Initial Characterization of a Novel Role of Shugoshin in Ciliated Neurons in *Caenorhabditis elegans*

A Thesis Submitted to the
College of Graduate and Postdoctoral Studies
in Partial Fulfillment of the Requirements
for a Master of Science Degree
in the Department of Biology
University of Saskatchewan
Saskatoon

Permission to use

In presenting this thesis/dissertation in partial fulfillment of the requirements for a graduate degree from the University of Saskatchewan, I agree that the Libraries of this University may make it freely available for inspection. I further agree that permission for copying of this thesis/dissertation in any manner, in whole or in part, for scholarly purposes may be granted by the professor or professors who supervised my thesis/dissertation work or, in their absence, by the Head of the Department or the Dean of the College in which my thesis work was done. It is understood that any copying or publication or use of this thesis/dissertation or parts thereof for financial gain shall not be allowed without my written permission. It is also understood that due recognition shall be given to me and to the University of Saskatchewan in any scholarly use which may be made of any material in my thesis/dissertation.

Requests for permission to copy or to make other uses of materials in this thesis/dissertation in whole or part should be addressed to:

Head of the Department of Biology
112 Science Place
W.P. Thompson Building
University of Saskatchewan
Saskatoon, Saskatchewan, S7N 5E5
Canada

OR

Dean
College of Graduate and Postdoctoral Studies
University of Saskatchewan
116 Thorvaldson Building, 110 Science Place
Saskatoon, SK S7N 5C9
Canada

Abstract

Across eukaryotic species, Shugoshin proteins perform several critical functions in meiotic and mitotic cells that ensures faithful chromosome segregation and the preservation of genomic stability. In the centromere, they function as adaptor proteins, mediating spindle attachment and cohesin phosphorylation to promote sister chromatid association and delay anaphase entry. In centrosomes, Shugoshin maintains centriole cohesion and regulates centrosome maturation in preparation for spindle nucleation. These functions implicate Shugoshin in regulating transient microtubule-related structures in the cell. Here I introduce a new function of Shugoshin in yet another tubulin-derived structure, the cilium. Using *Caenorhabditis elegans* (*C. elegans*) as a model, I investigated the possible localization of SGO-1 in sensory cilia of adult neurons and in the embryonic primordia of sensory organs. Finally, I identified TAC-1, a member of a conserved microtubule regulator protein family, as an SGO-1 interacting protein. Together, these results suggest the involvement of a similar genetic toolkit in the regulation of diverse cellular functions and reveal the first evidence of Shugoshin activity in a fully differentiated cell type.

Acknowledgements

I would like to thank my research supervisor Dr. Carlos Carvalho for giving me the opportunity to participate in this project. The experience gained both in lab and in life from Dr. Carvalho will continue to impact my life for many years to come. His never-ending support throughout this project enabled me to push myself beyond my limits and challenge myself to leave my comfort zone. I would also like to thank Dr. Troy Harkness for all his expertise troubleshooting and guiding me through unfamiliar protocols in my project. The members of Dr. Carvalho's lab, both past and present, also deserve some thanks for their help in and around the lab. I would to thank the funding sources for making this project possible. Dr. Carvalho is funded by an NSERC-Discovery grant as well as the Canadian Foundation for Innovation, and without them this project would have not got off the ground. I would also like to thank my parents for their constant support not only throughout this project, but throughout my entire university experience. Whether it was finically or motivationally, I owe a great deal to my parents and their continued support.

Table of Contents

Permission to use i
Abstract ii
Acknowledgments iii
Table of Contents iv
List of Tables vii
List of Figures viii
List of Abbreviations ix
1 Introduction 1
1.1 Overview of Shugoshin proteins 1
1.1.1 Cohesin in mitosis and meiosis 3
1.1.2 SGO isoforms in yeast 7
1.1.3 SGO isoforms in mammals 9
1.1.4 Tensile relocation of SGO 10
1.1.5 SGO functions in chromosome biorientation and cell cycle delay 11
1.2 Chromosomes of *C. elegans* 13
1.3 Cohesin in *C. elegans* 14
1.4 *C. elegans* as a model organism 17
1.5 Polarity shapes the cell 19
1.6 The sensory organs of *C. elegans* 20
1.7 Sensory dendrite extension in *C. elegans* 23
1.8 Cilium biogenesis in *C. elegans* 24
1.9 Tubulogenesis in *C. elegans* 27
1.10 Introduction figures 28
2 Hypothesis and Objectives 36
2.1 Hypothesis 36
2.2 Objective 1 36
2.3 Objective 2 36
2.4 Objective 3 36
3 Material and Methods 37

3.1 Materials 37
3.1.1 *C. elegans* Strains 37
3.1.2 Transgenes and arrays 39
3.1.3 Plasmids 40
3.1.4 Reagents 41
3.2 Methods 45
3.2.1 Worm growth conditions 45
3.2.2 Immunofluorescent staining 45
3.3 Injection protocols 47
3.4 Yeast 2-Hybrid 49
3.4.1 2-Hybrid overview 49
3.4.2 False positives 51
4 Results 54
4.1 Neuronal expression of *sgo-1* 54
4.2 Embryonic localization of SGO-1 57
4.3 SGO-1 marks the contact point for dendrite extension in amphids 59
4.4 SGO-1 occupies specific cilia domains 60
4.5 SGO-1 is compartmentalized to the cilia channel in the late embryo 61
4.6 Genetic requirements for SGO-1 loading in the developing amphid 63
4.7 A genetic null raises questions about the α-SGO-1 antibody specificity 65
4.8 Searching for the true embryonic SGO-1 localization 66
4.9 Screening for SGO-1 interacting proteins 67
4.10 Identification of hits 68
4.11 Results figures 69
5 Discussion 86
5.1 SGO-1 is a cilia protein 86
5.2 Microtubule regulators are used in different cellular domains 89
5.3 Significance of the TAC-1/SGO-1 interaction in the centrosome and cilia 92
5.4 Novel meiotic roles of SGO-1 in *C. elegans* oogenesis and spermatogenesis 94
5.5 Future directions 95
6 Appendices 98

Appendix A 98
Appendix B 98
Appendix C 99
Appendix D 99
Appendix E 100
Appendix F 101
Appendix G 101
Appendix H 101
Appendix I 102
Appendix J 102
Appendix K 102
Appendix L 103
Appendix M 104
Appendix N 104
Appendix O 105
Appendix P 105
Appendix Q 107
Appendix R 108
Appendix S 109
Appendix T 110
Appendix U 110
Appendix V 110

References 112

List of Tables

Table 3.1: Strains used in this study 37
Table 3.2: Transgenic arrays generated in this study 39
Table 3.3: Plasmids used and generated in this study 40
Table 3.4: Reagents used 41
Table B.1: Antibodies 98

List of Figures

Figure 1.1: SGO protein family 29

Figure 1.2: Cohesin protection during mitosis and meiosis 30

Figure 1.3: Tensile relocation of SGO 31

Figure 1.4: Diagram of sensory organ location and their components 32

Figure 1.5: Embryonic stages of *C. elegans* 33

Figure 1.6: Cilia structure in *C. elegans* 34

Figure 1.7: IFT in *C. elegans* 35

Figure 4.1: *sgo-1* sequences 70

Figure 4.2: Expression of *sgo-1* and subcellular localization of SGO-1::GFP in adult worms 71

Figure 4.3: SGO-1::tdTomato is present in sensory rays of male tails 72

Figure 4.4: Depletion of *sgo-1* results in *bonafide* cilia mutant phenotypes 73

Figure 4.5: WT embryos stained with α-SGO-1 74

Figure 4.6: α-SGO-1 detects signal in *sgo-1* mutant embryos 75

Figure 4.7: α-SGO-1 signals are juxtaposed to the dendrite anchorage proteins DYF-7 and DEX-1 in the anterior depression region 76

Figure 4.8: α-SGO-1 signals appear in close contact with known cilia proteins 77

Figure 4.9: α-SGO-1 signal insert in between a cellular pocket defined by adherens junctions in adjacent glia cells in the developing amphid 78

Figure 4.10: PAR proteins delineate the developing pocket defined by the presence of α-SGO-1 signals 79

Figure 4.11: α-SGO-1 signals in the sensory depression/head of cilia mutant embryos 80

Figure 4.12: α-SGO-1 signals are not lost in *sgo-1(sas02)* null embryos 81

Figure 4.13: HA-SGO-1 is detectable only in mitotic cells of the embryo 82

Figure 4.14: TAC-1 interacts with SGO-1 in a yeast two-hybrid assay 83

Figure 4.15: TAC-1 coding sequence and alignment 84

Figure 4.16: Confirmation of TAC-1/SGO-1 binding by reversing bait/prey clones 85

List of Abbreviations

aECM	Atypical extra cellular matrix
ALMS	Alström Syndrome
APC	Anaphase promoting complex
aPKC	Atypical protein kinase C
BBS	Bardet-Biedl Syndrome
BLAST	Basic local alignment search tool
bp	base pair
BSA	Bovine serum albumin
C. elegans	*Caenorhabditis elegans*
CDK	Cyclin dependent kinase
cDNA	complimentary DNA
CPC	Chromosome passenger complex
CRISPR	Clustered regularly interspaced short palindromic repeats
D. melonagaster	*Drosophila melanogaster*
DAPI	4′,6-diamidino-2-phenylindole
DIC	Differential interference contrast
DMF	Dimethylformamide
DMSO	Dimethyl sulfoxide
DNA	Deoxyribonucleic acid
dNTP	Deoxyribonucleotide triphosphate
E. coli	*Escherichia coli*
ECM	Extracellular matrix
EDTA	Ethylenediaminetetraacetic acid
GEF	Guanine nucleotide exchange factor
GFP	Green fluorescent protein
GTP	Guanine triphosphate
HA	Human influenza hemagglutinin

His	Histidine
IFT	Intraflagellar transport
IgG	Immunoglobulin G
IP	Immunoprecipitation
LB	Lysogeny broth
Leu	Leucine
MCAK	Mitotic centromere-associated kinesin
MCC	Mitotic checkpoint complex
MMP	Million Mutation Project
mRNA	messenger RNA
MTOC	Microtubule organizing center
NBP	National Bioresource Project
NCBI	National Center for Biotechnology Information
NGM	Nematode growth media
PAR	Partitioning
PCM	Pericentriolar material
PBS	Phosphate buffered saline
PBS-T	Phosphate buffered saline with Tween 20
PEG	Polyethylene glycol
PLK	Polo like kinase
PP2A	Protein phosphatase 2 A
RFP	Red fluorescent protein
RNA	Ribonucleic acid
RNAi	RNA interference
RPGR	Retinitis pigmentosa GTPase regulator protein
S. cerevisae	*Saccharomyces cerevisae*
S. pombe	*Saccharomyces pombe*
SAC	Spindle assembly checkpoint
SDS	Sodium dodecyl sulfate

SGO	Shugoshin
SMC	Structural maintenance of chromosomes
TACC	Transforming acidic coiled coil
TRP	Transient receptor potential
Trp	Tryptophan
Ura	Uracil
Y2H	Yeast-2-Hybrid

1 Introduction

1.1 Overview of Shugoshin Proteins

Over the past few years, the Shugoshin (SGO) protein family has emerged as critical players in cell division that can be found in a variety of organisms ranging from yeast to humans (1). The first homolog of SGO was uncovered in the early 1990's, when researchers studying *Drosophila melanogaster* discovered a meiotic mutant (MEI-S332) with increased chromosomal nondisjunction in both meiosis I and II (2). In these mutants, centromeres are prematurely depleted of cohesin, the 'glue' that sustains sister chromatid association. The untimely collapse of chromosome cohesion leads to dissociation (disjunction) of homologs and sister chromatids, preventing proper attachment to the spindle and resulting in the formation of chromosomal bridges and missegregation. Ultimately, aneuploid daughter cells are produced. Mutants with this characteristic meiotic defect were subsequently isolated in yeast, mice and *Xenopus*. These mutants, while displaying the same cell cycle defects, did not immediately point to the involvement of a single evolutionarily conserved gene family. In fact, only the subsequent cloning of the genes responsible for these defects and the identification of two small and poorly conserved sequence motifs present in these proteins revealed a common ancestry. This allowed further *in silico* identification of other putative Shugoshin genes in invertebrate and vertebrate organisms, from worms to humans (3, Figure 1.1).

The conserved domains mentioned above lie in the N and C termini of SGO proteins. A coiled coil domain near the N terminus and a canonical SGO motif at the C terminus are the most conserved structural domains (3). Thus, while at the sequence level, SGO homology between species is minimal, the consistent defects of Shugoshin mutants demonstrate a surprising level of functional conservation for SGO proteins across eukarya. Interestingly, this functional

conservation, as far as chromosome segregation is concerned, appears dependent on a monocentric chromosomal architecture where the centromere centralizes kinetochore assembly (see below).

The identification of SGO-specific domains shed light on how these genes evolved in different species and revealed the existence of orthologs in some species in which the *sgo-1* locus was duplicated. Some organisms, such as budding yeast and *D. melanogaster*, contain only a single isoform of SGO performing multiple functions while others, such as humans and mice, contain two separate forms of SGO. In these, the different SGO proteins appear to have functionally specialized, with different expression patterns and modes of action (3). Irrespective of these differences, there is a general consensus about the main functions of this protein family. SGO proteins have been found to act mainly during meiosis and mitosis to ensure the proper segregation of chromosomes (3). These studies revealed two critical aspects of Shugoshin's function that underlie its involvement in the cell cycle as we understand it today: 1) SGO proteins transiently localize to the centromere in metaphase and are removed from the centromere prior to sister chromatid segregation and 2) SGO proteins are required for the proper centromeric localization of proteins with catalytic activity (4). The discovery of specific spatial and temporal recruitment of SGO to the centromere, together with the phenotypic consequences of SGO depletion and its protein binding properties, pointed to a role of SGO proteins in shielding centromeric cohesin by acting as a tether to attract regulators of cohesin stability to the site of cohesin protection. Since cohesin is lost differentially from centromeres in mitotic and meiotic chromosomes, the unraveling of SGO's specific roles in these different cell divisions ultimately helped to explain how the stepwise segregation of homologs and chromatids is

possible in meiosis. A review of cohesin in mitosis and meiosis can be found below, and comments on the differences between some this species variance and function discussed after.

1.1.1 Cohesin in Mitosis and Meiosis

Mitosis and meiosis are processes through which cells duplicate their genome and either, divide to generate genetically identical daughter cells during tissue growth/maintenance, or form haploid gametes for sexual reproduction respectively. After DNA replication in mitosis, sister chromatids must faithfully segregate away from each other to opposite poles in order for the new cells to inherit a complete copy of the genome. Conversely, in meiosis, gametes receive only half of the genetic information as to allow for the reconstitution of the species ploidy upon fertilization.

This reduction in ploidy and subsequent DNA content in meiosis happens in a step wise manner that requires that homologous chromosomes segregate from each other first (meiosis I) before sister chromatids separate (Meiosis II). At the molecular level, chromosome association and segregation are regulated by the recruitment and dissociation of cohesin on chromosomes. Cohesin loads between sister chromatids as DNA replicates in S phase and is required for several aspects of chromosome behavior in mitosis and meiosis such as, chromosome resolution and correct attachment to the spindle in a bipolar mode that positions chromosome correctly along the metaphase plate. In addition, cohesin has also been shown to be involved in non-cohesion-related roles such as transcriptional control and double strand break repair (5). Removal of cohesin from chromosomal domains, licences chromosome segregation and, is therefore under strict regulation as to avoid the premature collapse of chromosome association. When this process is not lethal, it leads to genome instability.

In mitosis, cohesin must be completely removed from arms and centric regions after the transition beyond the spindle assembly checkpoint (SAC), which occurs upon the correct bipolar attachment of chromosomes to the spindle. With the onset of anaphase, chromosomes are cohesin-free and can be pulled away from each other allowing for sister chromatid segregation. On the other hand, in meiosis I, when homologs attach in a monopolar configuration to the centromere relative to the spindle pole, chromosomes must retain centromeric cohesin as to preserve sister chromatid association until meiosis II segregation. It is only after this initial separation that cohesin can be completely removed and sister chromatids allowed to separate. Problems in regulating the two-step removal of cohesin from meiotic chromosomes, results in: nondisjunction of chromosomes; the production of aneuploid gametes; and sterility (4).

The mitotic cohesin complex consists of four subunits. Structural maintenance of chromosomes (SMC) proteins Smc1 and Smc3, a kleisin subunit Scc1, and an accessory subunit Scc3 form the core of the complex (6). A fifth subunit, Pds5, recruited through Scc1 also associates with the complex and functions in part with the help of the destabilizing Wapl protein to remove cohesin from the chromosome (3). This cohesin complex however does not stably associate with chromosomes and the complex loads and unloads rapidly. Establishment of cohesin requires the acetylation of the Smc3 subunit by an Eco1 acetyltransferase which recruits sororin (3). Sororin competes with Wapl for Pds5 binding, thereby displacing Wapl from the complex. In preparation for chromosome alignment and spindle attachment in metaphase, removal of mitotic cohesin follows two separate paths: the prophase pathway; and the separase-dependent cleavage pathway.

The prophase path removes the majority of mitotic cohesin from the arms of chromosomes before metaphase through the action of Wapl. Cyclin dependent kinase (CDK)

and the Aurora B kinase phosphorylate sororin preventing its binding to the Pds5 subunit, allowing Wapl access to the cohesin complex to promote cohesin removal (3). The Polo-like kinase (PLK) also participates in cohesin removal through an unknown mechanism (3). Though most of cohesin is removed through the prophase pathway, functionally chromosomes remain associated as long as centromeric cohesin is intact. Upon correct spindle attachment, centromeric cohesin is removed via a proteolytic cascade that relies on the activation of separase, a caspase-like protease (7).

This separase mediated path targets the remaining cohesin subset bound near to the centromere by cleaving the Scc1 subunit (6). Separase is held inactive prior to the onset of anaphase by its inhibitor securin, which is tagged for degradation in a cell cycle-dependent manner through ubiquitination by the anaphase promoting complex (APC) (3). The APC is constrained by the SAC, thereby ensuring cohesin is only removed after chromosomes have properly aligned (6).

Errors during mitosis can cause chromosome instability, which in turn can lead to aneuploidy, DNA damage and loss or gain of whole chromosomes (8). Chromosomal instability has been indicated as a driving force for tumorigenesis as aneuploidy is prevalent in many forms of solid tumors (9). As the SGO protein family has implicated functions in chromosome segregation, it is not unreasonable to think mutations in this family can increase tumorigenesis. Not surprisingly, one study found that in forty-six cases of human colorectal cancer, Sgo-1 expression was down regulated (9). Heterozygous knockout mice for Sgo-1 displayed a marked increase in aberrant cryptic foci and colonic tumours as compared to the wild type after treatment with a carcinogen (9). Yet another study found that heterozygous Sgo-1 knockout mice spontaneously generated hepatocellular carcinomas as well as had increased instances of DNA

damage (10). The identification of novel oncogenes and the elucidation of their carcinogenic mechanisms may prove beneficial for an aging population in the near future.

The meiotic cohesin complex is very similar to its mitotic counterpart, with a slight substitution in subunits. The protein Rec-8 takes the place of Scc1 in meiotic cohesin (6). The loss of cohesin also takes a slightly different path. Sister chromatids must remain together as homologous chromosomes segregate, so cohesin between sister chromatids must be maintained. Separase mediated cleavage removes cohesin only along the arms of the chromosomes during meiosis I, leaving cohesin between centromeres of sister chromatids intact (3). It is not until meiosis II, when sister chromatids are to segregate, that cohesin is cleaved by separase (6). As for mitotic chromosomes, SGO proteins also act as protectors of meiotic centromeric cohesin (11). Spindle attachment and tension generation across centromeres are key to understanding how SGO can survive homolog segregation in the centromere of anaphase I chromosomes, but is removed in mitotic chromosomes and in anaphase II of meiosis. A description of cohesin removal during mitosis and meiosis is summarized in Figure 1.2 and the role of tension generation is discussed in more detail below.

Alongside the protection of cohesin, a handful of other accessory functions important for accurate chromosome segregation have also been reported in this protein family. Much like the protection of cohesin between sister chromatids, SGO has been proposed to also protect centriole cohesion. During the cell cycle the centrosome, comprised of centrioles and pericentriolar material, of a cell must duplicate so that two separate poles form for which chromosomes to segregate to (12). As the centriole is duplicated in S phase, the daughter centriole remains associated with the mother centriole so that a mother and daughter centriole each move to the same pole during M phase. However, upon completion of M phase these mother/daughter

centriole pairs must dissociate from each other to allow for another round of centriole duplication (12).

The centriolar pairs are held together by cohesin, similar to that of cohesin between sister chromatids. The proposed mechanism of centriole cohesin protection follows closely to that of the protection of sister chromatid cohesin. The recruitment of SGO to the centriole brings with it protein phosphatase 2 A (PP2A), which can dephosphorylate the Scc1 subunit of cohesin and prevent its cleavage by separase (12). This centriolar SGO seems to be specific as it is a shorter splice variant that localizes to centrosomes (12). Not only does SGO seem to play a role in centriole cohesin, it also seems to be involved with kinetochore assembly. After phosphorylation by Aurora B kinase, Sgo1 is targeted to the kinetochore (13). This recruits Plk1, a key mitotic kinase that regulates centrosome maturation as well as mitotic entry and bipolar spindle assembly (13). Once tension is generated across the kinetochore, Sgo1 is phosphorylated by Plk1, causing the removal of both Sgo1 and Plk1 from the kinetochore (13). As Plk1 recruits many factors involved with mitotic signalling, the loss of Plk1 from the kinetochore may silence the activity of the SAC and allow the cell cycle to continue (13). Differences do exist between various species and the functionality of these proteins, some of which are discussed in the following sections.

1.1.2 SGO Isoforms in Yeast

In the budding yeast *Saccharomyces cerevisiae* (*S. cerevisiae)*, a single SGO homolog (*sgo1)* has been identified. Sgo1p in this system has been found to localize to kinetochores of mitotic cells in all stages of the cell cycle except anaphase (14). Deletion of *sgo1* in this system produces an increased rate of nondisjunction in mitotic cells, similar to that of mutants for the mitotic checkpoint kinase Bub1p and the spindle assembly checkpoint subunit Mad2p. These

results suggest that yeast *sgo1* is required for proper chromosome segregation in mitosis. However, it may not be involved directly in the maintenance of cohesin as precocious separation of sister chromatids was not observed in metaphase arrested cells of *sgo1* mutants (14). Unlike mitosis, *sgo1* does seem to be directly involved in maintenance of cohesin in meiosis. Diploid colonies with a homozygous *sgo1* deletion were found to have an increased rate of sister chromatid missegregation during meiosis I (14). Other studies have shown that *sgo-1* binds and localizes PP2A to centromeric cohesin, allowing PP2A to dephosphorylate the Rec8 subunit of cohesin preventing its cleavage and removal by separase (15).

The reversible phosphorylation and dephosphorylation events are crucial for the proper functions of cohesin. Not only does phosphorylation of cohesin itself make it an available target for separase cleavage, but phosphorylation of other chromosomal associated proteins can promote or inhibit the removal of cohesin. For instance, Aurora B kinase phosphorylates sororin to promote the removal of cohesin while Sgo1p functions to keep sororin in a dephosphorylated state. Illustrating the complexity in these phosphorylation events, Aurora B, which is antagonized at the centromere by SGO activity, can in turn phosphorylate yeast Sgo1 to promote its binding to PP2A. In this sense, Aurora B contributes to SGO antagonism of itself. The fine tuning of PP2A and Aurora B activities underline much of this balancing of phosphorylation and dephosphorylation acts that decides on the fate of centromeric cohesin and ultimately, cell cycle progression.

In contrast to *S. cerevisae*, in the fission yeast *Saccharomyces pombe* (*S. pombe*), two isoforms of SGO have been identified. *S. pombe sgo1* has been shown to function during meiosis to protect cohesin between sister chromatids, much like *sgo1* in budding yeast (16). Without *sgo1*, fission yeast is viable and sister chromatids segregate to the same pole in meiosis

I, but their segregation in meiosis II is random (16). Rec8 was also found to disappear from centromeres after anaphase I, suggesting that without *sgo1* cohesin is not maintained between sister chromatids (16). Indeed, this system uses some of the same players as budding yeast to protect cohesin between sister chromatids during meiosis (3). The other SGO isoform, *sgo2*, was found to have functions during both meiosis and mitosis. Deletion of *sgo2* in concert with the heterochromatin deficient *swi6* mutation resulted in defective chromosome segregation, suggesting Sgo2p interacts with heterochromatin factors to promote segregation during mitosis (16). Defects in meiosis I were also observed in *sgo2* mutants, although the functions of *sgo1* and *sgo2* in meiosis are likely non overlapping as *sgo1* does not display a meiosis I defect and the double mutant does not enhance the defect found in *sgo2* mutants (16). It is interesting to note that the kinetochore kinase Bub1, an integral part of SAC, seems to have an important role in localizing both Sgo1p and Sgo2p to centromeres in meiosis and mitosis respectively, suggesting, as discussed below, a connection between spindle attachment and cohesin protection via SGO function (16).

1.1.3 SGO isoforms in Mammals

Much like the fission yeast, two separate isoforms of SGO have been identified in mammals. Sgo1 is thought of as the mitotic SGO, as it protects cohesion from removal by the prophase pathway during mitosis (3). Phosphorylation of Sgo1 by CDK initiates its binding to cohesin, allowing PP2A to dephosphorylate sororin which can then compete with and displace Wapl from cohesin, thereby preventing its removal (3). Sgo2 on the other hand has been described to possess meiotic functions. As previously stated, the Scc1 subunit of cohesin is replaced with Rec8 in the meiotic form of cohesin. As homologous chromosomes are segregating, Sgo2 transiently binds to cohesin at the centromere, bringing with it PP2A much in

the same way it does during mitosis. However, in meiosis the main target of PP2A dephosphorylation is Rec8 in place of sororin (3). In its unphosphorylated state, Rec8 is immune to cleavage by separase, leaving centromeric cohesin intact while cohesin along chromosome arms is degraded (3). Then during the second round of segregation in meiosis II, Sgo2 is displaced from the centromere allowing for the phosphorylation and degradation of Rec8 promoting the release of cohesin. The displacement of SGO from the centromere happens not only in meiosis, but in mitosis as well. How these proteins sense when to cease their protecting function is somewhat tied into their accessory functions, which are reviewed in the proceeding sections.

1.1.4 Tensile Relocation of SGO

In order to allow for sister chromatid segregation, centromeric cohesin must be removed. Because SGO loading onto chromosomes underlies cohesin protection, this would require the removal or inactivation of SGO at the centromere. Evidence has been mounting to support the idea that SGO only functions at the centromere when sister chromatids are not under tension (3). Once bound to opposite spindle poles, the force pulling sister chromatids apart also re-localize SGO into a new sub-domain in the centromere where it can no longer efficiently localize PP2A to dephosphorylate sororin (17). This tension-generated reconfiguration of molecular domains within the centromere/kinetochore, means that SGO-dependent cohesin protection is only possible prior to bipolar attachment when tension is not yet exerted. After correct chromosome attachment to the spindle, SGO associates with phosphorylated histone 2A instead, and PP2A recruitment has no further consequence to sororin phosphorylation and cohesin protection (17). Histone 2A is phosphorylated by Bub1 which is involved in mitotic checkpoint signaling and error correction (18). Binding of SGO to phosphorylated histone 2A initially localizes SGO to

the kinetochore, while the phosphorylation of SGO itself promotes its own binding to cohesin at the inner centromere (3). Thus, the chemical environments of these separate locations recruit kinases and phosphatases that allow SGO to switch its protective function on and off (3). While this tensile mechanism has been characterized in mitosis, it seems the tensile relocation of the SGO proteins is also responsible for cohesin maintenance during meiosis.

During meiosis I, it is the homologous chromosomes that segregate away from each other. The pairs of sister chromatids do not experience tension across their centromeres, since both sister chromatids attach to the same spindle pole. This lack of tension allows the SGO proteins to remain near to cohesin and promote the continuous dephosphorylation of Rec8 (19). Since homologs are bound at this stage solely by chiasmata which represent recombined regions of non-sister association where cohesin is never protected (with the centromere playing no role in this association), homolog separation and segregation progress once the SAC requirements are fulfilled. However in meiosis II, when sister chromatids are to segregate, the attachment of each sister chromatid to the spindle generates tension across the centromeres, as in mitosis, thereby displacing SGO from cohesin and allowing the separase mediated cleavage of cohesin (19). A diagram of this relocation can be found in Figure 1.3.

1.1.5 SGO functions in Chromosome Biorientation and Cell Cycle Delay

Apart from protection of cohesin, SGOs have also been implicated in proper spindle attachment to kinetochores of sister chromatids, an event that needs to occur to allow for cohesin protection as indicated above (3). SGO is responsible for the centromeric localization of the chromosome passenger complex (CPC), that includes Aurora B, which can remove microtubules from kinetochores that have failed to generate tension (20). The lack of tension across a kinetochore is an indication of improper spindle attachment, which if left uncorrected could

cause defects in chromosome segregation. These unattached kinetochores can then activate SAC to delay cell cycle progression and allow for further attempts to establish correct, tension-generating kinetochore attachments (3). SGO further links these processes together by interacting with the Mad2 subunit of the SAC, acting as an adapter between these two complexes and localizing them together at the centromere (3). Mad2 has been found to localize to unattached kinetochores whereas Bub1 localizes to both unattached kinetochores and kinetochores lacking tension (21). Both Mad2 and Bub1 are core components of the SAC, of which the APC is a downstream target.

The APC requires the accessory protein Cdc20 to inactivate its cell cycle delay functions (21). Mad2 binds to Cdc20 in a complex with Mad1, thereby sequestering Cdc20 and preventing activation of the APC (21). This sequestering of Cdc20 alone has been suggested to be insufficient to inhibit the APC. The Mad1-Cdc20 interaction has been found to complex with another subset of proteins, Bub3 and Mad3, which form the mitotic checkpoint complex (MCC), and has a more powerful inhibitory activity of APC than the Mad2-Cdc20 complex alone (21). Bub1 can also phosphorylate Cdc20, further inhibiting the APC (21). The checkpoint is switched off in response to multiple mechanisms. Once proper attachment to the kinetochore has been accomplished, Mad2 is transported down the microtubules by dyneins thereby preventing further inhibitory signals (21). Phosphorylation of Mad2 also prevents its association with Cdc20, allowing the APC to bind Cdc20 and become active (21). Once the inhibitory signals have been removed, the APC can activate separase allowing sister chromatids to separate and the continuation of the cell cycle. SGO also recruits the mitotic centromere associated kinesin (MCAK), which is involved in spindle formation and error correction of improperly attached kinetochores/microtubules (22). While these functions are unrelated to the canonical protection

of cohesin, they are nonetheless involved in accurate chromosome segregation, understating the modular and flexible role of SGO proteins and posing the interesting question of which function(s) the ancestral SGO protein originally held.

The intricate picture of SGO transient loading and repositioning on chromosomal domains during the cell cycle, as detailed above, suggests that SGO functions are highly constrained by and dependent on the presence of the centromere. By centralizing the last point of contact of sister chromatids prior to segregation to a small domain on the chromosome, the centromere facilitates the process of cohesin protection and removal. Centromeres, however, are characteristic of only one of the two major types of chromosomal architectures in eukaryotes, in which the attachment of chromosomes to the spindle occurs in a monocentric way. To fully understand the evolutionary relationship of SGO and the mechanics of chromosome segregation, it was necessary to investigate the role of SGO outside the context of monocentric systems.

1.2 Chromosomes of *C. elegans*

The chromosomes of *C. elegans* have a somewhat unique structure. Unlike many other systems with discrete singular centromeres on their chromosomes, *C. elegans* chromosomes are holocentric. Microtubule attachment sites are distributed along the entire length of *C. elegans* chromosomes instead of at a single location, essentially forming hundreds of centromeres per chromosome (23). Centromeric satellite sequences are scattered throughout the genome of the nematode and determine the location and distribution of the centromeres (24). Despite its uncharacteristic structure, *C. elegans* chromosomes must establish and remove cohesin-dependent cohesion to prompt mitotic and meiotic chromosome segregation in a similar fashion as observed in all monocentric species studied. In contrast to monocentric species, however, worms must accomplish this without a single centromere.

How do meiotic chromosomes, that lack this spatial cue, organize the protection of sister chromatid cohesion? The answer lies in a dramatic re-organization of chromosomal domains that reveal sites for cohesin protection in meiosis I. In *C. elegans*, bivalents undergo an intense re-configuration of cohesin domains around the region of the single crossing over, which always occurs off center in the chromosome. Following the formation of the chiasmata between homologous chromosomes, which involves a collaboration between the crossover sites and sister chromatid cohesion complexes, structural remodeling and condensation of the chromosomes results in a cruciform bivalent that displays a long and short axis (25). These two structurally different domains represent the interface between homologs (short arms) and sister chromatids (long arms).

Studies aimed at understanding the functional relevance of these domains revealed a striking difference in their molecular composition, and the identification of short and long arm-specific factors that are required to drive the proper removal of cohesin. As described below, most of these factors, with the notable exception of Shugoshin, appear to have representatives in the phosphorylation regulatory machinery that coordinates chromosome attachment and segregation in the centromere of monocentric species (3). Thus, worms appear to use a similar gene toolkit to promote the stepwise removal of meiotic cohesin on a completely different chromosomal template: first short axis cohesin, allowing homologous chromosomes to segregate in meiosis I, then long arm cohesin in meiosis II to promote sister chromatid dissociation.

1.3 Cohesin in *C. elegans*

C. elegans has evolved a mechanism for the protection of cohesion that is independent of SGO-1. Like in other systems, an Aurora B kinase phosphorylates the REC-8 subunit of the cohesin complex promoting the removal of cohesin from chromosomes (26). Unlike other

systems, *C. elegans* also contains two nearly identical and functionally redundant α-kleisin proteins, COH-3 and COH-4, that function alongside REC-8 to mediate meiotic sister chromatid cohesin (27). This REC-8, COH-3, COH-4 complex will be referred to as REC-8 for the remainder of this section. The sole Aurora B kinase in *C. elegans* responsible for REC-8 phosphorylation is AIR-2 (28). In order to prevent phosphorylation and removal of cohesion on the long arms of the bivalent, the phosphatase GSP-2 is recruited through the action of the worm-specific protein LAB-1. LAB-1 loads early in prophase I along other axis proteins such as HTP-3 to establish the cohesion domains necessary to trigger correct synaptonemal complex polymerization and recombination.

During the early stages of meiosis, LAB-1 brings GSP-2 into close proximity of the cohesin complex, where it can remove any phosphorylation events that occur on the REC-8 subunit (29). Upon crossover completion in zygotene and chromosome resolution in diplotene, LAB-1 is actively removed from the region that will become the short arm in the condensed cruciform bivalent (proximal to the crossover site). As bivalents attach to the spindle in metaphase I, cohesin is removed from the short arm domain, allowing for AIR-2 phosphorylation of REC-8. LAB-1 is retained along the long arm where cohesin survives past meiosis I via the recruitment of GSP-2 activity. Thus, in contrast to monocentric systems, homologs dissociate in worms by removing an overall small subset of cohesin on chromosomes, leaving chromatid cohesion intact in the remaining two thirds of chromosomes. Analogous to SGO regulation in the centromere of monocentric systems, sister chromatid disjunction is accomplished in worms by the dissociation of LAB-1 from the short arm at the end of metaphase II when the remaining REC-8 on chromosomes is cleaved off via AIR-2-mediated separase (SEP-1) activity.

Therefore, while meiotic chromosome segregation in *C. elegans*, as in monocentric species, relies in the same antagonistic activity of kinase and phosphatases, a different cohesin protection system evolved in worms that bypasses the lack of a centromere. Instead of transiently targeting cohesin protecting machinery (SGO-dependent) to a specific and relatively small chromosomal locus, *C. elegans* instead specifically removes a unique axis protein (LAB-1) previously loaded along the whole chromosome and whose presence is required to antagonize AIR-2 activity. By using the single chiasma to orient bivalent resolution, spatial information is transduced to the establishment of different molecular domains on meiotic chromosomes that mark the regions to be differently targeted for cohesin removal in meiosis I and II. In essence, 'centromere'-like molecular identities are progressively constructed on the chromosomes around the crossover site. First, on the short arms to regulate homolog dissociation, and then, on long arms, to segregate sister chromatids.

Remarkably, disrupting crossover control in worms to generate multiple cross overs, for example, leads to abnormal cohesin removal and chromosome segregation, presumably because of the disruption in the acquisition of correct chromosomal domains during resolution, pointing to the interconnectivity between recombination and cohesin removal in *C. elegans* (25). This novel mechanism, importantly, renders a SGO-like activity unnecessary in meiosis and defines LAB-1 as the functional analog of Shugoshin in worms, required for protection of meiotic cohesin (26). Since a potential function of LAB-1 in mitosis has not yet been described, it is still possible that SGO-1 retains a role, though redundant, in this division. These findings are consistent with the normal fertility of *sgo-1* mutants. and raise the intriguing question of what novel, if any, functions, SGO-1 would have evolved in organisms with holocentric chromosome architectures in which SGO cohesin protection functions may no longer be required.

1.4 *C. elegans* as a Model Organism

C. elegans is an excellent organism to study many different aspects of biology. They are free-living nematodes found in temperate soils (30). With a fully developed adult length of less than two millimeters, it is feasible to maintain large quantities of worms in simple petri dishes (30). They are in constant search of a food source, which is mainly bacterial growth. Laboratory strains of *E. coli* grown in agar petri dishes provide a cheap and sustainable food source for entire populations of worms. *C. elegans* is hermaphroditic, with males occurring in approximately in 0.1% of the population (30). This is advantageous as individual lines can easily be maintained by selfing of the hermaphrodites or new genes/mutations can be introduced by crossing hermaphrodites with males.

Each hermaphrodite can produce up to 350 progeny on her own, and combined with a short three day life cycle large amounts of progeny can be obtained in a few days (30). Progeny develop through a series of molts, beginning at the L1 larval stage after hatching and ending after the fourth and final molt between L4 and adult (30). If larvae experience unfavourable conditions, they may enter a delayed development stage called dauer. Energy is conserved and growth is halted while a new more suitable environment is found. They can survive as dauer for many months before finding a new suitable food source and resuming development (30).

C. elegans has a simple body plan. Two concentric tubes separated by a pseudocoelom form the body structure in its most basic description. The outer tube separates the interior of the animal from the environment. Here the epidermis secretes a thick collagenous cuticle which restricts the passage of molecules into and out of the worm (30). The inner tube consists of the pharynx and the intestine, which perform functions of food intake and digestion respectively (30). Most of the neuronal cell bodies of *C. elegans* are concentrated in a ring around the

pharynx termed the nerve ring (30). They extend processes out to the head, along the body and down to the tail where sensory information is obtained via a major ventral and dorsal nerve cords. The nerve center then integrates this information to form a physical response to environmental stimulus.

In adult hermaphrodites, two identical yet independent gonad arms are responsible for progeny production. Oocytes develop in the proximal arm of a gonad and pass through a spermatheca for fertilization before being allowed to further develop in the uterus (30). Eggs are then deposited outside the worm through a common uterus. In males a single gonad arm is found in place of two. Meiotic cells in the proximal arm progress through spermatogenesis inside the gonad before the mature sperm cells are stored in seminal vesicles for later copulation (30). Males display complex mating behaviors required to identify hermaphrodites, dock the tail fan around the vulva, insert the spicule and inject sperm. These behaviors are controlled by extra male-specific neurons that richly innervate the rays of the tail where sensory (tactile) information is relayed via ciliated neurons (31).

One of the most significant advantages of *C. elegans* as a model organism is its transparency. When viewed under a simple light microscope, internal structures and single cells of adults, as well as embryos, can be easily recognized. This transparency aided the determination of the entire cell fate map of worms and the acquisition of detailed electron microscopy images and continues to provide researchers with a simple way to view fluorescently tagged proteins *in vivo* (30). *C. elegans* remains the only multicellular organism in which the entire cell lineage map is known. Cell fates for all cells starting from the two-cell zygote up to the fully developed adult have all been characterized (30). An accurate number of somatic cells has also been determined. 959 somatic cells are present in the hermaphrodite and 1031 somatic

cells are present in the males (30). The extra set of cells found in males is accounted for by accessory neurons and structures required for mating. Not only does the number of cells remain constant between individuals, but the placement of the cells within the body is non-variable as well (30).

1.5 Polarity Shapes the Cell

Similar to other eukaryotes, cellular differentiation in worms requires the establishment of cell polarity. The acquisition of cellular asymmetry early on is recognized as a key event during development, behind cell fate decisions and the morphogenesis of different tissues types and specialized structures. Many of these structures rely on polarity cues inside the cell to determine their proper location. The partitioning (PAR) proteins provide cells with initial polarity cues, allowing for the determination of apical/basal surfaces in the developing embryo, for example (32). The initial event surrounding cellular polarity occurs already at the first division of the single celled zygote. This first division produces two asymmetric daughter cells; a larger anterior cell (AB cell) and a smaller posterior cell (P cell). These are progenitors of all somatic and germ cell lineages, respectively (33). Distribution of PAR-3 and PAR-6 closer to the anterior cortex of the cell with PAR-1 and PAR-2 more near to the posterior cortex helps position the first mitotic spindle ensuring the asymmetric cleavage (33). It is thought that a cytoplasmic flow generated by actomyosin contractions in the early embryo is responsible for relocating PAR-3 and PAR-6 to the anterior cortex (34). These events lead to an asymmetric partitioning of maternally provided cytosolic and membrane components that will trigger the cascading cell fate decisions to generate the main cell lineages in the early embryo.

Recent evidence suggests that aside from regulating asymmetric cleavage in the early embryo, the PAR proteins also function to promote patterning during later embryonic processes.

As epithelial sheets forms, information is needed on which surface will be apical and which basolateral so that adherens junctions may be properly placed at their boundary (32). PAR-3 has been shown to localize with PAR-6 and HMR-1 (E-cadherin) as foci in the interior of the cell that travel apically across epithelial cells and cluster (35). This suggests that the PAR proteins are not only responsible for early polarization events but may directly influence the location of adherens proteins in epithelial tissues. PAR proteins also interact with cytoskeletal components. Studies in *Drosophila* indicate that the PAR proteins are involved in regulation of actin myosin contractions (36). The Rho-GTPase CDC42 has been found to act in concert with PAR6 and the atypical protein kinase C (aPKC) to regulate the formation of actin filaments in epithelial cells (37).

1.6 The Sensory Organs of *C. elegans*

The main sensory organ of *C. elegans* is the amphid (reviewed in 31). They can be found in the head region of the animal in a pair, flanking either side of the mouth opening. The amphid is composed of twelve sensory neurons as well as support cells termed the socket and sheath cells (38, Figure 1.4). The neuronal cell bodies as well as the socket and sheath cells originate near the pharynx but extend anterior processes all the way to the tip of the nose (39). The socket and sheath cells form a channel through the cuticle of the animal through which some of the encompassed sensory neurons can make contact with the outside environment, with the socket cell forming the actual pore and the sheath cell sealing against the socket cell enclosing the base of the pore (40). The amphid channel forms between the comma and 1.5-fold stages of embryogenesis and depends on the cooperation of DAF-6 and CHE-14 (40). DAF-6 is a Patched related protein that localizes to amphid lumen and other tubes found in *C. elegans* (41). CHE-14 is one of the two *C. elegans* homologs of Dispatched and is found to localize at the apical

surfaces of the epidermis, excretory cell and the support cells of sensory organs (42). These two proteins have been proposed to regulate vesicle dynamics during tubulogenesis (41). These events take place in two specific regions in the cortex, where cells invaginate, resulting in larger cell-free pockets between the embryonic core and the inner egg-shell layer. Under DIC, these regions in the 1.5-fold embryo can be easily identified as small depressions and have therefore been termed anterior (amphid region) and posterior (phasmid) sensory depressions which mark the position of the future head and tail.

Inside, the channel is filled with a matrix material, some of which is secreted by the sheath cell (39). Eleven of the twelve sensory neuronal dendrites enter into this channel, but only eight out of those eleven make direct contact with the environment (40). The eight that are exposed end in slender cilia and are mostly responsible for sensing water soluble chemicals (30). The three neuronal dendrites that enter the channel but are not directly exposed to the outside have flat, branched cilia that terminate in the sheath cell. These are responsible for detecting volatile odours and are termed "wing" cells (30). The sole neuronal dendrite that never enters the channel also terminates in the sheath cell but has a complex branching pattern. This neuron senses temperature and its many fine branching points have earned it the name of "finger" cell (30). A diagram of the various sensory organs of *C. elegans* can be found in Figure 1.4.

Aside from the amphid sensillum, other sensilla also reside in the head region. They are innervated to a lesser degree than the amphid and also surround the mouth opening. Cephalic sensilla contain a single neuron and embed in the cuticle and serve as a mechanosensors (40). Inner and outer labial sensilla are also present surrounding the mouth opening. Inner labial sensilla contain two sensory dendrites, one exposed to the environment for chemo sensation and one embedded in the cuticle for mechanosensation, while outer labial sensilla contain only

dendrites embedded in the cuticle for mechanosensation (40). Posteriorly, the phasmid, a cilia-based sensory organ can be found. Built around the posterior ganglion, the phasmid contains only two sensory neurons (31). Much like in the amphid, these neurons terminate in cilia that extend through a channel formed by the socket and sheath cells to make contact with the outside environment. The lesser degree of innervation limits the phasmid to chemosensation, as opposed to the multiple stimulus detected by the amphid (31).

Finally, yet another specialized sensory organ exists in the specialized *C. elegans* male tail. The male tail contains a fan like structure that houses nine bilateral pairs of finger-like ray projections (42, see Figure 1.4). Each ray consists of a pair of sensory dendrites that are contained within a tube-like lumen, comparable to the situation found in the amphids and phasmids. However, in place of the socket and sheath cells found in the amphid/phasmid, a single ray structural cell forms this lumen (43). All rays are open and exposed to the environment at their tip except for a single ray (43). Cilia at the tips of these sensory dendrites are mostly responsible for the male mating behaviour. Here they detect cues regarding the location of a potential mate as well as the identification of a potential mate through chemo and mechanosensation (44). These cues not only guide male worms to a hermaphrodite, but also help to position the male tail near to the vulva of the hermaphrodite promoting successful copulation (44). Mutation of the cilium structure genes *osm-5* or *osm-6* result in males deficient in mate finding, male response to hermaphrodite cues, vulva discovery and sperm transfer (44). In summary, sensory perception in *C. elegans* that regulates a myriad of behaviors essential for survival and reproductive success relies on the development of ciliated organs in both head and tail.

1.7 Sensory Dendrite extension in *C. elegans*

The cell bodies of sensory neurons that will be part of amphids lie near the nerve ring, but as embryogenesis progresses, they need to extend their dendrites a considerable distance out to the nose. The apparent mechanism for this extension in the developing sensory organs during embryogenesis is quite unique. Rather than having a stationary cell body that projects a dendrite to the nose (axon pathfinding), it has been proposed that the dendrite remains stationary as the cell body migrates away. The cell body is born near the tip of the nose and extends a small dendrite out to the nose. Then as the cell body migrates away, the dendrite grows to accommodate the distance in a process termed retrograde extension (45). Dendrite extension occurs at the bean or comma stage of embryogenesis, similar to the time of development of the amphid (45). A schematic of the various embryonic stages can be found in Figure 1.5.

In the last 5 years, the isolation of the first mutants with defects in sensory neuron migration in *C. elegans* started to clarify the mechanism involved in this process. This process relies on the cooperation of two proteins, DEX-1 and DYF-7 that mediate membrane-matrix signaling. DYF-7 is a neuronal protein that contains a zona pellucida domain and DEX-1 contains a zonadhesin domain, although the cell type expressing DEX-1 has yet to be determined (45). These two domains are known to functionally interact in mice, as zona pellucida proteins comprise the matrix surrounding oocytes that zonadhesin proteins bind to (46). Both DEX-1 and DYF-7 are secreted into the extracellular space, where they can multimerize and form a dense matrix (45). Interestingly, these two proteins also share domain composition with the α and β tectorins found in the inner ear of mammals, another sensory organ (47). α and β tectorin make up the tectorial membrane inside the ear, which serves to anchor the sensory ends of hair cells to the membrane (47). Heiman and Shaham hypothesized that DEX-1 and DYF-7 form structures

in the extracellular matrix to which the dendritic tips can bind to, and later facilitate anchoring by either binding of the matrix to basement membranes or by steric hinderance of the matrix preventing its migration. How the dendritic tips interact with this matrix has yet to be uncovered.

1.8 Cilium Biogenesis in *C. elegans*

In animals, two major types of cilia, which are structurally similar but functionally diverse, exist. Primary cilia are non-motile structures specialized to sense environmental cues and mediate signal transduction events (48). Secondary cilia, or motile cilia, on the other hand are considered more ancient than primary cilia and are normally responsible for locomotion (48). Motile cilia, or flagellum, were discovered first in unicellular organisms, primarily due to the visibility of their function. Non motile cilia were observed in cells of higher eukaryotes. Because primary cilia do not generate ciliary beating and their function was not obvious in stationary cells, they were for a long time considered vestigial structures in cells, a left-over product of evolution (48).

The realization that primary cilium has critical signaling function became evident in recent years with the discovery of several human diseases and pathologies (ciliopathies) directly linked to defects in the structure and function of cilia in different tissues and organs. Today, cilia function and ciliogenesis are topics of intense research and clinical relevance (48). Bardet-Biedl Syndrome (BBS) is ciliopathy with a wide range of symptoms. It can cause vision deficiencies, auditory deficiencies, renal dysfunction and obesity. It also has many secondary symptoms which can include speech disorders, diabetes, and developmental delay. Nineteen BBS genes have been identified, most of which affect the protein complex responsible for transporting

membrane proteins into and out of the cilia (49). One of these genes is directly involved in intraflagellar transport (IFT) (49).

Another ciliopathy is Alström Syndrome (ALMS). It is caused by an autosomal recessive mutation to a single gene *ALMS1* (50). ALMS1 localizes to centrosomes and basal bodies of primary cilia in humans and has similar symptoms to that of BBS (50). ALMS1 has been implicated in metabolic homeostasis, cell cycle control and cell differentiation, although its exact functions have remained difficult to determine (50). ALMS was first described in 1959, but it wasn't until recently that it was classified as a ciliopathy. This suggests that there are more known diseases that have yet to be recognized as a ciliopathy, so understanding the mechanism of action behind these known ciliopathies might help uncover new ones.

In worms, the only ciliated cells in *C. elegans* are sensory neurons which carry primary cilia (31). This is very different from the mammalian system where most cell types are ciliated (48). Normally cilia arise from a structure called a basal body with triplet microtubules organized in a ring, but in *C. elegans* the ring is formed of doublet microtubules and instead is termed a transition zone (31). This initial transition zone is followed by a middle segment, containing a similar arrangement of microtubules, and is proceeded by the distal segment, which experiences a change from doublet microtubules to singlet microtubules. This transitioning from doublet to singlet tubules has been observed in the sensory cilia of other organisms and is thought to be conserved (31). Diagrams of the middle and distal segments can be found in Figure 1.6. The cilia of *C. elegans* are also unique in that they do not undergo the rapid assembly and disassembly experienced by cilia in other systems (31). In most animal cells the primary cilium is only present during the G0/G1 phase, when the centrosome is not required to form the mitotic spindle (51). The cilium is then broken down and its components used to make

the spindle required for chromosome segregation before being regenerated in the resulting daughter cells (51). However, in *C. elegans* the centrioles that give rise to the basal body are placed during organogenesis when sensory organs are becoming innervated (52). Once the primary cilium has formed in these finally differentiated cells, it remains stable and does not undergo assembly and disassembly as in other systems (52).

Cilia development in the sensory organs begins around the 3-fold stage of embryogenesis (40) and depends heavily on IFT. Ciliary precursor proteins are transported from the transition zone at the junction of the dendrite and cilium to the middle and distal segments. Two separate IFT motors of the kinesin-2 protein family, heterotrimeric kinesin-II and OSM-3, are responsible for moving IFT molecules and ciliary precursors to the middle and distal segments where they are used in signalling or cilium construction (31). The IFT molecules consist of two separate multiprotein complexes that have been termed A and B (53). In the middle segment, the two kinesin motors act together to transport cargo up the cilium, however only OSM-3 functions in transport to the distal tip (31). The retrograde IFT-dynein motor then returns the anterograde motors and presumably any turnover products back to the base of the cilium allowing for renewed transport of IFT particles (31).

Homologs of the BBS proteins in *C. elegans* have been shown to stabilize the IFT subcomplexes A and B when bound to the kinesin motors during transport (54). Another regulator of IFT in *C. elegans* is DYF-1. This protein loads the OSM-3 motor onto IFT particles and also spurs its motor activity thereby promoting cilium generation (55). A description of IFT is summarized in Figure 1.7. The identity of the cargo contained within the IFT particles has been somewhat elusive, although a handful of proteins have been recently described to be part of these complexes. The cilia specific TRP-type channel proteins OSM-9 and OCR-2 have been

shown to be part of the IFT cargo and that they experience IFT movement along the cilium (56, 57). These two proteins have been purposed to be involved in chemosensory responses (56). IFT components and associated proteins are highly conserved across animal phyla and defects in this axoneme transport is behind most identified ciliopathies so far (58). The homolog of mammalian *Tubby*, TUB-1, has also been visualized traversing the cilium. TUB-1 has implications in lifespan regulation and chemotaxis (59). Interestingly, many genes required for ciliogenesis are under the control of a promoter element called X box which is recognized by DAF-19, the master transcription regulator of cilia genes (60).

1.9 Tubulogenesis in *C. elegans*

Formation of a luminal cavity underlies the development of different organs and can be observed in a host of organisms and various cellular structures. In *C. elegans* these cavities can be found in the developing amphid/phasmid sensilla where a lumen houses the sensory dendrites as they transition to cilia and in the excretory system where channels form to dispose of wastes. Lumen formation has been best described in the excretory system of *C. elegans*. A canal cell, a duct cell and a pore cell in concert with a secretory gland and two sensory neurons make up the *C. elegans* excretory system, which has major functional implications in osmoregulation (61). The canal, duct and pore cells all form their own lumen, which connect with each other through apical junctions to form a continuous tube (61).

Much like epithelial cells, the apical or luminal surface of these tubes is delineated by the PAR3/6 proteins which function in the proper placement of the connecting apical junctions (61). These developing lumens also fill with a fibrous apical extracellular matrix (aECM) thought to give shape and strength to the cavity (62). The filling of the lumen with an ECM seems to be conserved across various types of lumen, as an ECM also fills the amphid/phasmid channel (45).

The extensive branching and elongation experienced by the canal cell during development is partially regulated by neuronal guidance cues, much like the amphid/phasmid channel (63, 39). These findings suggest that channel and tubular lumen formation may be controlled by similar mechanisms and proteins.

1.10 Introduction figures

Figure 1.1

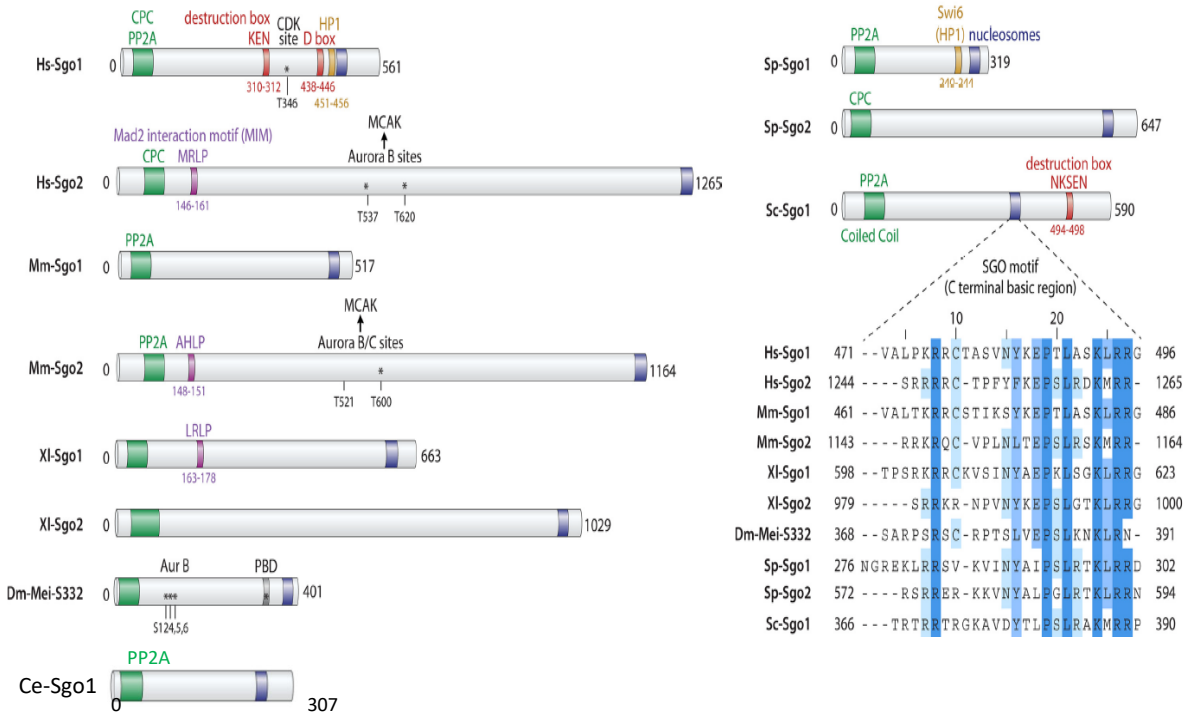

Figure 1.1: SGO protein family

A schematic description of the various domains found in the species specific SGO homologs. The minimal conservation between the canonical SGO motif can be found in the blown-up view of the final homolog. Hs - *Homo sapiens*, Mm - *Mus musculus,* Sc - *Saccharomyces cerevisiae*, Sp - *Saccharomyces pombe*, Xl - *Xenopus laevis*, Ce- *C. elegans* and Dm - *Drosophila melanogaster.* (modified from Marston, 2015)

Figure 1.2

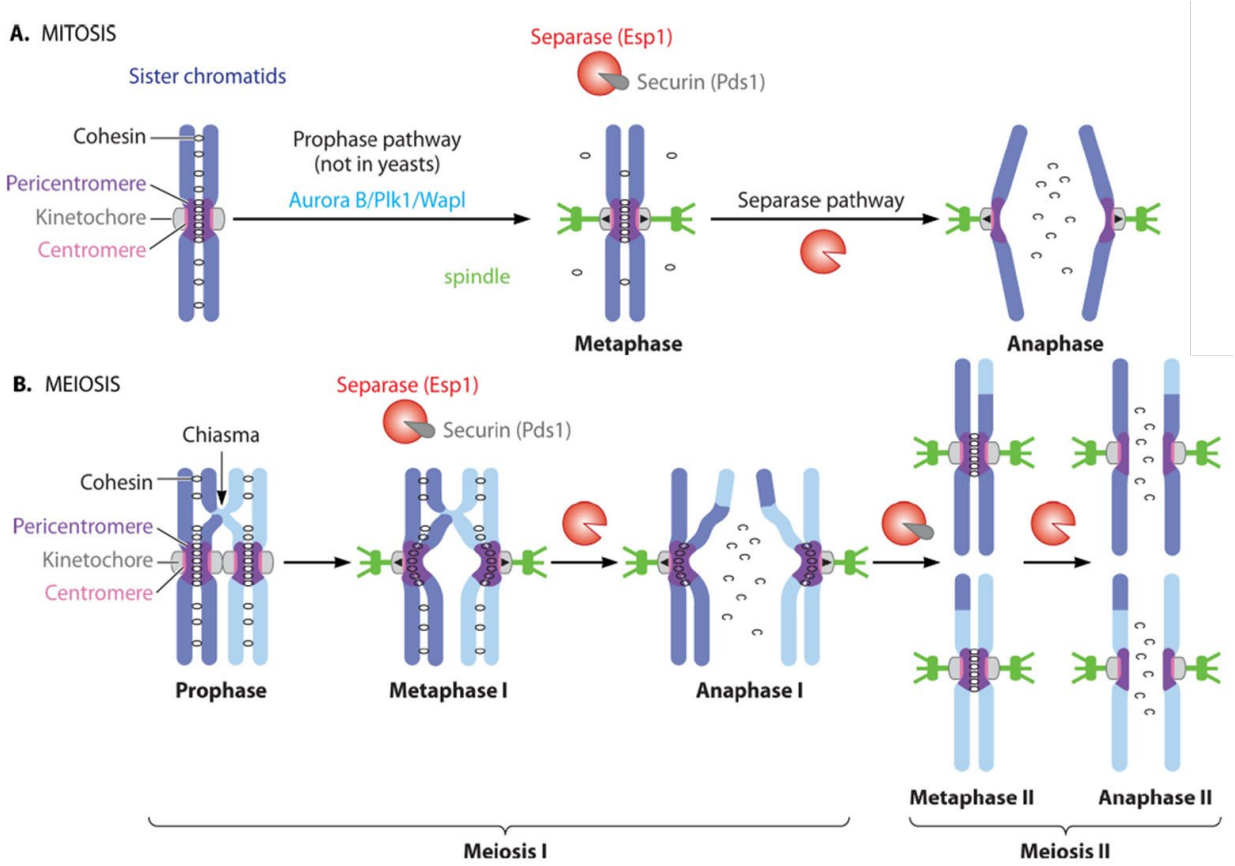

Figure 1.2: Cohesin protection during mitosis and meiosis

A) Protection of cohesin during mitosis. The prophase pathway removes the majority of cohesin along the chromosome arms leaving centromeric cohesin intact. Upon chromosome biorientation separase cleaves cohesin allowing the sister chromatids to segregate. B) Protection of cohesin during meiosis. Cohesin along the chromosomal arms is cleaved by separase allowing homologs to segregate while cohesin at the centromere between sister chromatids is protected by SGO. At the onset of anaphase II SGO is removed from the centromere, allowing for the separase-mediated cleavage of cohesin and segregation of sister chromatids. (from Marston, 2015)

Figure 1.3

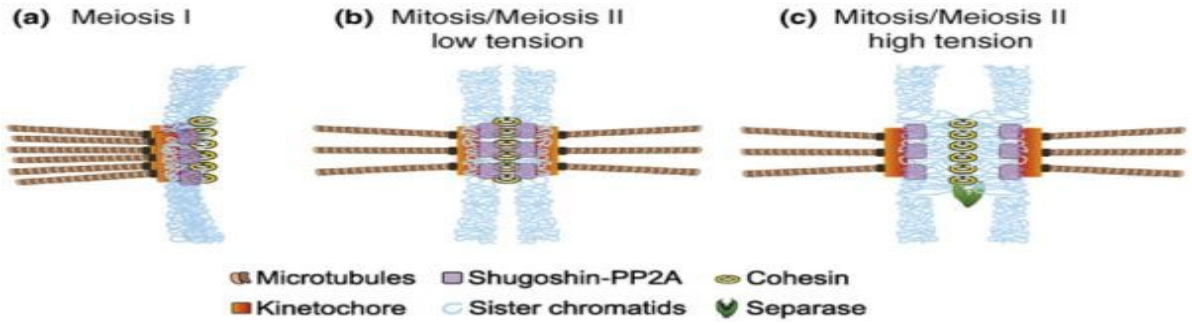

Figure 1.3: Tensile relocation of SGO

A) Attachment of only a single sister chromatid to the spindle during meiosis I does not generate tension across centromeres of sister chromatids, allowing SGO-PP2A to localize near to cohesin. B) Tension mounts between sister chromatids as the spindle forms and attaches to both sister chromatids during mitosis and meiosis II. C) As the spindle exerts more force on the sister chromatids, SGO-PP2A is "pulled" away from cohesin thereby allowing cleavage and removal of cohesin and sister chromatid segregation. (from Gregan *et al*, 2008 used with permission ID number: 4607151285233)

Figure 1.4

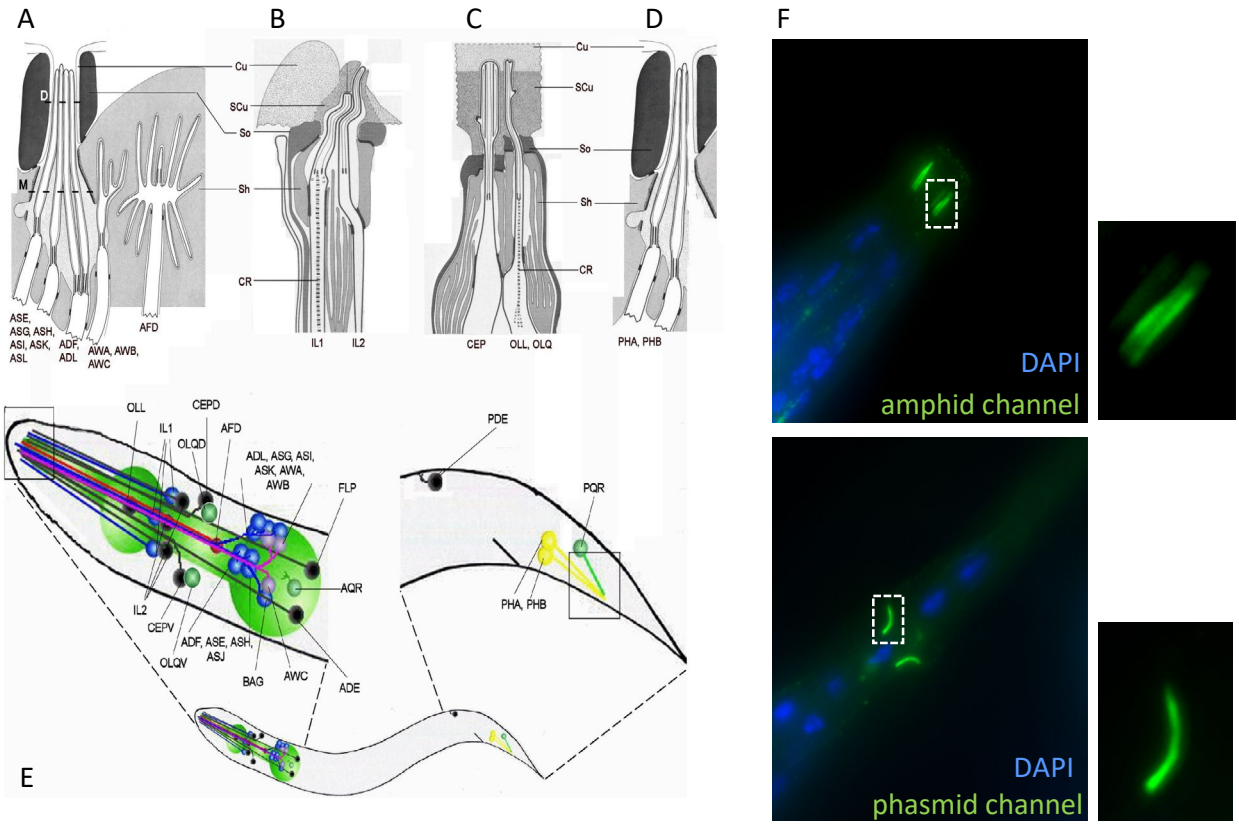

Figure 1.4: Diagram of sensory organ location and their components

Diagrams depicting the anatomical structure of the amphid and phasmid sensilla. A) Amphid showing the position of the sensory neurons and their glia within the organ. B) Positions of the inner labial sensilla and their neurons and glia. C) Cephalic/outer labial sensilla neurons and their glia. D) Phasmid and its associated neurons and glia. E) The location of the neuronal cell bodies and their processes innervating these structures. F) IF of whole worm showing amphid channel in head region (top, inset) and phasmid in the tail (bottom, inset). An uncharacterized monoclonal antibody 1-6/C10 generated in the lab that marks these structures was used. Cu: cuticle. CR: ciliary rootlet. SCu: sub cuticle. So: socket cell. Sh: Sheath cell. From WormBook©

Figure 1.5

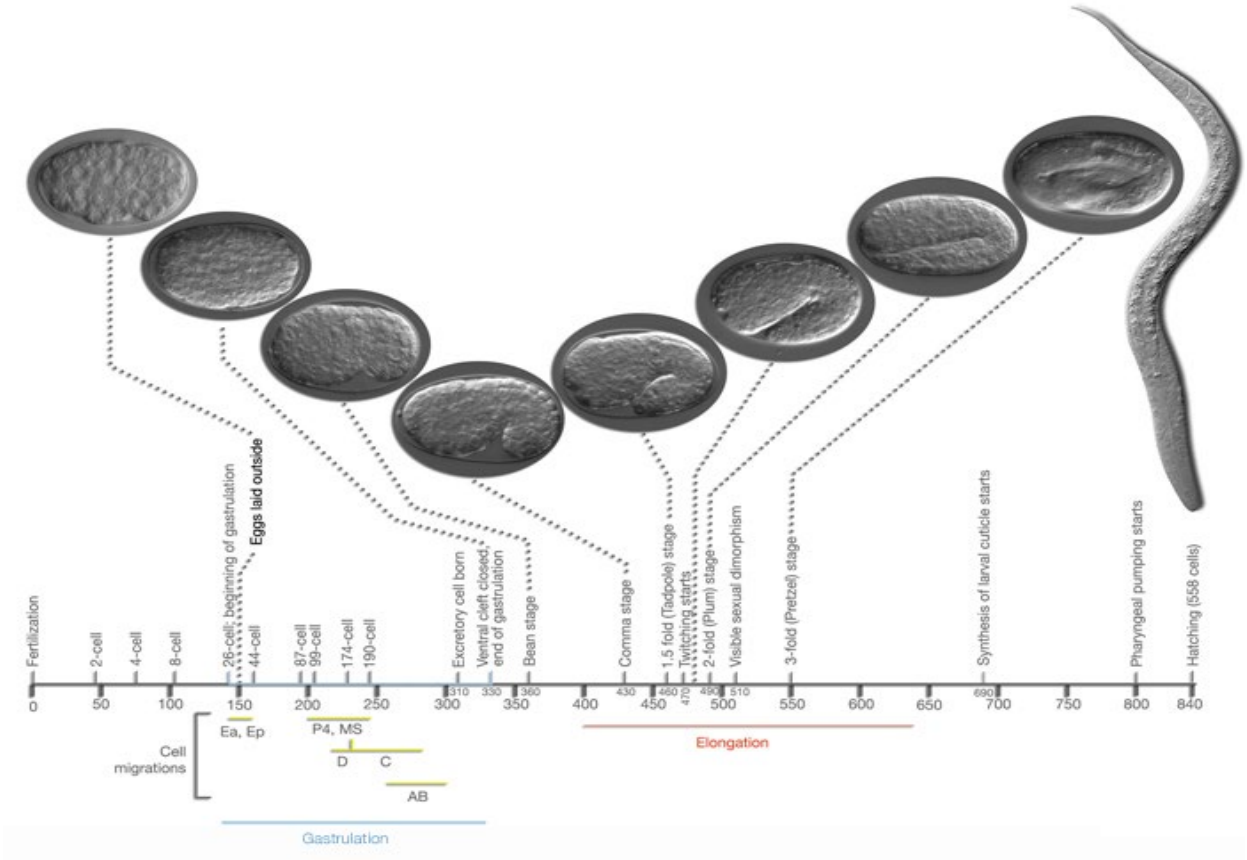

Figure 1.5: Embryonic stages of *C. elegans*

A timeline of the stages of *C. elegans* embryonic development beginning from fertilization and ending with hatching. Note the shape and time of development for the bean, comma, 1.5-fold and 3-fold (pretzel) stages. From WormAtlas©

Figure 1.6

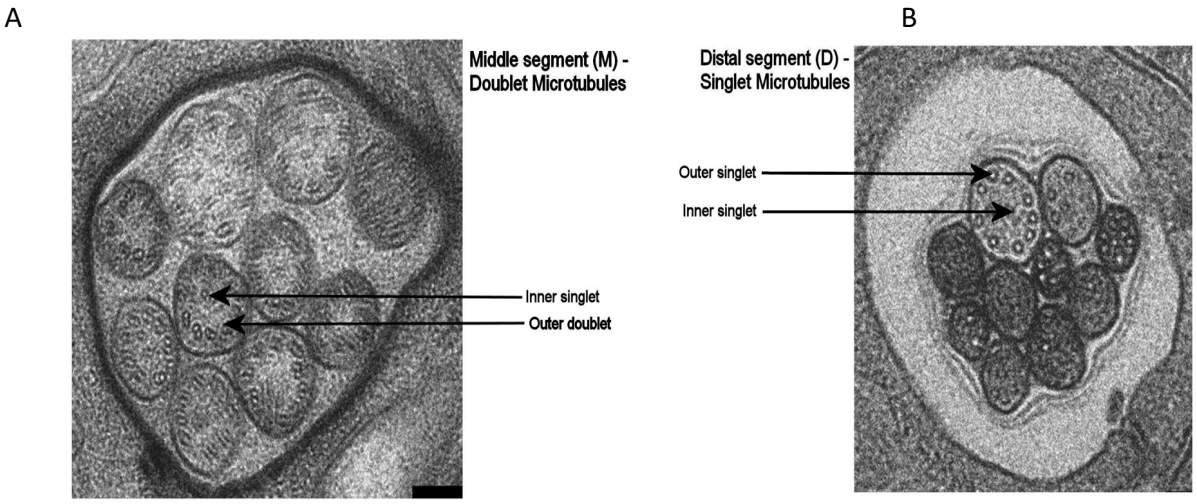

Figure 1.6: Cilia structure in *C. elegans*

A) Electron micrograph of the middle segment of *C. elegans* cilia. B) Electron micrograph of the distal segment of *C. elegans* cilia. From WormBook©

Figure 1.7

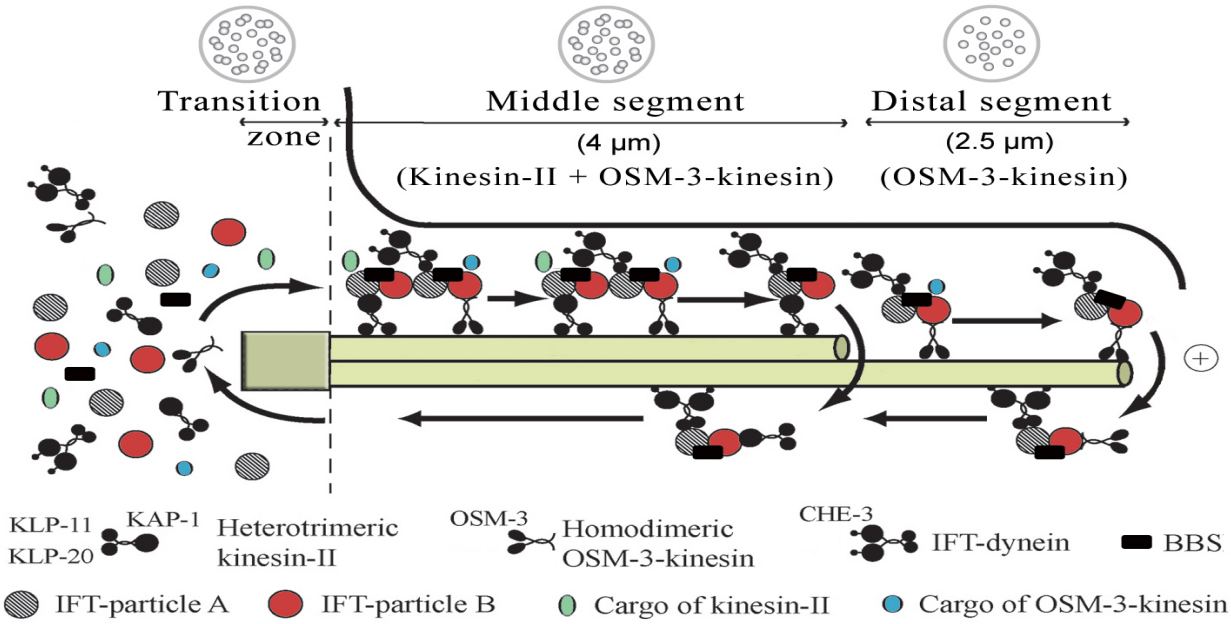

Figure 1.7: IFT in *C. elegans*

At the transition zone, ciliary precursors and cargo are bound by OSM-3 and heterotrimeric kinesin-II and load onto the microtubules of the cilium. Both kinesin motors function together to bring cargo to the middle segment, but only OSM-3 is responsible for transport to the distal segment. BBS proteins stabilize the cargo complex while bound to a motor protein. The IFT-dynein motor then transports all components back to the transition zone for repackaging and transport of new precursors. From WormBook©

2 Hypotheses and Objectives

2.1 Hypothesis

Since *C. elegans* seems to have evolved a system of cohesin protection independent of SGO-1, I propose that SGO-1 in *C. elegans* may carry roles outside the context of cell division. Given that *sgo-1* loss of function mutants display phenotypes similar to that of *bona fide* cilia mutants (see Results), this undiscovered function may have implications in cilium structure/function or the underlying neuronal connections made to the sensory cilia. Because of the lack of viability of *sgo* mutants non-worm systems, it is possible that this novel function, while conserved, has remained undetected in monocentric species where SGO activity is required early on for embryonic development. In worms, where SGO is dispensable for cell cycle progression, this ancestral function of SGO could then be revealed in adult animals. Conversely, the novel functions of SGO in the nervous systems could have evolved exclusively in worms after the relaxation of selective pressure on the *sgo-1* locus with the evolution of Shugoshin functional analogs such as LAB-1 and possibly others.

2.2 *Objective 1*: Characterize the embryonic signals identified in immunofluorescent images using a new anti-SGO-1 antibody generated in the lab and determine possible genetic interactions of SGO-1.

2.3 *Objective 2*: Determine the true localization of SGO-1 in adult worms and in embryos using transgenic approaches.

2.4 *Objective 3*: Screen for novel SGO-1-interacting proteins using a heterologous *in vivo* approach.

3 Material and Methods

3.1 Materials

3.1.1 *C. elegans* Strains

Table 3.1: Strains used in this study.

Strain Name	Genotype	Purpose	Source/Maker
N2	Wild type, Bristol strain	Control strain	*Caenorhabditis* Genetics Center (CGC)
CB1309	*lin-2(e1309) X*	Egg laying defect used for embryo collection	CGC
CV138	*sgo-1(tm2443) IV*	*sgo-1* loss of function, used in chemotaxis assays	CGC
MX1980	*ccep-290::GFP, rol-6(su1006) II*	To visualize the location of α-SGO-1 in respect to the transition zone	Leroux lab
MX1959	*ccep-290(ok415039)*	To see if transition zone disruption affects SGO-1 localization	Leroux lab
SP1735	*dyf-7(m537) X*	To see if dendrite extension defects affect SGO-1 localization	CGC
CEC191	*lin-2(e1309) X; sasEx36*	To see the localization of α-SGO-1 in respect to DYF-7	Carvalho lab
KK1248	*par-6::GFP*	To test the localization of α-	CGC

		SGO-1 in respect to PAR-6	
KK1216	*par-3::GFP*	To test the localization of α-SGO-1 in respect to PAR-3	CGC
CEC118	*unc-119(ed3)III;Is[psgo-1::sgo-1::GFP;unc-119+];Ex[pche-13::che-12::mCherry]*	To test the localization of α-SGO-1 in respect to the IFT transport protein CHE-13	Carvalho lab
CEC205	*sasEx42*	To test the localization of HA tagged SGO-1	Carvalho lab
CEC09	*sasEx01*	Transcriptional reporter of pSGO-1::GFP	Carvalho lab
CEC180	*lin-2(e1309);sasEx30*	To see the localization of α-SGO-1 in respect to DEX-1	Carvalho lab
DAM543	*nphp-4(tm925) V; mksr-2(tm2452) IV;ccep-290(tm4927) I*	To see if abolishing the entire transition zone affects α-SGO-1 localization	Dammermann lab
CEC214	*sgo-1(sas02) IV*	*sgo-1* null mutant, used to test the α-SGO-1 antibody	Carvalho lab
CB1377	*daf-6(e1377) X*	To see if amphid lumen formation defects affect α-SGO-1 localization	CGC
DR1720	*unc-4(e120); daf-19(m86) II*	To see if loss of cilia affects α-SGO-1 localization	CGC

VC40793	*gk815462*	To test α-SGO-1 in a loss of SGO-1 function background	CGC
VC200007	*gk952908*	To test α-SGO-1 in a loss of SGO-1 function background	CGC
VC20450	*gk325897*	To test α-SGO-1 in a loss of SGO-1 function background	CGC
CEC174	*him-5(e1467)V;lin-2(e1309)X;sasEx19*	To test the localization of SGO-1 in male tail rays	Carvalho lab
CEC03	*unc-119(ed3)III;Ex[psgo-1::sgo-1::GFP;unc-119+]*	Translational reporter of SGO-1 subcellular localization	Carvalho lab

3.1.2 Transgenes and arrays

Table 3.2: Transgenic arrays generated in this study.

Gene/Array	**Protein/Role**
sasEx36	*pdyf-7::dyf-7::GFP;rol-6(su1006)*
sasEx42	*psgo-1::HA::sgo-1cDNA::unc-54 3`UTR*
sasEx01	*psgo-1::GFP;rol-6(su1006)*
sasEx30	*pdex-1::dex-1::mCherry;rol-6(su1006)*
sasEx19	*posm-5::sgo-1::tdtomato;rol-6(su1006)*

3.1.3 Plasmids

Table 3.3: Plasmids used and generated in this study.

Plasmid ID	Plasmid information	Maker/source	Purpose
N/A	pDONR-221	ProQuest™ Two-Hybrid System with Gateway® Technology from Invitrogen	Initial plasmid used in the Gateway® procedure to generate the entry vector
N/A	pDEST-32	ProQuest™ Two-Hybrid System with Gateway® Technology from Invitrogen	Destination plasmid for Gateway® cloning, generates the expression bait vector
N/A	pDEST-22	ProQuest™ Two-Hybrid System with Gateway® Technology from Invitrogen	Destination plasmid for Gateway® cloning, generates the prey expression vector
N/A	pSCB	Aligent Technologies	Used to generate transgenic fusion proteins
pCEC34	pEntr-221-sgo-1	Brandon Waddell	Entry vector with *sgo-1* cDNA insert, used to make the expression bait vector
pCEC35	pExp-32-sgo-1	Brandon Waddell	Expression bait vector with *sgo-1* as the insert, used in the Y2H screen
pCEC39	pExp-22-tac-1	Brandon Waddell	Expression prey vector with *tac-1* as the insert, used in the Y2H screen
pCEC38	pExp-32-tac-1	Brandon Waddell	Expression bait vector with *tac-1* as the insert, used to reconfirm the TAC-1/SGO-1 interaction
pCEC36	pExp-22-sgo-1	Brandon Waddell	Expression prey vector with *sgo-1* as the insert, used to reconfirm the TAC-1/SGO-1 interaction

pCEC07	p32.8	Carvalho lab (unpublished)	Used to visualize SGO-1::tdTomato in the cilia

3.1.4 Reagents

Table 3.4: Reagents used.

Reagent	**Manufacturer**	**Catalogue Number**
NaCl	Bioshop	SOD001.205
Bacto Peptone	Fisher Scientific	BP1420-500
Agar	Anachemia	02116-380
$MgSO_4$	Bioshop	MAG513-500
$CaCl_2$	Bioshop	CCL555.500
KH_2PO_4	Bioshop	PPM302.1
KOH	Bioshop	PHY202.1
Na_2HPO_4	Bioshop	SPD307.1
Glycerol	Fisher Scientific	BP229-1
Tris Base	Bioshop	TRS001.1
EDTA	VWR	BDH0232-500G
SDS	Bioshop	SDS001.500
Proteinase K	Bioshop	PRK403.100
β-mercaptoethanol	VWR	97064-588
Tryptone	Bioshop	TRP402.500
Yeast Extract	Bioshop	YEX401.500
HEPES	Bioshop	HEP001.100
Formaldehyde	Bioshop	FOR201.500
KCl	Bioshop	POL999.500
Tween20	Bioshop	TWN510.500

22x22 mm Coverslips	VWR	48366-227
22x50 mm Coverslips	VWR	48393-194
25x75x1 mm Superfrost Plus Microscopy Slides	VWR	48311-703
Precision Glide 0.4x13 mm Needles	BD	305109
60x15 mm Polystyrene Petri Dish	Fisher Scientific	FB0875713A
25 mL Serological Pipette	Fisher Scientific	13-678-11
200 µL Pipette Tip	Fisher Scientific	13-611-117
100x 15 mm Polystyrene Petri Dish	Fisher Scientific	FB0875712
1.5 mL Locking Lid Microcentrifuge Tube	Fisher Scientific	14-666-319
50 mL Conical Centrifuge Tube	Fisher Scientific	06-443-18
1000 µL Pipette Tip	VWR	83007-384
10 µL Pipette Tip	VWR	613-0259
15 mL Conical Centrifuge Tube	Thermofisher Scientific	339651
PEG 3350	Sigma Aldrich	202444-500G
L-Leucine	Sigma Aldrich	L8000-25G
Yeast Synthetic Dropout Medium w/o Histidine, Tryptophan, Leucine or Uracil	Sigma Aldrich	Y2001-20G
LiAc	Acros Organics	AL447712500
Yeast Nitrogen Base w/o Ammonium Sulfate or Amino Acids	Sigma Aldrich	Y1251-100G
4 mm Glass Beads	Fisher Scientific	11-312B
D-Glucose	Sigma Aldrich	G8270-1KG

Acrodisc 32 mm Syringe Filter w/ 0.2µm Supor Membrane	PALL Life Sciences	4652
10 mL Syringe	BD	302995
100 µL Filtered Pipette Tip	Neptune Scientific	BT100
10 µL Filtered Pipette Tip	Fisher Scientfic	02-707-473
TitonX-100	Bioshop	TRX506.500
Ammonium Sulfate	BioBasic	AMP301.1
Kwik-Fil Borocilicate Glass Capillaries	World Precision Instruments	1B100F-4
3 mm Chromatography Paper	GE Healthcare	3030-6461
Halocarbon Oil 700	Sigma Aldrich	H8898-100mL
DMSO	Amresco	0231-500mL
Agarose for Electrophoresis	Bioshop	AGA002.100
Agarose for Injection Pads	Amresco	0710
Frosted Microscope Slides 25x75x1 mm	Fisher Scientific	12-544-2
X-gal Assay membranes	GE Healthcare Life Sciences	1003-070
$5^{3/4}$ inch Borosilicate Glass Pasteur Pipette	Fisher Scientific	13-678-20A
NaOH	Bioshop	SHY500.1
Bromophenol Blue	Amresco	0449-50G
Xylene Cyan FF	Bioshop	XYC001.5
Bovine Serum Albumin	Amresco	0332-100G
Phenol/Chloroform/Isoamyl Alcohol	Fisher Scientific	BP1752I-400
Isopropyl Alcohol	VWR	BDH1133-1LP
Ampicillin Sodium Salt	Sigma Aldrich	H9518-25G
Trizol	Ambion by Life Technologies	15596026

Ethyl Alcohol	Chemistry Stores	01157
DMF	VWR	BDH1117-4LP
High Fidelity Phusion Polymerase	New England Biolabs	M0530S
Taq	Grown and purified in lab	
High Fidelity Bsrg I	New England Biolabs	R3575S
Parafilm	BioBasic	PF002
1 Kb Sharp DNA Marker	RBC Bioscience	RD001
3AT	Sigma Aldrich	A8056-25G
X-gal	BioBasic	BB0083
Salmon Sperm DNA	Invitrogen	15632-011
BP Clonase II	Invitrogen	11789-020
LR Clonase	Invitrogen	11791-020
Stratclone Blunt PCR Cloning Kit	Aligent Technologies	240207-5
Superscript II One Step RT-PCR w/ Platinum Taq	Invitrogen	10928-034
GeneJET Plasmid Maxi Prep Kit	Thermo Scientific	K0491
Clear Nail Polish	Electron Microscopy Sciences	72180
Prolong Gold Antifade Reagent	Invitrogen	P36930
L-Histidine	Sigma Aldrich	H8000-25G
L-Uracil	Sigma Aldrich	U0750-25G
L-Tryptophan	Sigma Aldrich	T0254-25G
Ethidium Bromide		
HiYield Gel/PCR DNA Fragments Extraction Kit	RBC Bioscience	YDF100
HiYield Plasmid Miniprep Kit	RBC Bioscience	YPD100

Ez-10 Spin Column DNA Gel Extraction Miniprep Kit	BioBasic	BS654
Ez-10 Spin Column Plasmid DNA Miniprep Kit	BioBasic	BS614

3.2 Methods

3.2.1 Worm growth conditions

All strains of *C. elegans* were grown on Nematode Growth Media (NGM, refer to Appendix U) in a 20˚C refrigerated incubator unless otherwise stated for temperature sensitive mutants. 10ml of molten agar media were uniformly poured in 60mm sterile petri dishes using an automatic media dispenser to standardize growth conditions. All worms were fed a slow growing laboratory strain of *E. coli* OP50. Worms were moved onto fresh food plates whenever food ran out or contamination occurred. A Nikon SMZ745 stereo microscope was used to observe and manipulate worms with standard *C. elegans* techniques.

3.2.2 Immunofluorescent (IF) staining

Two separate strategies were used to harvest embryos for staining. For strains carrying a *lin-2* mutation, worms were grown until L4 and then fifteen to twenty of the desired phenotype were transferred to a new plate and allowed to fill with embryos. Due to their vulva developmental defect, *lin-2* mutants cannot lay eggs and newly fertilized oocytes continuously accumulate in the uterus as a result, making it ideal to harvest a large number of embryos for staining. On the day of the dissection, worms were transferred to a plate without food for fifteen to thirty minutes, allowing them to crawl off excess bacteria and expel any they were digesting. Once clean, they were added to a drop of water on a cover slip supported by a glass slide, and under a microscope dissected by sectioning at the midsection using a pair of needle tips to expose the embryos. Carcasses of the parents were discarded, and about half of the remaining

water in the drop was removed. For all other strains not carrying the *lin-2* mutation, embryos were picked directly from the plate and transferred to a drop of water on a coverslip supported by a glass slide. To remove bacteria coating the embryos, the drop was flushed with more water to swirl and stir the sample, and then half of the volume pipetted off. After two to three washes with water, samples were exposed to freeze & crack protocol. A coverslip was placed on top of the water drop and samples were immediately placed on a pre-chilled (-80ºC) metal plate. After rapid freezing, the coverslip was pried away from the sample (freeze & crack) using a razor blade to permeabilize the egg-shell. Without allowing the sample to thaw, slides were submerged into -20ºC cold methanol for one minute, to quickly fix the sample. The methanol was removed, carefully not to disturb the sample area, and post-fixed in a paraformaldehyde solution (4% FIX, refer to Appendix A) for thirty minutes in a humid chamber at 20˚C. Alternatively (mh27 antibody staining) slides were fixed for 30 minutes in cold methanol only. After three five-minute washes in wash buffer (phosphate buffered saline with Tween 20 (PBS-T), refer to Appendix A), slides were blocked for one hour at 20˚C in blocking solution (0.5% bovine serum albumin (BSA) in PBS-T). After removing excess blocking solution, sample area was covered in primary antibody diluted in blocking solution (as described per antibody in the Appendix B.1) and then covered with cut outs of parafilm. Slides were incubated overnight at 4˚C in a humid chamber.

The next day the parafilm was carefully removed by allowing it to float to the surface of a coplin jar filled with PBS-T, and the slides subsequently washed twice more for five minutes. After drying excess buffer, secondary antibody diluted in PBS-T at a dilution rate of 1:500 for all antibodies except goat- α-rabbitIgG-Cy3, which was diluted 1:1000, was added to the sample area and covered with parafilm. Following a two-hour incubation at 20˚C in a humid chamber,

samples were washed as before to remove the parafilm. Slides were DAPI stained in a 0.5 µg/mL DAPI in PBS-T solution for ten minutes and then destained in PBS-T for ten minutes. After careful drying, avoiding the sample area, a drop of Vectashield® (Vector Laboratories) or Prolong™ Gold was applied to reduce photobleaching and a coverslip sealed on top with clear nail polish. Slides could be viewed immediately or stored at 4˚C in a light-protected case.

All images were taken on a DeltaVision Elite wide field fluorescent microscope and processed in softWoRx by Applied Precision Inc. As fluorescent signal intensity varied widely from sample to sample, exposure parameters were set as high as possible without saturating the camera for each separate image. This allowed for the visualization of weak signals. When appropriate, and to control for false negative results, samples were co-stained with either a mouse α-GFP or mouse α-tubulin-α antibodies. All raw images were deconvolved using Softworx® ten stage iterative deconvolution with a medium (200 nm) noise filter.

3.3 Injection protocols

In order to generate strains expressing fluorescently tagged transgenic proteins used in this study, DNA microinjection was performed. Using an inverted microscope coupled with a needle manipulator, DNA mixtures containing the construct (plasmid DNA) as well as a dominant marker transgene (*rol-6*) were injected in the distal gonad of healthy adult worms immobilized on an agarose pad. In this anatomical region, many germ cell nuclei are clustered and sharing the common cytoplasm in the gonad syncytium. DNA taken up by germ cells is copied and concatemerized into large extrachromosomal arrays through homologous recombination that can be stably inherited for may generations (64). The use of the *rol-6* (*su1006)* selectable marker aids in identifying transgenic progeny by inducing a dominant rolling phenotype in animals carrying the transgene. F1 rollers can be easily be identified from non-

transformants in the progeny of injected P0 worms due to their characteristic circular movement patterns on bacterial lawns and can be propagated to select transmitting lines.

Delivery is accomplished by pulling borosilicate glass capillary needles that is then filled with 0.5 µL of a 100 ng/µL DNA injection solution. The needle is loaded into the injection apparatus and the needle point brought into focus above the sample. Before injecting, the needle tip must be gently broken by tapping on a glass slide to allow solution to flow through. Care must be taken to avoid creating too large of a break to minimize damage done to the animals. Samples are prepared by individually adding worms to the bottom of a 2% agarose pad covered by a drop of halocarbon oil to avoid dehydration. Worms are carefully pushed down to the agarose surface with the help of a fine brush made from an eyelash until they adhere and stop moving. Animals are brought into focus under 10x magnification and the distal gonad located under 40x magnification. By increasing magnification, the gonad is much easier to distinguish from intestine and the point of entry for the needle becomes visible. With gentle force, the needle is pressed onto the cuticle of the worm until it penetrates the outer surface. Too much force and the needle will exit the other side of the animal and greatly decrease viability.

A small puff of air is delivered using a Femtojet® (Eppendorf) microinjector connected to the building pressured air supply and the solution is injected into the animal. This can be observed by a temporary expansion of the gonad syncytium as it fills with liquid follow by its contraction. The 0.5 µL of injection solution can inject many worms, with slight deviations of volume injected per worm depending on the length of the air pulse. The needle is slid out of the animal, taking care not to create a large exit wound, and the animals recovered from the agar pad using a drop of M9 buffer (see Appendix U). Worms will float up from the agar and can be fished out with a worm pick and transferred to a plate of fresh food to recover. Injected (P0)

animals are allowed to self and F1 progeny checked for rollers. When available, at least 30 F1 rollers are singled and transmitter lines identified by checking for F2 rollers. On average, 5% of F1 rollers will produce transmitting lines. Transmission can vary greatly between lines. Because two arrays generated using the same injection mixture injected into the same P0 animal can potentially be different in composition, copy number and stability, at least two independently isolated transmitting lines were maintained from each transgene, as to validate the analysis and rule out strain-specific artifacts. When possible, a line with high (>70%) and low (<20%) transmission were selected. Once identified, transgenic strains carrying extra-chromosomal arrays were maintained by cloning animals expressing the dominant (roller) phenotype and aliquots frozen for storage purposes. Precise specifications can be found in Appendix C.

3.4 Yeast 2-Hybrid

3.4.1 2-Hybrid Overview

To probe for protein interactions between the proteome of *C. elegans* and SGO-1, a Yeast 2 Hybrid (Y2H) screen strategy as used. In this system the Gal 4 transcription factor of *S. cerevisiae* is separated into two distinct functional parts, its activation domain and DNA binding domain. To generate cDNA for *sgo-1*, a mixed population of *C. elegans* was subject to the mRNA isolation protocol in Appendix G. The resulting RNA sample was retrotranscribed into cDNA using the protocol in Appendix H. The *sgo-1* cDNA band was separated on a 1% agarose gel, gel extracted of the fragment (HiYield® Gel/PCR DNA Fragments Extraction kit) and used as a template in a PCR reaction with the Gateway® primers indicated in Appendix L. This PCR reaction added the Gateway® compatible sequences to the *sgo-1* cDNA fragment. The BP reaction found in Appendix E was used to generate the entry vector pEntr-221-*sgo-1*, which was sequenced using the primers found in Appendix N to ensure the cDNA

sequence was in frame with the Gal 4 domain. The entry vector was then subject to the LR reaction found in Appendix E to generate the expression vector pExp-32-*sgo-1*, which is the final bait vector used in the screen. Transformation of the BP and LR reactions into bacteria followed the protocol outlined in Appendix F.

A prey cDNA library of wild type C. *elegans*, representing the transcriptome of a mixed N2 population grown at 20ºC, was prepared by recombining cDNAs in frame with the Gal 4 activation domain, generating a library of prey plasmids (a gift from the Smolikove lab, University of Iowa). Storage of prey clones and library propagation in bacteria were carried out in the lab using the protocol found in Appendix M. Prior to screening, prey plasmids as well as the *sgo-1* bait vector were introduced into host yeast cell using the transformation protocols found in Appendix Q. Successful transformants were then screened for reporter gene activity as described in Appendix R. The particular host cell used has been engineered to have a set of reporter genes controlled by the Upstream Activation Sequence (UAS) bound by the Gal 4 DNA binding domain. Specifications on the host strain can be found in Appendix O. If the proteins encoded by the bait and prey plasmids interact inside the yeast cell, the UAS brings the DNA binding domain and activation domains together causing transcription of the reporter genes. The reporter gene *HIS3* allows growth on media without histidine, *URA3* allows growth on media lacking uracil, and *lacZ* produces a blue colour when exposed to the substrate β-galactosidase. Hits are scored based on their ability to perform during the reporter assays.

Once a positive hit is found, the plasmid DNA present in the yeast cell is extracted using the extraction protocol found in Appendix S and electroporated into bacterial cells using the protocol in Appendix J. The resulting bacterial colonies were then subject to the miniprep protocol in the HiYield™ Plasmid Minikit to extract the prey plasmid for identification by

sequencing using the sequencing reaction found in Appendix N. Initial hits were selected as follows. An aliquot of the bait/prey co-transformation was spread onto synthetic complete media plates lacking tryptophan and leucine, selecting for only the presence of the bait and prey plasmids and the resulting colony counts used to determine the total number of cells screened. The remaining bait/prey co-transformation was spread onto synthetic complete media plates lacking tryptophan, leucine and histidine (but containing 10 mM of 3AT to increase selection stringency) to begin the screening process. Vector maps of the bait and prey plasmids can be found in Appendix D.

3.4.2 False Positives

A major drawback of the Y2H approach is the occurrence of false positives. These colonies are positively selected in reporter assays and appear to contain interacting proteins, though they in fact represent leaky selection or artifacts and are not the product of real interactions. There are a few different causes for false positives. Proteins with large hydrophobic surfaces may have a low affinity for other proteins and may simply bind the bait protein to minimize exposed hydrophobic surfaces. Heat shock proteins that interact with a wide range of proteins may by chance bind to the bait protein. Transcription factors can directly bind to the UAS without the aid of the DNA binding domain and cause transcription of the reporter genes. Multiple prey plasmids may also be taken in by the cell causing making it difficult to discern which prey plasmid conferred the interaction. Mutations in the host cell could also occur that cause the inappropriate readout of phenotypes.

To reduce the number of false positives, the bait and prey plasmids are low copy number ARS/CEN vectors that prevent over-expression of the fusion proteins. Most of the other issues are circumvented by titrating selection conditions of the three reporter assays. If all assays

confirm interaction, that hit is most likely a positive interaction and should be examined in more detail. If only two of the assays are passed, the hit might be a weak interaction and still warrants further investigation. However, if only one or none of the assays are passed, then that hit is most likely a false positive. The level of activation is determined by comparing the reporter assay results of the hits to those of the controls. Five separate controls were used. Three of the five controls all contain the same bait plasmid, pExp-32-Krev1, however they differ in their prey plasmids. The strong positive control uses pExp-22-RalGDS as its prey plasmid, as Krev1 and RalGDS are known interacting partners (65). The weak positive control also uses pExp-22-RalGDS, however a mutation in the RalGDS sequence perturbs its interaction with Krev1. One of the negative controls utilizes a more detrimental mutation that abolishes its interaction with Krev1. The second negative control uses empty bait and prey plasmids, which ensures that the plasmids are not active on their own without gene inserts. The final negative control is experiment specific. This control uses an empty prey plasmid as well as the bait plasmid containing *sgo-1* cDNA. This control ensures that the presence of the insert does not cause self activation of the bait plasmid. By comparing the results of the hits to the controls, one can roughly gauge the strength of the interaction.

Host cell mutations and multiple prey plasmids were sorted out by retransforming a fresh host cell with the isolated prey plasmids. Prey plasmid DNA from hits in question were first isolated in *E. coli* and then reintroduced into the host cell alongside the bait plasmid. The reporter assays were performed a second time to ensure the phenotypes read out were the same. Hits were further confirmed by switching prey and bait that showed positive interaction, transforming the new clones into yeast, and observing the results of the reporter assays. True

interactions were assigned only if reporter assays in this configuration produced consistent results.

4 Results

4.1 Neuronal expression of *sgo-1*

Shugoshin proteins are essential for cell cycle progression and gamete formation in a host of other organisms. Published and unpublished results from our and other laboratories using RNAi, two deletion mutants (*tm2443* and *tm2344*) and several uncharacterized base pair substitution mutants from the Million Mutant Project (MMP - http://genome.sfu.ca/mmp/) indicated that depletion of *sgo-1* in worms does not significantly impact viability or fertility (26). These observations, however, are not entirely conclusive. The *tm2443* deletion was originally described as a frameshift mutation due to a 7-base pair (bp) insertion in exon 5 followed by a 204 bp deletion that encompasses intron 5 and 13 bp of exon 6 (National Bioresource Project – NBP, Japan). The predicted SGO-1^{tm2443} protein lacks the conserved basic C-terminal domain (*Sgo1* motif) associated in vertebrates with the interaction with phosphorylated histones and had been therefore assumed to represent the null *sgo-1* allele. Upon sequencing in our lab, however, the *sgo-1* cDNA from *tm2443* homozygous mutants indicated that the annotation for this allele was incorrect. In our hands, no insertion was present in the 3' of exon 5 of *sgo-1(tm2443)* cDNA clones, instead a 195 bp deletion of the entire intron 5 and 15 bp of the 5' of exon 6 was confirmed. This results in an *in-frame* deletion that predicts a putative protein missing 47 residues as compared to wild type SGO-1, but retaining intact N and C terminal domains (Figure 4.1). This discrepancy likely represents possible splicing alternative events taking place in the early descendants of the original deletion animals before locus stabilization. It remains possible, therefore, that the lack of overt phenotypes in *tm2443* worms, similarly to animals homozygous for *tm2344* (another *in frame* deletion in the same overall region) are explained by the weak loss-of-function effect of these mutations. When considered together with the limitations in RNAi

penetrance in worms, particularly in the germline and nervous system, these results raised concerns that the deletion mutants and RNAi-knock downs did not represent the null phenotype of *sgo-1*. In an initial attempt to bypass this issue and reveal the true functional implications of SGO-1 depletion in worms, two approached were taken: 1) isolation of a full gene deletion by CRISPR/Cas9 (see below) and 2) mapping the expression profile of *sgo-1* in *C. elegans* using transcriptional and translational reporters. If SGO-1 in worms participates in the same canonical processes of spindle attachment, cohesion protein and anaphase entry as is the case with other characterized Shugoshin homologs, I predicted that SGO-1 would be found exclusively in mitotically active cells and the knockout mutants would be inviable.

Exploring the transgenic technology in *C. elegans*, a transcriptional reporter was generated for *sgo-1* by fusing promoter sequences to a GFP cassette. A cassette containing 1.5 kb of the 5' sequence of *sgo-1* fused to GFP and stabilized by 3'UTR sequences of *unc-54* was injected into N2 worms, the wild type *C. elegans* strain. Lines stably transmitting *Psgo-1::GFP* extrachromosomal arrays were isolated and propagated. Live worms were viewed under a fluorescent microscope. With the exception of the mitotically proliferating germ cell population in the gonad, cells of adult *C. elegans* are finally differentiated. Since chromosomal arrays are generally silenced in the germline, it was expected that *Psgo-1::GFP* expression would be observed exclusively in dividing embryonic cells. Surprisingly, strong GFP signals were clearly observed throughout the nervous system of adult worms as well as in developing embryos. In particular, the neuronal cell bodies of the nerve ring in the head were found to fluoresce quite brightly, with the dendrites of these neuronal cells extending anteriorly to the tip of the head and posteriorly to connect to the ventral and dorsal nerve rings also visible (Figure 4.2). These results represented the first evidence of a Shugoshin homolog present in a fully differentiated cell

type and hinted on a possible hitherto uncharacterized function of Shugoshin proteins beyond cell division.

Transcriptional reporters do not inform on the sub-localization of proteins in cells. To understand to which neuronal compartment SGO-1 is targeted, a translational reporter approach was used. A fosmid carrying genomic sequences of *sgo-1* fused *in frame* to GFP (Transgeneome Project, Max Planck Institute - https://transgeneome.mpi-cbg.de/transgeneomics/index.html) was injected into N2 gonads and transgenic lines expressing SGO-1::GFP animals identified via the presence of a dominant phenotype (roller). Fluorescence in these animals was no longer detectable in the cell bodies or along the length of the dendrites of the neuronal cells but appeared restricted to the extreme tips of neurons that make up the sensory organs in the tip of the head (amphid) and tail (phasmid – Figure 4.2). The presence of SGO-1::GFP (as well as signals from a SGO-1::tdTomato expressing strain generated in the lab) in the head and tail regions corresponding anatomically to amphid and phasmids of hermaphrodites and in the sensory rays in male tails (Figure 4.3) strongly suggested that SGO-1, a protein known to regulate microtubule events in the context of the chromosome/spindle/centrosome, may be a ciliary protein in worms.

Cilia function is key to enabling a plethora of behaviours in worms, coupling environmental cues with a systemic neuronal response. If SGO-1 is required in the development, maintenance or function of ciliary structures in the head and tail, depleting *sgo-1* should elicit abnormal behaviours similar to other *bona fide* cilia mutants. Partnering with researchers in Dr. Michel Leroux's lab at Simon Fraser University, the response of *sgo-1(tm2443)* in several cilia-related behaviors were thus examined in detail. One such test relates to the ability of wild type worms to detect and avoid environments with high glycerol osmolarity. In these osmotic

avoidance tests, worms are placed in the middle of agar plates surrounded by an osmotic barrier generated with 8M glycerol (66). Wild type worms perceive the barrier and avoid crossing whereas mutants such as *osm-10* and *che-3* worms that are impaired in cilia-dependent sensory perception, ignore the high osmolarity barrier and transverse it freely. As observed in Figure 4.4, a higher percentage (>50%) of *sgo-1(tm2443)* worms, as compared to wild type N2 animals (20%), tend to cross the osmotic barrier.

Cilia function is also essential for entry into the dauer developmental program in response to dauer hormones (daumones) released during stressful environmental and metabolic conditions (67). In this context, cilia mutants are generally dauer-defective. Consistent with a chemo sensation impairment in *sgo-1* mutants, these animals also failed to enter dauer stage after a prolonged period of starvation (Figure 4.4). Importantly, the introduction of an untagged genomic *sgo-1* construct into *sgo-1(tm2443)* worms can rescue dauer formation in these animals. The results presented in this section place *C. elegans* SGO-1 in the cilia region of the sensory organs and functionally implicate it with cilia-dependent sensory perception at the phenotype level. Though these unpublished results were performed outside the context of this thesis's work, they provided a logical rationale and experimental framework for the investigations that I designed and carried out, as described in the next sections.

4.2 Embryonic localization of SGO-1

While cilia function and maintenance have been topics of intense research in *C. elegans*, little is known about the embryonic origins of amphids and phasmids. In part this is due to the lack of cilia proteins expressed during amphid formation. Because ciliated organs in vertebrates are difficult to access during development, the formation of amphids and phasmids in nematodes offers simpler models to dissect and ascertain the genetic basis influencing the neuronal

architecture involved in wiring a permanently ciliated organ. My work therefore concentrated in characterizing the patterns of SGO-1 localization during embryogenesis while investigating a possible developmental role of Shugoshin in building ciliated organs in worms.

Since the translational reporters generated in our lab yielded weak signals, an antibody approach was used. As indicated in Introduction 1.1, sequence homology between SGO-1 orthologs is minimal, and hence cross species antibody use is not expected to be a viable option. To solve this problem, a series of polyclonal and monoclonal antibodies as well as immunostaining of embryos expressing tagged SGO-1 proteins were applied. Embryos lack the impermeable cuticle found in larvae and adult worms, allowing for the use of antibody staining without harsh permeabilization procedures that disrupt tissue morphology (68). Using an affinity purified rabbit polyclonal antibody raised against a C terminal peptide of Shugoshin (see Figure 4.1), a spatial and temporal assessment of SGO-1 localization during embryogenesis was performed. This antibody recognized transgenic SGO-1 signals in the embryo (see below) and adult worms (not shown) in IF experiments, suggesting it was specific. Antibody signals were not observed in early embryonic stages (blastula and gastrula), in contrast to the clear centrosomal signals in mitotically dividing cells observed with tagged GFP transgenes (26). Antibody signals appear from mid embryogenesis onwards ("bean" to "pretzel" stages), which marks the transition from 1.5 to 3-fold embryonic growth. During these elongation steps, when neuronal migration of sensory neurons and wiring of sensory organs is taking place, three major embryonic domains were clearly identified using this antibody: 1) Structures along the developing anterior sensory depression (future sensilla), where many small foci can be seen dotting the area where the mouth will form (69). This signal extends anteriorly as the mouth region develops and by pretzel stage is observed anteriorly of known TZ proteins (see below).

This localization overlaps with the expected region of the main sensory organ primordium, the amphid (40). 2) Near the midgut region, where the excretory duct and pore form (61) and 3) in the posterior sensory depression in the tail region where phasmids and male rays will develop (31, Figure 4.5). Thus, the embryonic domains in which SGO-1 appears to load and the time of development, match those of the forming sensory structures in the head and tail. Detecting signals assumed to represent native SGO-1 in these structures, most notably the sensory depressions where neurons will migrate towards to form structures that terminate in sensory cilia (40), was consistent with the SGO-1::GFP localization in adult animals and explained the functional implication of this protein to sensory perception described above. A counterargument against SGO-1 identify for the signals detected using this antibody in wild type embryos arose when embryos with mutations in *sgo-1* were tested. In these embryos, including the two in-frame deletions and several uncharacterized point mutations, the embryonic domains described above marked by the α-SGO-1 antibody in wild type embryos were also observed (Figure 4.6). In addition, the SGO-1::GFP signals in embryos have been only described in centrosomes of dividing cells and were not confidently found in sensory depressions, though as mentioned, these native GFP signals are very dim and hard to assess. Because it seemed reasonable to expect that all *sgo-1* mutants produced SGO-1 proteins that could properly localize, these results were not sufficient to disprove the specificity of the antibody. The rationale was that this assessment would only be possible once a strain carrying a full gene deletion allele was available.

4.3 SGO-1 marks the contact point for dendrite extension in amphids

In the anterior sensory depression of 1.5-fold embryos, SGO-1, as marked by the antibody, can be seen in approximately twenty discrete structures along the developing head. This number is reminiscent of the pores for the growing ciliary channels that connect the cuticle

externally to the ciliary membrane of sensory dendrites internally. This finding raised the exciting possibility that SGO-1 marks the interface where migrating sensory neurons must dock and anchor to extend the ciliary channels during amphid development. To confirm the SGO-1 localization near the dendrite-cilia junction, worms were injected with a translational construct for the neuronal protein DYF-7 fused to GFP and then stained for SGO-1 (α-SGO-1) and DYF-7::GFP (α-GFP). As can be seen in Figure 4.7, SGO-1 and DYF-7::GFP signals appear juxtaposed. In fact, it would seem as though the SGO-1 domain almost wraps around the DYF-7::GFP signal, forming a sort of doughnut shaped channel for the dendritic tip to pass through and terminate. This is interesting, as DYF-7, in conjunction with another extracellular matrix protein, DEX-1, has been proposed to be involved with sensory dendrite anchorage during embryogenesis as stated in the Introduction. As expected, DEX-1::mCherry signals in the anterior sensory depression recapitulate the close association observed for SGO-1 and DYF-7-occupied domains (45, Figure 4.7 C). Overall, these results putatively placed SGO-1 in the base of the developing cilia during a critical junction during amphid development and suggested that SGO-1 may be involved in sensory neuron anchoring.

4.4 SGO-1 occupies specific cilia domains

The primary cilium is a complex structure made up of functionally different sub-domains (Figure 1.6). To narrow down possible functions of SGO-1 in the cilia, the location of the α-SGO-1 signals relative to other cilia proteins was investigated using strains carrying fluorescent constructs for sub-domain specific proteins. Because no other known cilia protein loads as early as 1.5 stage, these experiments had to be done looking at developed amphids from late embryos and adults. The transition zone protein CCEP-290 was found to localize posteriorly to SGO-1 in developing amphids, as can be seen in Figure 4.8. While some points of near contact can be

seen, SGO-1 for the most part seems to be more anterior than CCEP-290. It is important to note in late embryogenesis, the α-SGO-1 signals are observed more anteriorly in the amphid, around the tip of the nose. In adults expressing *sgo-1* transgenes, SGO-1 signals are detected in a more posterior position again, closer to the base of the cilium. This is clearly observed relative to the axonemal dynein heavy chain protein CHE-3, which in adult cilia appears anterior to SGO-1::GFP (Figure 4.8). These differences could indicate a shift in the cilia domain occupied by SGO-1 from early to late embryogenesis and again in adult cilia. Conversely, this could also be explained by a technical artifact of the antibody and/or transgene themselves.

4.5 SGO-1 is compartmentalized to the cilia channel in the late embryo

The cilia of amphids extend from the sensory dendrite harboring the basal body to the cuticle where it contacts the outside environment in order to access external cues (40). Glial cells surrounding the cilia prevent the outside environment from spilling into the worms, and vice versa. This is accomplished through the formations of adherens junctions between the glial cells, the cuticle and the dendrites themselves (40). This result is a pocket that houses the dendrites as they transition into cilia, with a channel extending out to the environment. To situate the SGO-1 domain in the developing cilia relative to the surrounding cells, embryos were co-stained with α-SGO-1 and an antibody against the adherens junction complex protein, AJM-1. As shown in Figure 4.9, SGO-1 signal runs along walls of AJM domains, representing the boundaries of the pocket. The smaller foci of α-SGO-1 signals that can be seen dotting the edge of the sensory depression may be marking other sensilla that are not innervated to the extent of the amphid. Interestingly, the compartmentalization in the amphid can also be found in the excretory pore. There, AJM-1 seems to form a ring around α-SGO-1 signals as it passes through (Figure 4.9). From a development standpoint, the morphogenesis of the amphid and the

excretory pore share similar genetic instructions necessary to form these tubular structures (61). These results, in combination, suggest that SGO-1 may be present in the ciliary channel of developing amphids, likely along the axoneme and/or in the transition zone, consistent with the results with SGO-1::GFP and SGO-1::tdTomato in the adult sensory organs (Figures 4.2 and 4.8).

During development, polarized cells have to spatially re-organize and re-position subcellular structures in the proper manner. The partitioning (PAR) proteins provide cells with a sense of polarity, allowing for identification of apical or basolateral surfaces (32). Aside from regulating early asymmetric cell divisions, PAR proteins also play a role in cell migration, gastrulation and epithelial tissue differentiation through their interactions with the cellular cytoskeleton (32). These PAR-related functions are particularly relevant during gut epithelium morphogenesis, which connects to the putative mouth in the anterior sensory depression. In fact, PAR-3 and PAR-6 have also been reported to localize in what appear to be non-gut cells around the mouth in a pattern similar to SGO-1, though their function in this context has not been explored (35, 70). Considering PAR-3/6's role in regulating apical junctions in epithelia and their nearby localization in and around the sensilla, it was important to clarify whether, as SGO-1, these proteins are present in the pocket. Indeed, PAR-3/6 are detected lining up the posterior cup-shaped end of the pocket with SGO-1 running through the channel (Figure 4.10). The similarity between this disposition and the one observed with AJM-1 suggested that PAR proteins are marking the same structures, likely the glia cell walls. As with other proteins in the cilia tool kit, SGO-1 and PAR-6 also appear together at the excretory duct (Figure 4.10).

4.6 Genetic requirements for SGO-1 loading in the developing amphid

The sections above revealed specific domains in the developing cilia where α-SGO-1 signals are detected, suggesting SGO-1 could have a determinant role in cilium morphogenesis. To explore genetic dependencies of SGO-1 activity, the localization of α-SGO-1 signals in these domains were checked in null mutants in which the structure of the cilium is known to be disrupted. CCEP-290 helps stabilize the microtubules of the sensory cilia (71). In *ccep-290* mutant embryos, however, α-SGO-1 signals are normally present (Figure 4.11). Disturbing the organization of the cilia microtubules is therefore not sufficient to abolish SGO-1 loading. To investigate if further disrupting the transition zone could impact the correct localization of α-SGO-1 signals, a triple mutant with mutations disrupting all three transition zone protein complexes was analyzed. Strain DAM543 has mutations in three core TZ subdomain proteins (CCEP-290, NPHP-4 and MKSR-2), the combination of which results in a complete loss of the transition zone (71). While cilia formation was found to be normal in these mutants, they fail to extend into the amphid channel (71). As observed in Figure 4.11, α-SGO-1 signals can still be found in the head region of developing embryos. While disruption of all TZ domains prevents cilia from inserting into the amphid channel, cilia are still formed in these mutants. To determine if the complete absence of cilia would affect α-SGO-1 signals, embryos from *daf-19* homozygous mutant embryos were examined (strain DR1720). *daf-19* is the master transcription regulator involved in coordinating the expression of several key cilia genes and in DAF-19-depleted animals, cilia are absent (72). Surprisingly, α-SGO-1 signals in *daf-19* embryos was not disrupted (Figure 4.11), and is normally detected in the sensory depression, excretory duct and phasmid. These results suggested that the formation of cilia may not be a requirement for SGO-1 localization. Cilia are not the only structures present in the amphid. There are also glial

cells which form the lumen that houses the cilia as they transition to the outside environment. This lumen requires the action of patched domain containing protein 1 homolog DAF-6 to properly form and bundle the cilia together (41). In *daf-6* mutants (CB1377), however, α-SGO-1 signals in the embryo were again similar to those observed in wild type embryos. These results were confounding, as the initial expectation was that cilia or pocket malformations would likely disrupt SGO-1 loading. However, it is possible that SGO-1 association to these regions happen independently of the formation of cilia and channel.

If neither the cilium itself nor the adjacent pocket are critical to SGO-1 loading in these regions, perhaps SGO-1 relied on extra-cellular matrix signals to properly access these embryonic regions. As described above, α-SGO-1 signals appear to first load to the region in early bean stage when migrating sensory neurons are reaching their targets in the anterior sensory depression. Therefore, I checked if the appearance of α-SGO-1 signals relied on cues provided from these neurons in the dendritic membrane as guiding cues. DYF-7 and DEX-1 are conserved regulators of amphid development where they mediate dendrite anchorage and retrograde extension (45). DYF-7 and DEX-1 also share close association with SGO-1 domains in the sensory depressions and excretory channel regions. Indeed, when embryos lacking DYF-7 (SP1735 strain) were examined, no detectable α-SGO-1 signal was observed in the depressions or the excretory channel. This was found in both early (bean) and late (3-fold) embryonic stages (Figure 4.11). These results indicate a requirement of DYF-7 presence for α-SGO-1 signals to appear in the embryo suggesting a genetic interaction between *dyf-7* and *sgo-1* that could reflect, considering the localization of these proteins in the depression (Figure 4.7), by a direct protein-protein association, though this has yet to be determined.

4.7 A genetic null allele raises questions about the α-SGO-1 antibody specificity

An important constraint in the characterization of potential SGO-1 functions in embryos had been the lack of a true *sgo-1* null mutant which also prevented adjudicating the specificity of the α-SGO-1 antibody. Indeed, the α-SGO-1 embryonic signals detected in IFs are not disrupted in the existing *sgo-1* mutants (Figure 4.12), potentially because SGO-1 carrying the C-terminal domain against which the polyclonal antibody was generated was produced and correctly localized in these embryos (Figure 4.1). To complicate matters further, neurons are extremely recalcitrant to RNAi in worms, such that post-transcriptional knock downs were not effective as a strategy to verify the specificity of the antibody. The localization to ciliary structures in the embryos in IFs using this antibody is consistent with behavioural phenotypes observed in *sgo-1* mutants and the localization of SGO-1 transgenes in adult animals. However, the lack of centrosomal signal in wild type embryos and the presence of signals in IFs using *sgo-1* mutant embryos raised the possibility that this reagent was in fact detecting a cross-reacting antigen in embryos, different than SGO-1. It is important to mention that though the rabbit antibody fails to detect native centrosomal SGO-1 in embryonic cells, it recognizes the robust signal from overexpressed SGO-1::GFP and HA::SGO-1 in embryonic centrosomes as previously described (26, Figure 4.13), suggesting that some anti- SGO-1 IgGs is indeed present in the polyclonal antibody.

Since this thesis work started, several high efficiency CRISPR/Cas9 protocols for *C. elegans* have been described. Though a few uncharacterized *indel* alleles in the *sgo-1* locus were generated in the lab, ultimately a complete gene deletion was commissioned from Sunnybiotech (China). A homozygous [*sgo-1(sas02)*] line with a deletion of the entire coding *sgo-1* genomic locus (first ATG to TGA) was produced (Figure 4.12). Sequencing of the *sgo-1* locus in *sas02*

worms verified the deletion. Homozygous *sgo-1(sas02)* animals are viable and showed no overt embryonic lethality or increased male frequency (Him phenotype), consistent with other *sgo-1* mutants and supporting the proposed non-essential role for this gene. However, whether *sas02* worms display cilia defects and how these compare to chemosensation impairments observed in *tm2443* animals needs to be confirmed to better characterize the null *sgo-1* phenotype. Importantly, *sgo-1(sas02)* embryos showed the same sensory structures when stained with the polyclonal α-SGO-1 antibody (Figure 4.12). These results definitively proved that the sensory structures highlighted by this antibody in the embryo and discussed in the sections above as representing native SGO-1 signals are in fact not formed by SGO-1, but another unknown ciliogenesis-related protein.

4.8 Searching for the true embryonic SGO-1 localization

The *sas02* results threw in doubt the assessment of SGO-1 functions during amphid development, though at the same time opening an opportunity for future reverse characterization of a potentially novel gene acting in amphid development. At this point, it was important to clarify the correct SGO-1 localization in embryos. For that, a new transgenic strategy was devised. C-terminal SGO-1 fusions with fluorescent proteins revealed weak signals in embryos that rapidly photobleached, complicating imaging. These signals, however, were only observed in centrosomes and never recapitulated the antibody structures observed in the sensory depressions, consistent with the results captured with the new knockout *sgo-1* mutant. To address the signal intensity issue, as well as the potential functional disruption of SGO-1 localization by a C-terminus GFP cassette, as the reasons for these differences, worms carrying a N-terminus human influenza hemagglutinin (HA) tag fused to SGO-1 were generated and HA::SGO-1 detected in fixed embryos using an α-HA antibody. The differences between the α-

SGO-1 images and the α-HA::SGO-1 images are striking. The α-HA::SGO-1 antibody did not display any detectable signal in the sensory depressions or excretory pore region as marked by the α-SGO-1 antibody. Instead, and consistent with SGO-1::GFP localization in live embryos, α-HA::SGO-1 signals could be seen coating chromosomes and loading onto centrosomes of dividing cells (Figure 4.13). This is reminiscent of the mitotic localization of vertebrate Shugoshin in kinetochores (which in *C. elegans* spreads along the whole length of chromosomes) and centrosomes, suggesting that in worms, as in other systems, SGO-1 may retain some function in mitotic chromosome segregation, albeit not essential. What exact functions these would be require further in-depth investigations.

4.9 Screening for SGO-1 interacting proteins

The data implicating SGO-1 in cilia localization and function in the adult did not involve the use of the antibody and therefore did not need to be re-interpreted in view of the null mutant IF results. Together with the HA::SGO-1 localization studies, these results clarified the true localization profiles of SGO-1 in embryos (centrosomes, spindle and chromosomes in mitotic cells) and adults (basal body and axoneme in ciliated neurons). As a reasonable follow up step to reveal the possible mechanisms of SGO-1 action in the context of mitotic cells and ciliated neurons, a yeast two-hybrid approach was used. Interacting proteins were identified by screening a cDNA prey library constructed from mRNA extracted from a mixed population of *C. elegans* (which contains embryos at various stages as well as larvae and adult worms) and using the entire *C. elegans* SGO-1 protein as bait. Of the 5.78×10^6 cells screened, five hundred potential positive hits were obtained. A subset of sixteen of these positive hits was subject to the reporter assays described in the Appendix section R. Confirmed positive hits were then sequenced, and a basic local alignment search tool (BLAST) search performed against a National

Center for Biotechnology Information (NCBI) database of *C. elegans* genes. Subsequently, thirty-four potential positive hits were subject only to sequencing reactions, for reasons described below.

4.10 Identification of hits

Of the initial sixteen potential positives hits that were assayed, fourteen of them were confirmed as positive interactions by completing the reporter assays described in the Materials and Methods and Appendix R sections. All fourteen were sent for sequencing with prCC333 forward primer and prCC335 reverse primer and the results entered into a BLAST search. These primers anneal to the backbone of the vector, flanking either side of the recombination site but outside of the recombination region. All fourteen clones were found to contain the entire cDNA sequence of the *C. elegans* transforming acid coiled coil (TACC) homolog *tac-1* as the insert (Figure 4.15). Although a single forward sequence read did not contain the entire *tac-1* sequence, a combination of forward and reverse reads was able to place the entire cDNA sequence within one clone. The remaining two false positive hits that were unable to pass all three reporter assays were also sequenced to confirm they were indeed false positives. These two hits were found to have the sequence for the *C. elegans* ribosomal protein *rpl-22*. Ribosomal proteins have been shown to frequently occur as false positives due to their inherent "sticky" nature that allows them to interact with a broad range of other proteins (73). To check for saturation of the screen, hits were subject directly to sequencing to reduce redundant colony testing. Untested *tac-1* clones were assumed to respond equally to the reporter assays. In total, thirty-four extra potential positive hits were sequenced, and all were found to contain *tac-1* sequences. A representative set of reporter assay results can be found in Figure 4.14.

The independent isolation of multiple *tac-1* clones suggested this is not a false positive interaction. At the same time, the lack of other hits raised the question of reduced library complexity and ubiquitous cDNA overrepresentation. To confirm the interaction with TAC-1, bait and prey inserts were switched. A bait *tac-1* construct and a prey *sgo*-1 construct were introduced into a yeast cell and the resultant colonies subjected to the reporter assays. Along with this retransformation, a new *tac-1* bait/empty prey control was also generated. Since the bait vector was changed, there also needed to be a change in the negative control containing the bait plasmid and an empty prey plasmid to ensure the bait alone did not interact with the prey plasmid itself. To confirm the false positive nature of the *rpl-22* hit, and the functionality of the assay, *rpl-22* was also retransformed as a prey vector and allowed to interact with the new *tac-1* bait. These interactions were confirmed with the retransformation assay, as can be seen in Figure 4.16.

In summary, these results revealed a previously uncharacterized interaction of SGO-1 with the a TACC family member. TAC-1 represents the first SGO-1-interacting protein in worms, though this association needs to be confirmed *in vivo* using protein lysates. Whether this interaction is functionally relevant to SGO-1 in centrosomes, where TAC-1 is required for spindle growth, and/or in the cilia, where TACC functions have not yet been reported in any system, requires further work.

4.11 Results figures

Figure 4.1

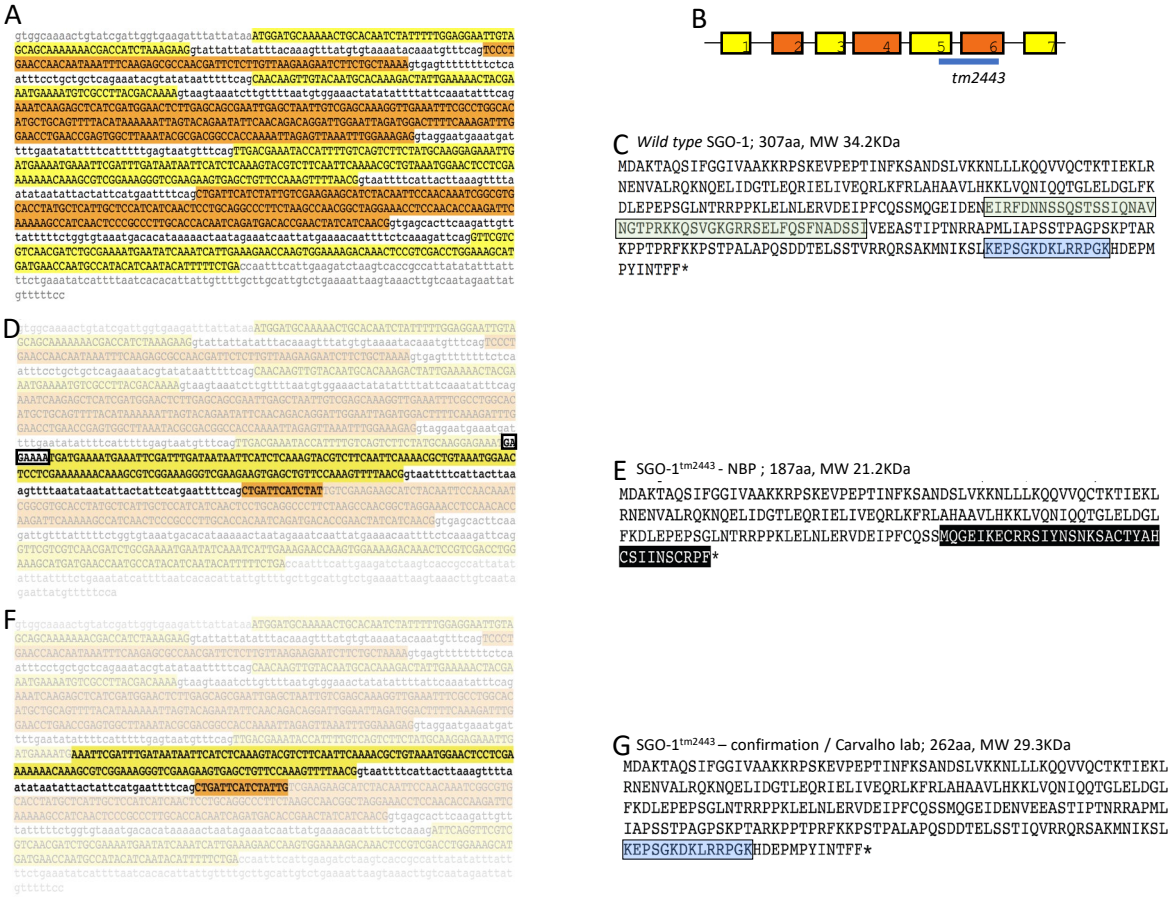

Figure 4.1: *sgo-1* sequences

A) Wild type *sgo-1* (C33H5.15 cosmid sequence) genomic locus. B) Diagram of genomic locus. Exons are shown as numbered boxes. The location of the *tm2443* deletion, presumed initially to be a frameshift allele, is shown by a bar underneath. C) Conceptual translation of the WT SGO-1 protein. Sequence highlighted in green shows deleted region confirmed in *tm2443* (see G below). Blue highlight marks the protein region used to generate the C-terminal rabbit polyclonal antibody characterized in this study. D) Reported tm2443 allele (NBP-Japan). The upstream and downstream boundaries of the reported deleted region are faded. The putative 7bp insertion is boxed, followed by the remaining portion of exon 5 (yellow highlight), intron 5 and start of exon 6. E) The predicted protein based on the NBP-reported *tm2443* deletion. A frameshift caused by the insertion substitutes the wild type C-terminus peptide (including the antibody recognition region) with an aberrant 34 residue before a stop codon in position 188 (black highlight). F) The resolved *tm2443* genomic region. Cloning and sequencing of *sgo-1* cDNAs from *tm2443* clarified the correct deletion in these mutants. No insertion was observed in exon 5. The deletion takes out most of exon 5, all intron 5 and the first 15bp of exon 6 but does not alter frame. G) The corrected prediction for SGO-1^{tm2443} sequence. A 47 residue region in the center of the protein (marked in green in C) is absent. Note that the C-terminal domain is not affected and carries the antibody peptide region. Exons are highlighted in alternating orange and yellow and are also denoted by uppercase letters.

Figure 4.2

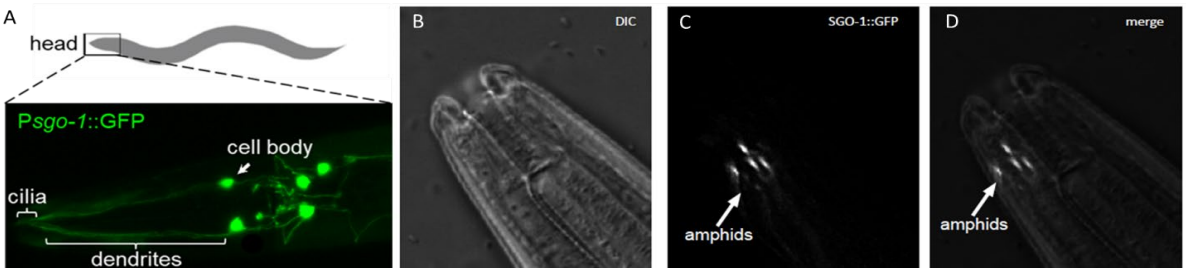

Figure 4.2: Expression of *sgo-1* and subcellular localization of SGO-1::GFP in adult worms

A) Diagram of an adult worm (anterior-left, posterior-right). The amphid region located in the tip of the head region is marked by a box. Live zoomed image of the corresponding head region of a worm expressing P*sgo-1*::GFP is shown in the bottom. The cell bodies of the sensory neurons are identified in the nerve ring more posteriorly. Dendrites from these neurons extend anteriorly to the end in the cilia region, also marked. B-D) Amphid region in worms expressing SGO-1::GFP. The tip of the mouth is visible in the top left of the panel in the DIC image. In these optical sections, SGO-1 signals are observed in amphids located in the ventro-lateral side.

Figure 4.3

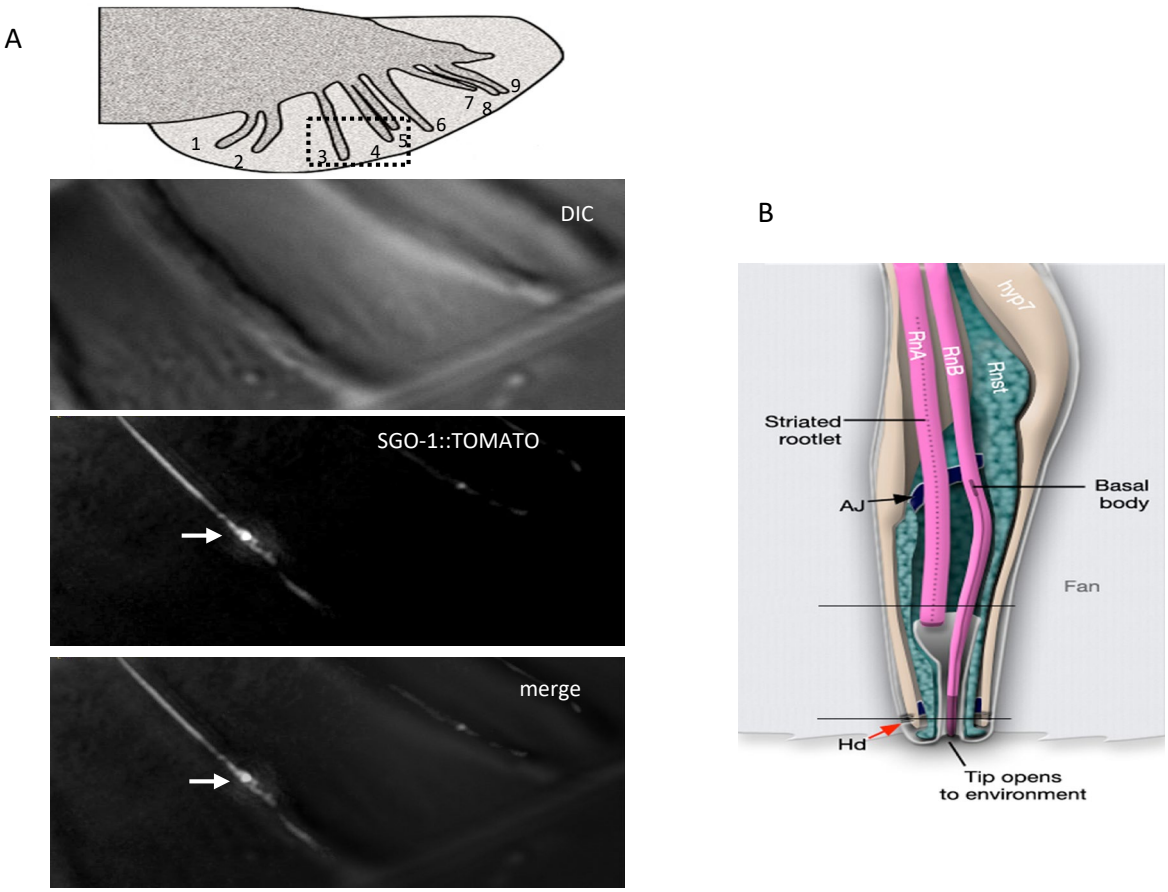

Figure 4.3: SGO-1::tdTomato is present in sensory rays of male tails

A) Lateral view diagram of a male tail with the 9 rays indicated (modified from Wormbook®). The corresponding region imaged in the panels below is boxed. Males expressing SGO-1::tdTomato driven by a cilia promoter (*Posm-5*) is shown below. Note the accumulation of SGO-1::tdTomato past the midsection point of the ray, where the basal body is located. B) A diagram of a ray, with the basal body position indicated (Wormbook®). Top-proximal, bottom-distal. The dendrites from RnA,B neurons are shown in pink. AJ- Adherens junctions; Hd- hemidesmosomes; hyp- hypodermal cells.

Figure 4.4

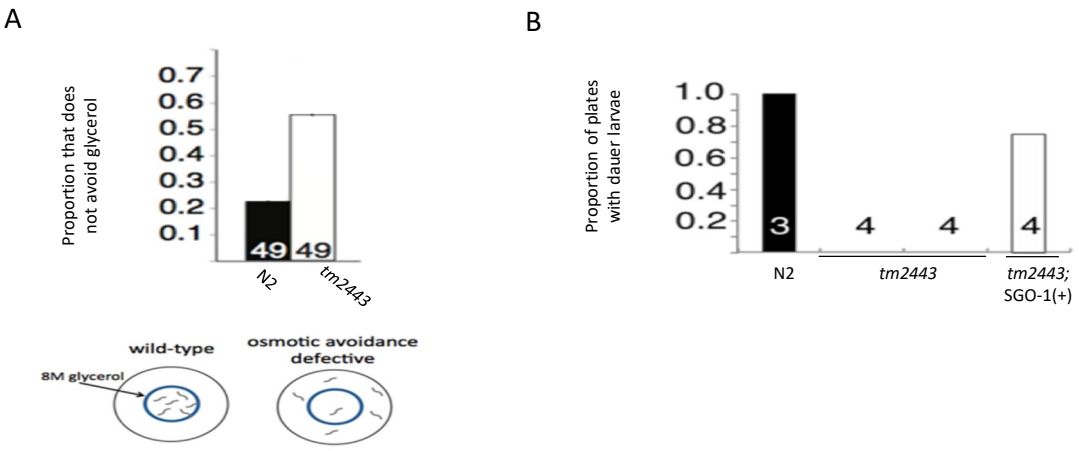

Figure 4.4: Depletion of *sgo-1* results in *bonafide* cilia mutant phenotypes

A) Osmotic avoidance behaviour in wild type (N2) and *sgo-1(tm2443)* worms. Three replica experiments with n=49 worms are represented. B) Dauer formation in starved plates. Plate numbers in each experiment are shown in the bars. A genomic rescue construct (SGO-1+) restored dauer formation in a *tm2443* mutant background (far right bar). Unpublished results from Tiffany Timbers.

Figure 4.5

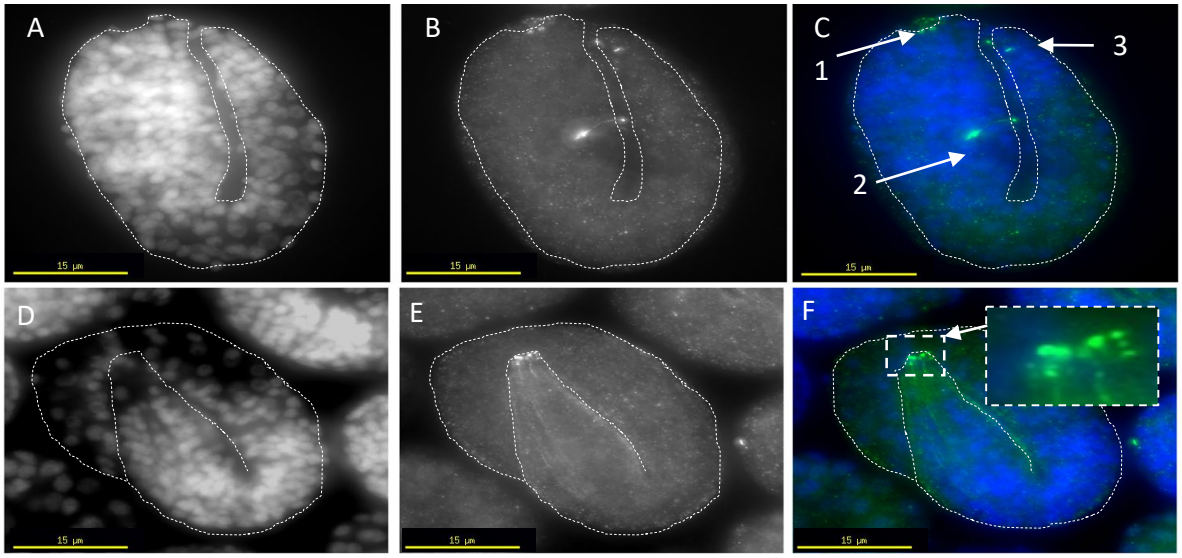

Figure 4.5: WT embryos stained with α-SGO-1

A-C) A 1.5-fold embryo. Arrow 1 shows the position of the anterior sensory depression, arrow 2 the excretory pore and arrow 3 the putative phasmid region. D-F) A 3-fold embryo. The developing head region is highlighted in the inset. Signal is seen in the tip. Blue-DAPI; green-α-SGO-1.

Figure 4.6

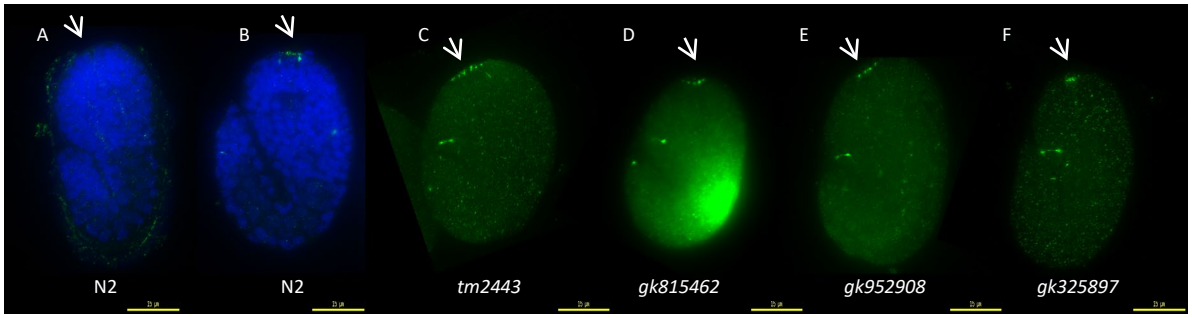

Figure 4.6: α-SGO-1 detects signal in *sgo-1* mutant embryos

1.5-fold embryos stained with a pre-serum (A) and α-SGO-1 (B-F) are shown. Wild type embryos (A and B) were also stained with DAPI. tm2443 is a 195 base pair deletion mutation predicting a shorter, *in frame sgo-1* cDNA. All other mutants are missense nucleotide substitutions: The *gk815462* allele (strain VC40793) is a C>T transition predicting a D288N modification. *gk952908* (strain VC200007) is a G>A transition predicting a P27L modification as *gk325897* (strain VC20450) which predicts a P242S modification (Million Mutation Project - http://genome.sfu.ca/mmp/search.html). Arrows indicate the anterior sensory depression region where α-SGO-1 can be observed.

Figure 4.7

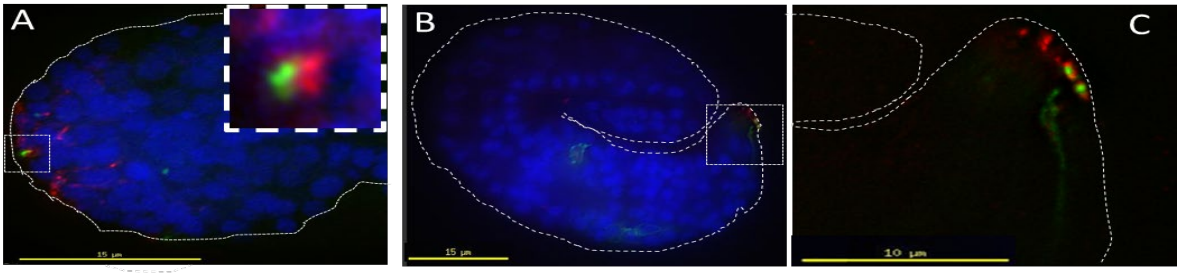

Figure 4.7: α-SGO-1 signals are juxtaposed to the dendrite anchorage proteins DYF-7 and DEX-1 in the anterior depression region

A) A 1.5-fold embryo. Marked region zoomed in in the inset. Green-α-SGO-1; red-DEX-1::mCherry (using α-RFP); blue-DAPI. B) A 3-fold embryo. Red-α-SGO-1; green-DYF-7::GFP (using α-GFP); blue-DAPI. C) Same embryo as in B, under higher magnification highlighting the proximity of SGO-1 and DYF-7::GFP. (marked box in B).

Figure 4.8

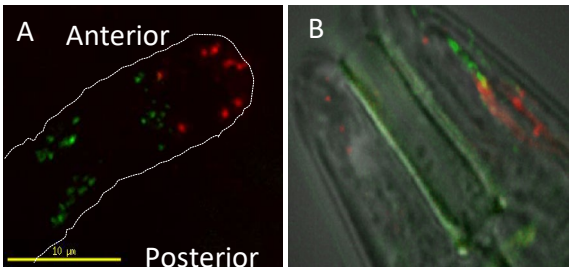

Figure 4.8: α-SGO-1 signals appear in close contact with known cilia proteins

A) IF of the head region of a 3-fold embryo (top right-anterior) showing CCEP-290::GFP (using α-GFP) in green and α-SGO-1 in red. B) Live fluorescence image of the head in an adult worm showing CHE-13::GFP in green and SGO-1::tdTomato in red.

Figure 4.9

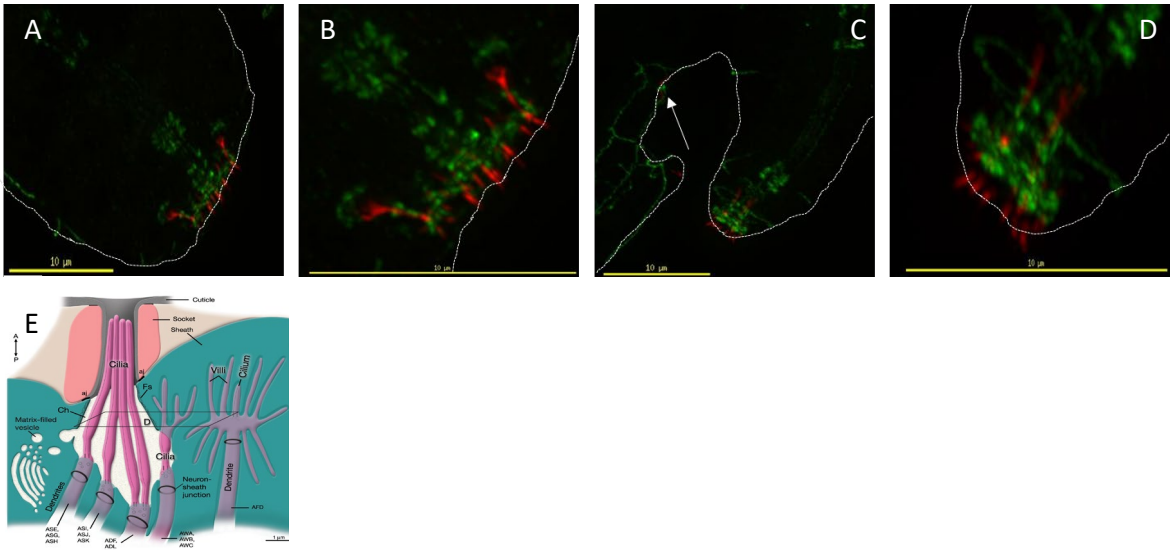

Figure 4.9: α-SGO-1 signal insert in between a cellular pocket defined by adherens junctions in adjacent glia cells in the developing amphid

A) A 1.5-fold embryo stained with α-AJM-1 in green and α-SGO-1 in red. B) A different optical place from the same embryo as in (A), to highlight the pocket. C) A 3-fold embryo showing α-AJM-1 in green and α-SGO-1 in red. Note the "channel" of AJM-1 through which α-SGO-1 seems to go through. The arrow marks the location of the excretory pore. D) A magnification of the same embryo as in (C), to highlight the pocket. E) Illustration of the amphid glial cells forming the amphid channel (Wormbook®). The socket cell is shown in pink and the sheath cells in green.

Figure 4.10

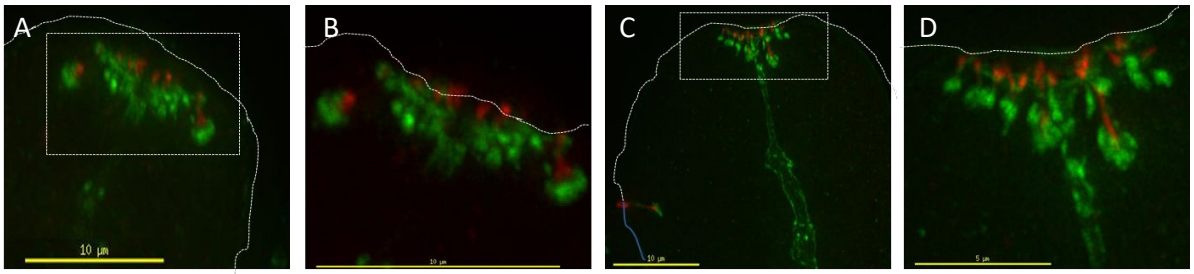

Figure 4.10: PAR proteins delineate the developing pocket defined by the presence of α-SGO-1 signals

IF 1.5-fold embryos expressing *par-3::GFP* (A) or *par-6::GFP* (C) transgenes. A) PAR-3::GFP signal in green (using α-GFP) and α-SGO-1 in red. B) Zoom in of the inset in (A). C) PAR-6::GFP is seen in green (with α-GFP) and α-SGO-1 in red. D) Zoom in of the inset in (C). Note the signal near the excretory duct also seems compartmentalized, as in the sensory depression (arrow).

Figure 4.11

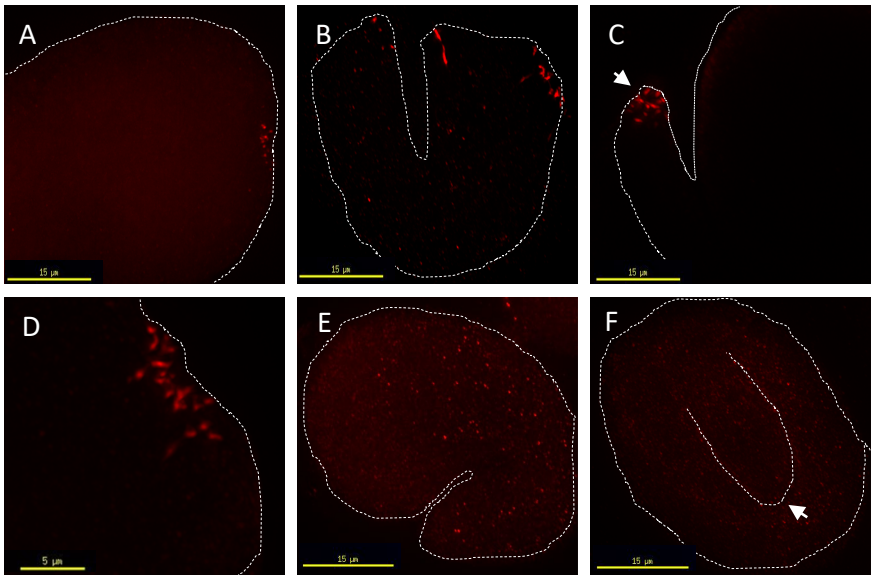

Figure 4.11: α-SGO-1 signals in the sensory depression/head of cilia mutant embryos

A) A 1.5-fold embryo of a *ccep-290* mutant with normal α-SGO-1 signals. B) A 1.5-fold embryo of a *daf-19* mutant showing α-SGO-1 signal in the sensory depression, excretory pore, and phasmid. C) A 3-fold embryo of a *nphp-4;mksr-2;ccep-290* triple mutant showing α-SGO-1 signal in the developing head region. D) A 1.5-fold embryo of a *daf-6* mutant showing α-SGO-1 signal in the sensory depression. E) A 1.5-fold embryo of a *dyf*-7 mutant showing absence of α-SGO-1 signal in the sensory depression, excretory duct and phasmid. F) A 3-fold embryo of a *dyf*-7 mutant showing an absence of α-SGO-1 signal in the developing head region. α-SGO-1 signal is shown in red. Arrows indicate the anterior sensory depression (1.5-fold embryos) and head region (late 3-fold region).

Figure 4.12

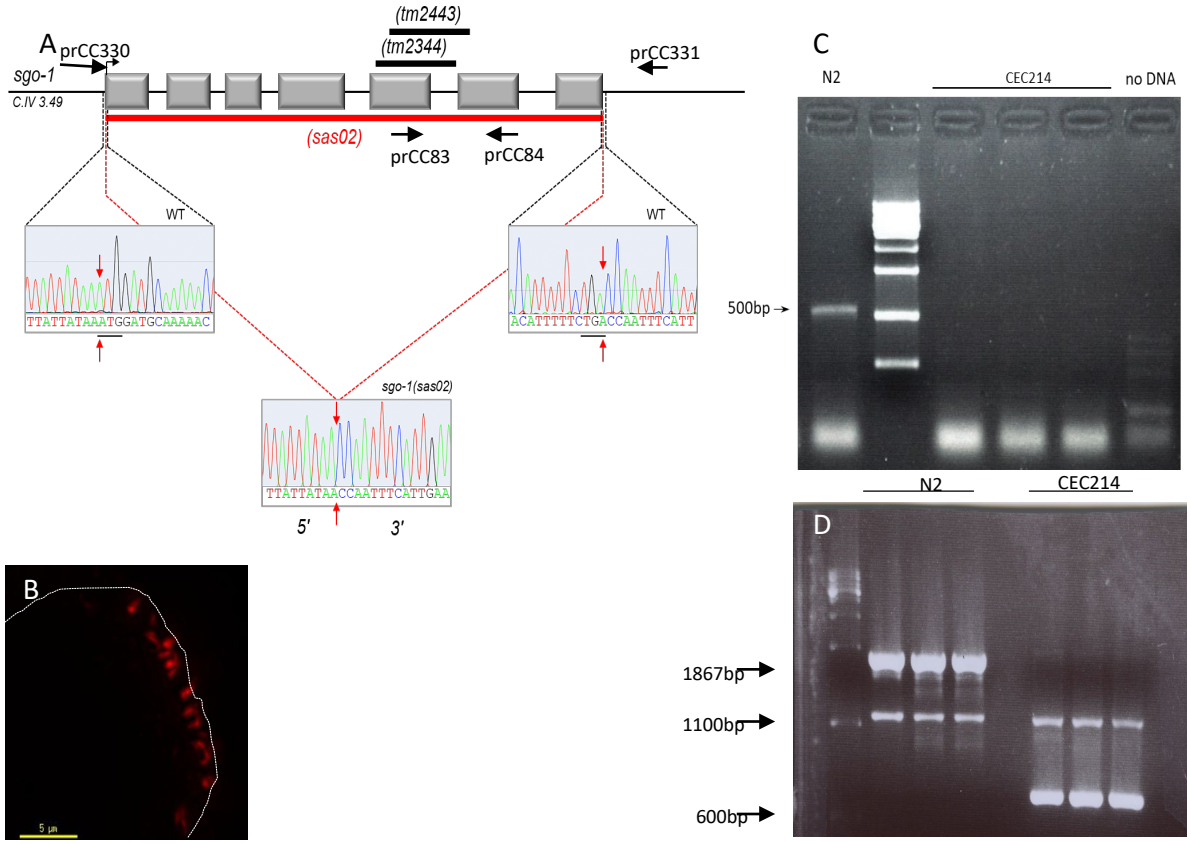

Figure 4.12: α-SGO-1 signals are not lost in *sgo-1(sas02)* null embryos

A) Diagram depicting the region of *sgo-1* deleted using CRISPR/Cas9 editing. B) A *sgo-1(sas02)* embryo (1.5-fold stage) showing normal α-SGO-1 signals in the sensory depression. C) Single worm PCR of wild type (N2) and *sgo-1(sas02)* worms using prCC83 and prCC84. The predicted amplicon in N2 worms is 500 bp, and this locus should be missing in *sgo-1(sas02)* worms. D) Single worm PCR of N2 and CEC214 using prCC330 and 331. The wildtype locus is 1879 bp and the null locus is 600 bp. A nonspecific band can be seen at 1100 bp.

Figure 4.13

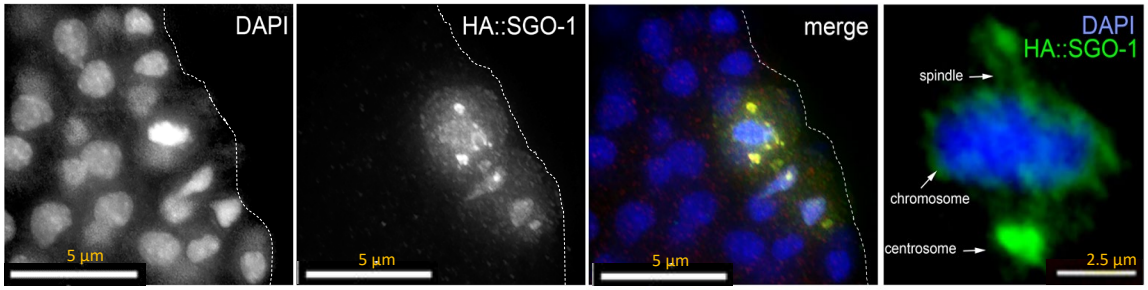

Figure 4.13: HA-SGO-1 is detectable only in mitotic cells of the embryo
IF of an early embryo expressing HA::SGO-1 using an α-HA antibody. HA::SGO-1 in observed in mitotic figures where it marks metaphase (top cell) and anaphase (bottom cell) chromosomes (presumably at kinetochores), centrosomes and the spindle. Later during gastrulation HA::SGO-1 signals are not seen in the sensory depressions (not shown).

Figure 4.14

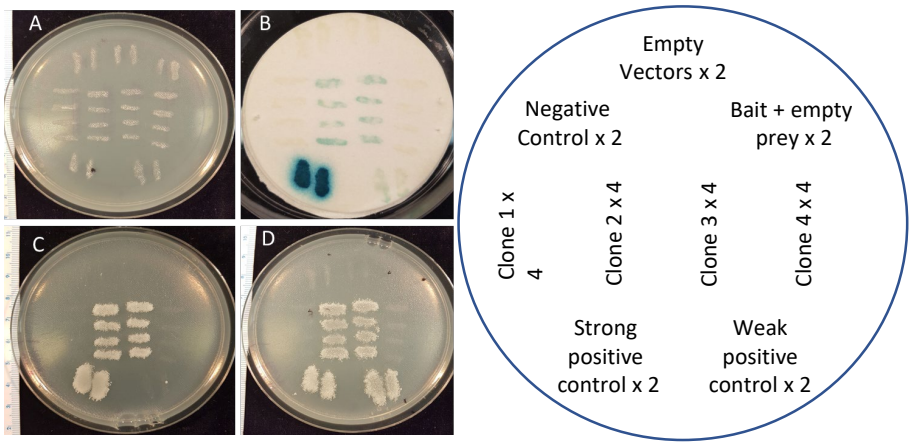

Figure 4.14: TAC-1 interacts with SGO-1 in a yeast two-hybrid assay

Representative growth response selection and reporter assay tests in a yeast two-hybrid screen using full length SGO-1 as the bait. A guide is provided in the right. Initial screening plate before identification of hits. A) Master plate of non-selective media used to replicate colonies onto the assay plates. B) LacZ assay filters after 24 hours. C) Growth on selective media without uracil. D) Growth on selective media with 10mM 3AT added and without histidine.

Figure 4.15

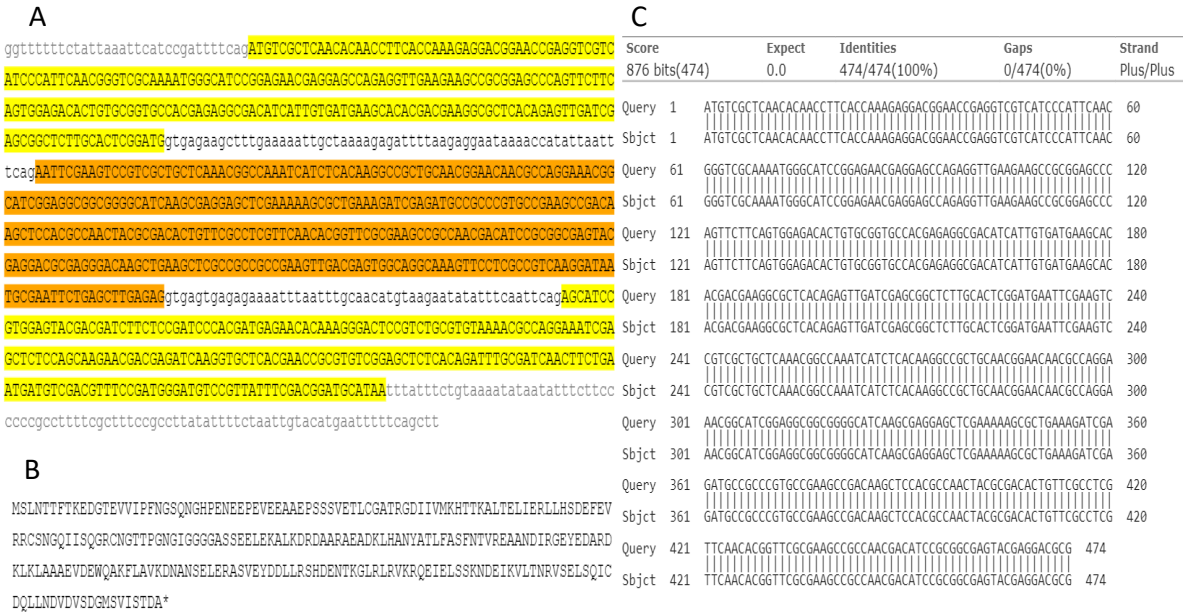

Figure 4.15: TAC-1 coding sequence and alignment

A) Wild type *tac-1* (Y54E2A.3.1 cosmid sequence) genomic locus. Exons are highlighted in alternating orange and yellow while also being in uppercase. B) The predicted translation of the *tac-1* sequence. C) BLAST alignment of a positive hit with the cDNA sequence of *tac-1*. Query is the cDNA sequence submitted for analysis and subject is the sequence the query was aligned to.

Figure 4.16

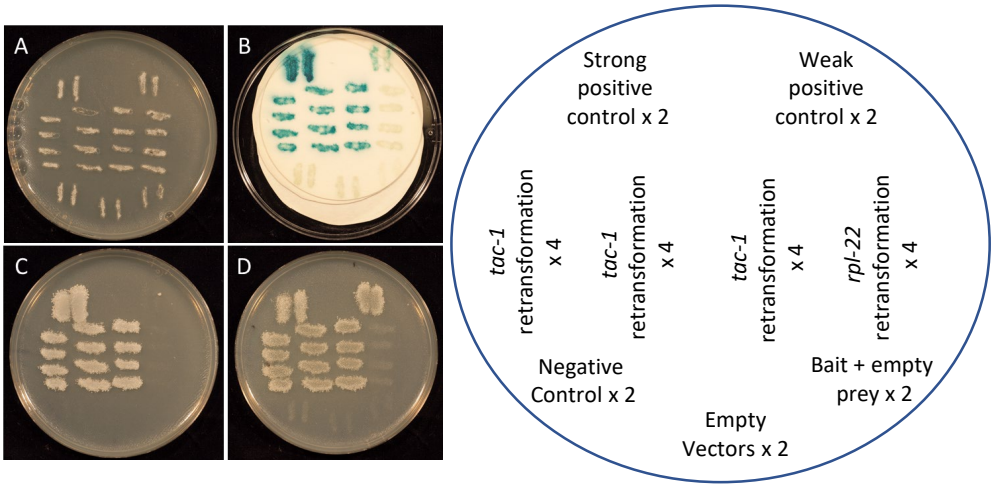

Figure 4.16: Confirmation of TAC-1/SGO-1 binding by reversing bait/prey clones

Growth response selection and reporter assay tests in a yeast two-hybrid screen using full length TAC-1 as the bait and SGO-1 as the prey. A guide is provided in the right. A) Master plate of non-selective media used to replicate the colonies onto the assay plates. B) LacZ assay filter after 24 hours C) Growth on selective media without uracil. D) Growth on selective media with 10mM 3AT added and without histidine.

5 Discussion

5.1 SGO-1 is a cilia protein

Since the isolation of MEI-S332 mutants in *Drosophila*, Shugoshin proteins have been shown to be nearly universally important for cell cycle progression from yeast to humans. The understanding on how Shugoshin mediates proper chromosome segregation in meiosis and mitosis has had tremendous implications in explaining crucial differences in the mechanics and outcomes of these two very different cell divisions. These studies, however, were conducted in organisms that share the same chromosomal architecture, where focalized chromosomal attachment and kinetochore assembly is possible because of the presence of a single centromere. *C. elegans* represents a paradigm shift in this respect, as chromosomes in these worms, while using a similar regulatory toolkit and enzymatic apparatus to modulate cohesion, cannot rely on spatial information provided by the centromere.

The mechanism through which *C. elegans* removes cohesin from chromosomes in meiosis has been shown to be Shugoshin-independent, though recent evidence has emerged of novel meiotic roles for this protein (see below). In addition, a role of SGO-1 in mitosis cannot yet be ruled out in *C. elegans*. In fact, this thesis provides further confirmation that SGO-1 localizes to mitotic chromosomes, centrosome and spindle in dividing cells of the early embryo. Despite this, *sgo-1* mutants do not show phenotypes consistent with defects in mitosis, such as embryonic lethality. As *sgo-1* mutants, including the new whole gene deletion animals described in this thesis, undergo normal cell division and have no other overt developmental defect, it is possible that SGO-1 function in this context (cohesin removal and/or bipolar attachment) is

redundant with other cell cycle regulators. Further work isolating *sgo-1* synthetic lethal mutants should tease out these genetic interactions.

The SGO story in *C. elegans* could have ended with these conclusions if it weren't for the finding that SGO-1::GFP signals were detected in the nervous system of adult worms. *C. elegans* follows a pre-determined development program with the establishment of irreversible cell lineages. Aside from the germline, all somatic cells in adult worms, including neurons, are therefore arrested in interphase. Shugoshin localization in neurons raised the intriguing possibility of a completely novel function for this canonical cell cycle protein. A more precise picture started to emerge when the subcellular localization of SGO-1 in the ciliary compartment of sensory organs was determined. Primary cilia are specialized microtubule organizing centers with critical and conserved signaling functions. In several organisms, including worms, ciliated structures underlie sensory perception. This thesis work started at this junction and intended to shed further light on: a) where is SGO-1 loading in developing and adult cilia and b) what is the function of SGO-1 in the cilium. Ultimately, this work should contribute to understanding the larger picture on the evolution and functional connections of SGO proteins and its interacting partners in different cellular domains.

A significant part of the work concerned the characterization of a potential SGO-1 localization in the developing cilia using a novel anti-SGO-1 antibody that revealed, in IF experiments, a series of tubular structures surrounding the mouth. The developing amphid and adjacent structures have been poorly characterized at the fluorescence microscopy level such that previous descriptions of similar structures in the sensory depressions are not available in the literature. By assessing the location of these embryonic structures relative to the anatomical position of the sensory sensilla in the adult worm, a fairly good correspondence could be

determined. It seemed probable that SGO-1 labelled the developing channels in the amphid primordia where cilia from sensory neurons eventually assemble. Since robust genetic evidence for a null *sgo-1* phenotype was lacking at the time, the presence of these structures in the available *sgo-1* deletion embryos was not enough to readily discard the antibody signals as non-specific. The finding of a genetic interaction between *sgo-1* and *dyf-7*, involved in ensuring proper docking and positioning of sensory neuron dendrites in the base of what will become the ciliary channel, further strengthened a probable cilia-domain localization for the antibody signal, and therefore, SGO-1.

As explained above in detail, it is now clear that the anti-SGO-1 antibody detects signals other than SGO-1 in the sensory depressions. Because these signals are not observed with control sera and are absent in *dyf-7* mutants, they cannot be explained by simple trapping and deposition of IgGs in the depression, a 'filling' effect known to occur in the adult ciliary channel. Instead, it seems more likely that IgGs in this antibody recognize a discrete embryonic protein that, coincidentally, marks the region of the developing sensilla. DYF-7 would be a primary candidate for such a protein, based on its published localization. However, DYF-7 signals do not fully co-localize with the signals detected using the anti-SGO-1 antibody (Figure 4.7), suggesting the antibody is detecting a protein other that DYF-7 in this domain. While these findings do not directly contribute to understanding a role of SGO-1 in the development of these structures, they represent an opportunity to further characterize the downstream events triggered by DYF-7/DEX-1-dependent regulation of amphid formation. Screening cDNA expression libraries with this antibody may indeed allow for the identification of the true identity of the anti-SGO-1 signals in embryos.

Several cilia proteins in *C. elegans* characterized in adult are first observed only in larvae. At this point, there is no evidence to suggest that SGO-1 is any different. Assessment of SGO-1 localization in the adult has been previously done using several fluorescent tagged constructs that suggest a basal body/transition zone localization. Because signals using these native promoter constructs are weak, alternative options using strong cilia-specific promoters like *posm-5* driving *sgo-1* sequences are more effective to address subcellular localization. In fact, *posm-5::sgo-1::tdTomato* lines show strong SGO-1 cilia signals in the basal body, transition zone and, possibly, axoneme (Figure 4.3). Determining the specific sub-cilia localization of SGO-1 relative to other cilia proteins and possible genetic and biochemical interactions will be critical, since residence in these domains imply different roles in cilia structure and function.

5.2 A shared genetic toolkit to regulate microtubule-derived structures

What links the SGO-1 functions in the chromosome, centrosome and cilia? These structures represent coordinating centers for assembly and disassembly of microtubule-based structures (namely: kinetochores, spindle and axoneme). In the past few years several examples of proteins with functions in different cellular domains responding to cell cycle-dependent contexts pointed to the existence of a shared genetic toolkit used to transiently regulate these structures. For instance, the chromosome segregating machinery made up of cohesin, separase, SGO and PP2A, originally characterized in the centromere, has been shown to be present in the centrosome where they regulate, in a biochemically similar way, centriole disengagement, a critical process controlling centrosome duplication required for mitotic entry. Cohesin (Smc1) immersed in the pericentriolar material (PCM) is targeted and removed by separase during the prophase pathway to dissociate the two connected centrioles. This, in turn, is antagonized by the recruitment to the centrosome of PP2A by SGO. Shugoshin, therefore, is a protector of centriole

cohesion as much as of sister chromatic cohesion (74). In humans, these roles are performed by two distinct alternative splicing variants of Sgo1 whose transcripts carry pro-centrosomal or pro-chromosomal target sequences. Remarkably, the transcriptome of cells undergoing ciliogenesis appears to replicate a centrosome-like program of gene expression (75). These findings revealed a striking parallel in the coordination of chromosomal and centrosomal cycles.

Conversely, other centrosome/kinetochore proteins have been found to regulate cilia formation. For instance, Plk1 is known to interact with components that signal to the SAC that the cell is not ready to divide (13). However, Plk1 has also been described as having functional implication in cilia disassembly in mammals. In RNAi studies, knockdown of Plk1 was found to decrease the rate of ciliary resorption (74). The same study found that Plk1 also localizes with nephrocystin-1 (NPHP1) in the transition zone of primary cilia, and that NPHP1 was a phosphorylation target of Plk1 (74). NPHP1 has been described as a scaffold protein important for actin cytoskeleton organization in areas of epithelial cell-cell adhesion and in cell-matrix adhesion (76). Budding uninhibited by benzimidazole-related 1 protein (Bubr1) is another dual function protein related to this context. It is a known SAC component that binds to Cdc20 in M phase to prevent the untimely activation of the APC (77). However, during G0 the APC binds to Bubr1 to tag Cdc20 for ubiquitin mediated degradation (77). This then allows the APC to bind a second activator, Cdc20 homolog 1 (Cdh1), which alters the APCs function. When bound to Cdh1 the APC targets Disheveled (Dvl), an important regulator of Wnt signalling, for ubiquitin mediated degradation (77). When Dvl is present in too high or low of quantities, defects in ciliogenesis arise due to issues in apical docking of basal bodies (77). By changing the time of action, Bubr1 is able to mediate ciliogenesis as well as the progression through M phase. As SGO interacts with the SAC through Mad2, it is in a position to target the SAC complex to both

the cilium and the kinetochore. Separate phosphorylation events could target SGO to either domain, bringing with it the components of the SAC. This could bring Bubr1, and potentially the APC, into proximity of the cilium allowing for the degradation of Dvl and proper cilia formation. The presence of SGO on kinetochores recruits Plk1, so the presence of SGO in cilia could also recruit Plk1 to the cilia, allowing for Plk1 interactions with NPHP1. SGO could also bring with it PP2A, which could antagonize the actions of kinases present in either domain. More importantly, the discovery of these overlapping mechanisms regulating separate pathways in the chromosome, centrosome and cilia may help to explain the etiology of still poorly understood diseases.

Finally, similar regulatory machinery in the spindle midzone (midbody) required for cytokinesis, yet another microtubule-dependent event in animal cells, have been recently shown to be co-opted to promote cilia functions. *C. elegans* central spindle proteins such as SPD-1 and ZEN-4, which are essential for furrow formation in dividing cells, also localize to the basal body in cilia and their mutants display cilia defects (78). While SGO-1 has not been shown to localize to the furrow or participate in cytokinesis, these findings further understate the adaptability of pathways controlling the assembly of microtubule-based structures.

In view of the role of SGO proteins in microtubule organizing centres, what could be the function of SGO-1 in the cilia of *C. elegans*? Though a role for the cohesin-regulatory machinery is not well established in cilia at this stage, recent evidence places the cohesin subunits Smc1 and Smc3 in the basal body and transition zone of cilia in photoreceptor cells where they associate with the guanine nucleotide exchange factor (GEF) Retinitis Pigmentosa GTPase Regulator protein (RPGR), a cilia/centrosome resident protein mutated in cases of retinitis pigmentosa. As a GEF, RPGR is expected to participate in signaling mediation, though

the specific pathway concerned is not known. Instead, RPGR has been proposed, via association to other IFT proteins, to be involved in ciliary transport assemblies. Interestingly, RPGR also binds CEP290, another transition zone protein, which itself carries a cohesin-like (SMC) domain (79). Moreover, while separase in *C. elegans* (SEP-1) has so far not been detected in cilia, the PP2A regulatory SUR-6 has recently been shown to localize to amphids (Carvalho lab, data not shown). There is, therefore, a precedence to expect at least some of the cohesin regulators to be acting in the cilia. However, if SGO-1's role in the cilia is cohesin protection via a conserved mechanism similar to that observed in the chromosome and centrosome, then a kleisin subunit should be required. So far, there are no reports of Scc1 in cilia. Basal body proteins function as gatekeepers to regulate entry and exit of cilia cargo up and down the axoneme. The presence of SGO-1 and cohesin in the basal body could indicate that cohesin-dependent microtubule interactions could be the target of SGO-1 activity. Further work investigating the presence of *C. elegans* cohesin subunits in the cilia and possible cilia defects in PP2A mutants are required.

5.3 Significance of SGO-1/TAC-1 interaction in the centrosome and cilia

Members of the transforming acidic coiled coil (TACC) family of proteins can be found in organisms ranging from yeast to humans (80). As SGO, TACC proteins have also been previously shown to localize to centrosomes where they regulate microtubule organization. The Y2H results in this thesis, however, is the first to demonstrate a possible functional connection between these proteins in any system.

Much like the SGO protein family, the similarity between the various TACC proteins lies on a conserved coiled coil domain found in the C terminus (80). Different organisms contain multiple isoforms of TACC proteins, but in *C. elegans* only one ortholog, TAC-1, exists (80). In *C. elegans* embryos exposed to RNAi mediated knockdown of *tac-1*, defects in pronuclear

migration are observed (81). Aside from pronucleus migration defects, incorrect attachment to the spindle is also detected. Chromosomes are seen attached to only a single centrosome in anaphase resulting in chromosome missegregation and multinucleated cells (81). These results suggested that TAC-1 in this system is required for microtubule-dependent processes. Consistent with these findings, astral microtubules in *tac*-1 (RNAi) one celled embryos fail to reach cell the cortex, explaining the defect in pronuclear migration (81). *tac-1* mutant embryos show normal localization of γ-tubulin, suggesting that TAC-1 plays a larger role in promoting microtubule growth from centrosomes without affecting their general nucleation (80). In *C. elegans*, TAC-1 appears on centrosomes prior to pronuclear migration before reaching peak expression at metaphase, followed by a decrease in expression up until telophase where small foci of GFP::TAC-1 can be seen associated with the newly duplicated centrosome. Importantly, the centrosomal localization of TAC-1 seems to be dependent on AIR-2 (Aurora-B), as depletion of AIR-2 by RNAi removes TAC-1 from the centrosome (81). While acting to localize TAC-1 to centrosomes, Aurora-B-mediated phosphorylation of centromeric substrates mediates proper spindle attachment and cohesin removal. Thus, Aurora B may be a key link between SGO-1 and TAC-1 functions in the chromosome and centrosome, respectively.

A less clear connection between TAC-1 and SGO-1 could be playing out in cilia, though neither TAC-1 nor AIR-2 have been localized to the sensory organs in *C. elegans* so far. Supporting a functional relevance to the Y2H interaction in the context of the cilium, current unpublished work in the Carvalho lab has demonstrated that *tac-1* mutants also display defects in a cilia-dependent phenotype: *tac-1* temperature sensitive worms are defective in osmotic avoidance, suggesting a sensory role. Assuming TAC-1 and AIR-2 are in the amphids, as SGO-

1, a possible scenario would have SGO-1 localizing TAC-1 to the basal body to antagonize AIR-2 activity and regulate axoneme growth and/or IFT processes.

5.4 Novel meiotic roles of SGO-1 in *C. elegans* oogenesis and spermatogenesis

Up until recently, it was believed that SGO-1 activity was not required for meiotic progression or chromosome segregation in worms. This was based on the lack of classic chromosome segregation defects in *sgo-1*-depleted meiocytes as well as an unclear localization of SGO-1 in the gonad. Work from the Bhalla lab, however, has for the first time shown that SGO-1 is indeed important for prophase I checkpoints regulating synapsis and DNA damage response. Interestingly, these are events that happen earlier than the canonical functions of SGO in the centromere of monocentric species, suggesting these functions are not necessarily related. Mutants for the synaptonemal complex protein SYP-1 prevent synapsis and recombination which in conjunction activate two meiotic checkpoints, the synapsis checkpoint and the DNA damage response. The induction of these two checkpoints leads in turn to increased levels of germ cell apoptosis, detectable in the gonad by CEP-1::GFP foci, an apoptotic maker (82). *sgo-1*; *syp-1* mutants showed reduced levels of germline apoptosis when compared to *syp-1* mutants, consistent with a role for SGO-1 as a checkpoint activator (83). In *cep-1;syp-1;sgo-1* triple mutants, where the CEP-1-triggered DNA damage response checkpoint pathway is impaired, wild type levels of germ cell apoptosis were observed, indicating SGO-1 is involved in the synapsis checkpoint pathway instead (83). A defect in checkpoint activation because of failure of meiotic chromosomes to synapse predicts errors in the resolution of double strand breaks (DSBs). Indeed, in addition to a role in the synapsis checkpoint, SGO-1 was also found to affect non-homologous DNA repair. Abundance of RAD-51::GFP foci, which loads on DSB sites to process strand exchange, can be used as a readout of repair efficiency (84). In a *syp-1;sgo-1* null

background, less RAD-51::GFP foci were detected in prophase I nuclei, compared to *syp-1* gonads, suggesting that depletion of *sgo-1* improves DSB repair, presumably because the failure to activate a DNA repair checkpoint (83).

These results pointed to a novel, non-canonical meiotic role of *C. elegans* SGO-1 beyond cohesin protection and chromosome segregation. Similar to a role of other SGO protein in sensory perception, subtle phenotypes such as in the early meiotic checkpoint could have been overlooked in other systems where the most dramatic outcome of SGO depletion is cell cycle collapse due to premature chromosome disjunction.

5.5 Future directions

Several new lines of research were identified in this study. An obvious next step forward would be the characterization of possible roles of known SGO interactors in the cilia. This would involve investigating possible amphid and phasmid localization of fluorescently tagged proteins known to partner with SGO-1 in the chromosome and centrosome. Functionally, any co-cilia localization could then be tested at the level of sensory defect using simple chemotaxis assays.

A more complex question is to resolve the actual role of SGO-1 in the cilia. As an adaptor protein, SGO-1 functions depend on its ability to recruit and localize proteins with catalytic activity to certain domains in the cell. Identifying these factors is therefore a gateway to determining the specific cilia role of SGO-1. TAC-1 is currently the only known interacting protein to *C. elegans* SGO-1. A thorough phenotypic characterization using temperature sensitive mutants for *tac-1* to bypass early defect in embryogenesis should provide more information on this functional connection. For instance, is SGO-1/TAC-1 interaction of an activating nature or this association is inhibitory? A potential way to functionally address these

questions would be to determine changes in the level of osmotic avoidance defects in *sgo-1;tac-1* double mutants as compared to single *sgo-1* and *tac-1* mutants. Since these mutants seem to be both defective in avoiding high osmolarity environments, one could predict that their interaction is needed to promote sensory function. In this case, it would be interesting to see if the double mutant shows an enhanced defect. These genetic interaction experiments could be then overlapped with cell-specific knockdown or rescue experiments using floxed CRISPR-induced deletions or expression of constructs driving SGO-1/TAC-1 to subset of sensory neurons to probe roles in specific behaviours.

Aside from expanding the Y2H analysis initiated in this thesis work, immunoprecipitation (IP) experiments with tagged SGO-1::GFP proteins followed by mass spectroscopy should also be attempted to identify other interacting proteins in native lysates and confirm Y2H interactions with antibodies.

A non-expected outcome of this work was the identification of an antibody that reacts with an unknown protein involved in sensory organ development. Further characterization of this antibody and the identification of the antigen would open a different venue to understand how sensory organs are formed. Studying sensory organ development is a complicated task in vertebrate systems where important constraints such as difficult anatomic access, hinder progress. The *C. elegans* amphid provide an immense advantage as an entry model to study the genetics and development of these important organs. Considering the conservation of cilia proteins across species and their relevance to disease, identifying novel genes involved in the development of sensory organs may enhance our understanding of as yet uncharacterized ciliopathies.

Overall, this work contributed to research in the field that suggests SGO are highly dynamic and adaptable proteins that have been co-opted to mediate different events in the life of a cell. The results presented here suggest that SGO can act beyond cell division. The cilia function of SGO-1 could have evolved exclusively in worms, where the evolutionary constraints on SGO-1 function were lowered because of a holocentric mode of chromosome segregation. Conversely, Shugoshin proteins in monocentric species could also participate in cilia structure or function, but this role may have so far been obscured by the essential cell cycle functions in early development.

6 Appendices

Appendix A: Immunostaining solutions

10X Phosphate Buffered Saline (PBS)	KCl	2 g
	KH_2PO_4	2.4 g
	NaCl	0.3 M
	Na_2HPO_4	14.4 g
	H2O	1 L
Wash Buffer (PBST)	PBS	1X
	Tween 20	0.1% v/v
4% FIX	PBS	1X
	HEPES pH 7.4	80 mM
	EDTA	0.8 mM
	Formaldehyde	4% v/v
	$MgSO_4$	1.6 mM
Blocking Solution	0.5% Bovine Serum Albumin in PBST	

Appendix B: Antibodies

Table B.1: Antibodies

Antibody Target	Dilution Factor	Production Company
rabbit-α-sgo-1	1:1000	GenScript
mouse- α-RFP	1:100	Rockland Immunochemicals, Inc
mouse- α-GFP	1:50	Developmental Studies Hybridoma Bank
mouse-α-tubulin-α (AA4.3)	1:50	Developmental Studies Hybridoma Bank
mouse-α-ajm-1 (mh27)	1:50	Developmental Studies Hybridoma Bank
goat- α-rabbitIgG-FITC	1:500	Jackson Laboratory

goat- α-mouseIgG-FITC	1:500	Jackson Laboratory
goat- α-rabbitIgG-Cy3	1:1000	Jackson Laboratory
goat- α-rabbitIgG-FITC	1:500	Jackson Laboratory

Appendix C: Microinjection

All injections were performed on a Nikon Eclipse TS100 outfitted with a Narishige injection needle holder. An Eppendorf FemtoJet 4x microinjector was used to regulate the output pressure of injection to one thousand hPa. A constant pressure of fourteen hPa was applied to the needle to prevent flow back from the worm into the needle. A Narishige PC-10 needle puller set to 65.1˚C was used to create the injection needles from Kwik-Fil™ Borosilicate Glass Capillaries by World Precision Instruments, Inc. Injection solution consisted of one in ten dilutions of both the marker construct and the construct of interest in sterile water. Bacteriological grade agarose was dissolved in water to a final concentration of two percent, a large drop sandwiched between a twenty-two by fifty mm glass coverslip and glass plate and allowed to solidify. The glass plate was removed, and pads were dried overnight at 37˚C.

Appendix D: Vector maps

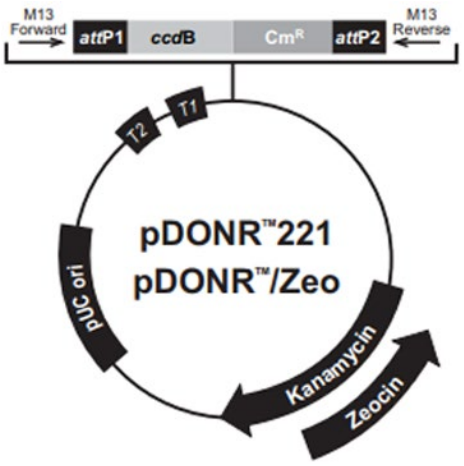

Gateway® Technology with Clonase® II manual

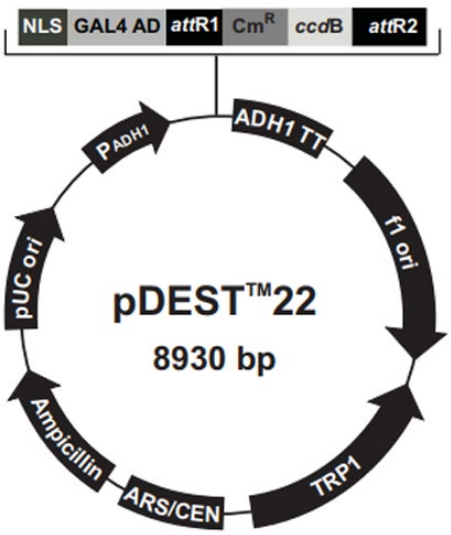

ProQuest™ Two-Hybrid System manual

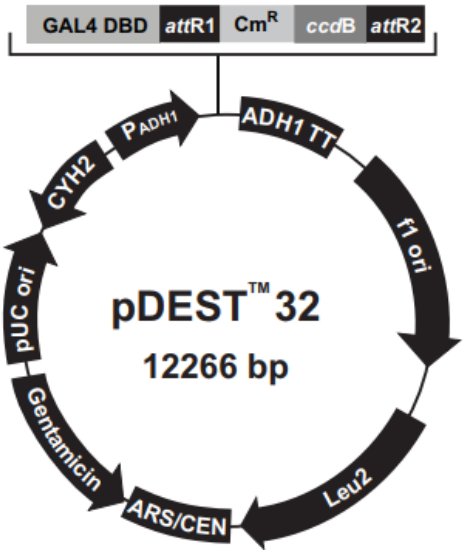

ProQuest™ Two-Hybrid System manual

Appendix E: Gateway reactions

BP Reaction	*att*-B flanked PCR product	1.5 µL
	pDONR-221	1.2 µL
	BP Clonase®	1.0 µL
	1X TE pH 8.0	1.3 µL

Mix components in a 1.5 mL microcentrifuge tube at room temperature and incubate at 25˚C overnight. The following day 1 µL can be transformed into a suitable bacterial host and plated onto LB + Kanamycin plates to yield entry clone pEntr-221-GOI.

LR Reaction	pEntr-221-GOI	1.5 µL
	pDEST-22 or pDEST-32	1.2 µL
	LR Clonase®	1.0 µL
	1X TE pH 8.0	1.3 µL

Mix components in a 1.5 mL microcentrifuge tube at room temperature and incubate at 25˚C overnight. The next day 1 µL can be transformed into a suitable bacterial host and plated onto

LB + Ampicillin for pDEST-22 to yield expression clone pExp-22-GOI or LB + Gentamycin for pDEST-32 to yield expression clone pExp-32-GOI.

Appendix F: Bacterial transformation

1. Thaw DH5α cells on ice.
2. Add 1 µL of either an LR reaction or a BP reaction into the cells and incubate on ice for 30 minutes.
3. Heat shock cells at 42˚C for 30 seconds and recover on ice for 2 minutes.
4. Add 250 µL of warm SOC medium and incubate at 37˚C for 4 hours.
5. Plate transformation onto appropriate selection plates.

Appendix G: mRNA isolation

1. N2 worms were grown on 3 separate plates until plates are saturated with worms and they have exhausted the food but are not starving.
2. Collect worms by adding 3 mL of M9 buffer to each plate, swirling to remove the worms, and transferring them into a 10 mL Falcon tube.
3. Place the tube on ice for 10 minutes, remove M9 and add 10 mL of clean M9. Place on ice for 10 minutes
4. Remove as much M9 as possible careful no to disturb the worm pellet and add 4 mL of Triazol.
5. Vortex to mix and place the tubes on ice for 1 hour, vortexing every 15 minutes.
6. Split the solution into 4 1. 5 mL microcentrifuge tubes and spin down at 13500 x g for 10 minutes at 4˚C.
7. Transfer supernatant to a new tube, add 200 µL of chloroform, vortex and place on ice for 3 minutes.
8. Spin for 15 minutes at 13500 x g at 4˚C and transfer the upper aqueous layer to a new tube.
9. Add 500 µL of isopropyl alcohol, mix, and place on ice for 10 minutes.
10. Spin for 10 minutes at 13500 x g at 4˚C to pellet RNA.
11. Remove supernatant, wash pellet with 100 µL of 70% ethanol in DEPC water then air dry the pellet for 20 minutes.
12. Add 25 µL of DEPC water, incubate at 60˚C for 10 minutes and store RNA at -80˚C.

Appendix H: cDNA synthesis

1. To a PCR tube add: 1 µL of genomic f (forward priner), 1 µL of genomic r (reverse primer), 2 µL of the RNA prep, 1 µL of 10 mM dNTPs, and 8 µL of DEPC water.
2. Set a thermocycler program to 65˚C for 5 minutes, 42˚C for 52 minutes and 70˚C for 15 minutes.
3. Heat the sample at 65˚C for 5 minutes, stop the cycle, chill on ice, quickly spin the sample down then add: 4 µL of 5X FS buffer, 2 µL of 0.1M DTT, and 1 µL of RNAse out.
4. Mix gently and continue the cycle.

5. 2 minutes into the 42˚C cycle, stop and add 1 µL of SuperScript II Reverse Transcriptase. Resume the cycle, and once finished store at -20˚C.

genomic f: CCTGTGGAAAACTGTATCGA

genomic r: TGGCGGTGACTTAGATCTTCA

Appendix I: Electrocompetent cells

* after harvesting cells, it is important to keep everything cold. Precool centrifuge rotor and all falcon tubes/microfuge tubes to 4˚C before beginning. Cells must also be kept on ice after the harvest step to keep them cold.

1. Prepare fresh colonies of DH5α on an LB plate.
2. Inoculate 1-5 mL of LB without NaCl with a single colony of DH5α and shake overnight at 37˚C.
3. The next morning, add 1 mL of the overnight culture to 100 mL of fresh LB without NaCl and shake at 37˚C until the OD_{600} is 0.35 to 0.4.
4. Place the culture on ice for 30 minutes swirling to evenly cool.
5. Split the culture into 2 50 mL falcon tubes and harvest cells at 1000 x g for 15 minutes.
6. Remove supernatant and wash each tube with 40 mL of ice cold 10% sterile glycerol.
7. Spin cells down at 1000 x g for 10 minutes.
8. Repeat steps 6 and 7 three more times.
9. After the final spin, remove the supernatant and resuspend each pellet in 500 µL of 10% glycerol.
10. Aliquot 30 µL of resuspended cells into separate microfuge tubes, flash freeze in liquid nitrogen and store at -80˚C.

Appendix J: Electroporation

1. Thaw electrocompetent cells on ice.
2. Add 1 µL of DNA to each tube, mix gently and place on ice. Also remove cuvettes from freezer and place on ice.
3. Set the electroporator to 1.8 kV, 200 Ω, and 25µF.
4. Remove a cuvette from the ice and wipe off any excess ice or water.
5. Without allowing the cuvette to warm, add the DNA/cell mixture from one tube into the cuvette. Gently tap the cuvette on the table to ensure solution spreads across the entire cuvette bottom. Try to avoid bubbles and splashing, this will decrease the chances of arcing.
6. Place the cuvette into the safety holder and slide the cuvette in between the electrodes.
7. Press and hold both red buttons down until a tone is heard and then release.
8. Add 1 mL of SOC into the cuvette to recover cells and transfer them to a 15 mL falcon tube.
9. Shake cells at 37˚C for 1 hour and plate onto selective plates.

Appendix K: Bacterial media

Lysogeny Broth (LB)	Tryptone	10 g
	Yeast Extract	5 g
	NaCl	10 g
	Agar (for plates)	15 g
	Water	to 1 L

After autoclaving, add the appropriate dilution of antibiotic to make antibiotic plates

Antibiotic Stock Solutions	Ampicillin	100 mg/mL
	Gentamycin	50 mg/mL
	Kanamycin	50 mg/mL

Super Optimal Broth with Catabolite Repression (SOC)	Tryptone	20 g
	Yeast Extract	5 g
	NaCl	0.5 g
	1 M KCl	2.5 mL
	Water	to 1L

After autoclaving, add 20 mL of 1 M filtered glucose and 10 mL of sterile $MgSO_4$

Appendix L: Adding Gateway sequences

Before proceeding with the first reaction, the cDNA of the gene of interest must be adapted with Gateway® compatible sequences. Once cDNA has been obtained, a PCR reaction containing primers with Gateway® compatible sequences is used to add these sequences onto the gene of interest. The primers are as follows:

Forward (nested Y2H f):

GGGGACAAGTTTGTACAAAAAAGCAGGCTGGGAGGTCACCACCATGGATGCAAAAACTGCA

Reverse (prCC334r):

GGGGACCACTTTGTACAAGAAAGCTGGGTGTCAGAAAAATGTATTGATGTATG

The Gateway® compatible sequence is bolded and the start and stop codons of *sgo-1* have been underlined. The forward primer has been designed with a yeast Kozak consensus

sequence to aid expression of the bait product and is also compatible with an in-frame N-terminal fusion for downstream applications.

1. On ice in a PCR tube, combine 5 µL of 5x Phusion™ buffer, 0.5 µL of 2 mM dNTPs, 0.5 µL of nested Y2H f, 0.5 µL of prCC334r, 17 µL of water, 1.0 µL of a 1:10 dilution of the band prepped RNA sample, and 0.5 uL of Phusion™ polymerase.
2. Mix the sample well, and add it to a thermocycler programed as follows:

94˚C	94 ˚C	55 ˚C	72 ˚C	72 ˚C	4˚C
3 minutes	[40 seconds	30 seconds	70 seconds]	5 minutes	Hold
	Repeat cycles 2 to 4 30 times				

3. Run the reaction on a 1% agarose gel at 100 volts for 45 minutes, then cut and extract the band of interest.

Appendix M: Library propagation

1. Thaw DH10B bacterial cells on ice. Use 4 eppendorf tubes with 250 µL of cells in each tube.
2. Dilute library plasmid stock 1:10 with TE buffer pH 8.0
3. Add 5 µL of the diluted plasmid to each tube and gently mix
4. Let stand on ice for 30 minutes.
5. Heat shock cells at 42˚C for 45 seconds and let them rest on ice for 2 minutes.
6. Add 1 mL of room temperature SOC to each reaction, pool them into a 15 mL conical centrifuge tube and shake at 37˚C for 1 hour.
7. Spin the cells down at 5000 x g for 5 minutes, remove the supernatant and dissolve the pellet in 1.2 mL of SOC.
8. Plate 200 µL onto 12 LB + ampicillin plates and grow overnight at 37˚C.
9. The next day, use 2-3 mL of LB to wash the resulting colonies off the plates and into a 50 mL conical centrifuge tube.
10. Spin the cells down at 5000 x g for 5 minutes and resuspend the pellet in 3 mL of LB.
11. Freeze an aliquot for storage and use the rest to inoculate 100 mL of LB.
12. Grow overnight shaking at 37˚C and perform a Maxiprep with the GeneJET plasmid Maxiprep kit.

Appendix N: Clone sequencing

Before performing the LR reaction, it is important to sequence the entry clone to ensure the gene of interest is in frame with its Gal 4 fusion protein. The entry clone sequencing primers are as follows:

Forward (prCC332):

CAACACATTGATGAGCAATG

Reverse (M-13):

CAGGAAACAGCTATGAC

After isolating prey DNA from positive hits, it is necessary to sequence the insert to determine which gene was responsible for the interaction. The prey sequencing primers are as follows:

Forward (prCC333):

TATAACGCGTTTGGAATCACT

Reverse (prCC335):

AGCCGACAACCTTGATTGGAGAC

Appendix O: Yeast host strain

The host yeast strain used in this was MaV203 from Invitrogen. It has been specifically engineered to contain the *HIS3, URA3,* and *LacZ* reporter genes under the control of the UAS of the Gal4 system. It has also been manipulated to contain auxotrophies for these genes so that the phenotype can be based solely on the expression of the reporter genes. The Gal4 transcription factor has been removed to prevent endogenous activation of the reporter genes. The *gal80* gene is a negative regulator of the Gal4 transcription factor and has been removed to prevent this inhibition. The genotype of the strain is as follows:

MATα; leu2-3,112; trp1-901; his3Δ200; ade2-101; cyh2R; can1R; gal4Δ; gal80Δ; GAL1::lacZ; HIS3UASGAL1::HIS3@LYS2; SPAL10::URA3.

Appendix P: Yeast media

Yeast Peptone Dextrose (YPD)	Peptone	20 g
	Yeast Extract	10 g
	Glucose	20 g
	Agar (for plates)	20 g
	Water	to 1 L

Autoclave

Synthetic Complete (SC)	Amino Acid Powder Drop Out powder (without Leucine, Tryptophan, Histidine or Uracil)	1.3 g
	Yeast Nitrogen Base (without Ammonium Sulfate)	1.7 g
	Ammonium Sulfate	5 g
	Glucose	20 g

	10 N NaOH	0.3 mL
	Agar (for plates)	20 g
	Water	to 1 L

After autoclaving, add 8 mL of the appropriate Amino Acid Stock Solution

For 3-Amino-1,2,3, Triazole (3AT) plates, add 3AT as a powder after autoclaving and swirl to dissolve before pouring plates and only uracil as an additive

3AT	10 mM	0.84 g
	25 mM	2.10 g
	50 mM	4.20 g
	75 mM	6.30 g
	100 mM	8.40 g

Amino Acid Stock Solutions	Histidine	100 mM
(all filter sterilized)	Leucine	100 mM
	Tryptophan	40 mM
	Uracil	20 mM

10X TE buffer	Tris Cl pH 8.0	100 mM
	EDTA pH 8.0	10 mM

Autoclave

1 M LiAc (10X)	pH 7.5

Filter sterilize

1X TE/1X LiAc	10X LiAc	10 mL
	10X TE	10 mL
	Water	80 mL

Filter sterilize

1X LiAc/ 0.5X TE	10X LiAc	10 mL

	10X TE	5 mL
	Water	85 mL

Filter sterilize

40% Polyethylene Glycol-3500 (PEG)/1X LiAc/0.5X TE/	10X LiAc	10 mL
	10X TE	5 mL
	PEG-3350	40 g
	Water	to 100 mL

Filter sterilize

Z- buffer	Na_2PO_4	60 mM
	NaH_2PO_4	40 mM
	KCl	10 mM
	$MgSO_4$	1 mM

Filter Sterilize

Triton Sodium Dodecyl Sulfate (SDS) Lysis buffer	Triton X-100	2% v/v
	SDS	1% w/v
	NaCl	100 mM
	Na_2 EDTA	1 mM

Appendix Q: Yeast transformation

Small Scale Transformation: for generating controls, retransformation of specific prey, and preparing for library scale transformation.

1. Inoculate 10 mL of YPD media with a colony of MaV 203and shake overnight at 30˚C.
2. Determine the OD_{600} of the culture and dilute to an OD_{600} of 0.4 in roughly 50 mL and shake an additional 2 hours at 30˚C.
3. Pellet the cells in the 50 mL Falcon tube at 1125 x g for 3 minutes. Discard supernatant and wash pellet with 40 mL 1X TE.
4. Pellet cells at 1125 x g for 3 minutes. Discard the supernatant and resuspend the pellet in 2 mL of 1XLiAc/0.5X TE and incubate the solution at 20˚C for 10 minutes.

5. For each transformation (up to 20), mix 1 µg of plasmid DNA (0.5 µg of each plasmid if doing a co-transformation) with 100 µg of denatured sheared salmon sperm DNA and 100 µL of yeast solution from step 4. Salmon sperm must be boiled for 5 minutes and chilled prior to adding.
6. Add 700 µL of the PEG/1X LiAc/0.5X TE solution to each transformation and pipette up and down to mix well. Incubate at 30˚C for 30 minutes.
7. Add 88 µL DMSO to each reaction and mix well, then heat shock at 42˚C for 7 minutes.
8. Pellet cells at 1125 x g for 2 minutes and remove supernatant.
9. Wash with 1 mL of 1X TE and pellet cells at 1125 x g for 2 minutes.
10. Resuspend the pellet in 100 µL 1X TE and plate onto 10 cm SC -Leu -Trp plates and grow 30˚C for 3 days.

Library Scale Transformation: used to transform a cDNA library into a host that has the bait plasmid.

1. In the early afternoon, inoculate 20 mL of SC -Leu media with a large colony of MaV 203 containing the bait plasmid and shake overnight at 30˚C.
2. The next morning, dilute the culture to an OD_{600} of 0.10 and shake at 30˚ C until an OD_{600} of 0.45 to 0.5 is reached.
3. Spilt culture into 4 sterile falcon tubes and harvest cells at 1125 x g for 5 minutes. Discard supernatant and continue harvesting until all culture is used.
4. Resuspend each pellet in 3 mL of sterile water and pool into one tube.
5. Pellet cells at 1125 x g and resuspend the pellet in 30 mL of sterile water.
6. Pellet cells at 1125 x g and resuspend in 1.5 mL of 1X LiAc/1X TE.
7. Add 1µg of library DNA and 50 µg of sheared denatured salmon sperm DNA to each of 30 1.5 mL microcentrifuge tubes. Add 50 µL of yeast from step 6 to each tube. The salmon sperm must be boiled for 5 minutes and then chilled before adding.
8. Add 300 µL of PEG/1X LiAc/0.5X TE to each tube and pipette up and down to mix well. Incubate at 30˚C for 30 minutes.
9. Add 40 µL of DMSO to each tube, mix well, and heat shock at 42˚C for 10 minutes.
10. To calculate efficiency of transformation, remove 100 µL from 1 transformation and dilute 1:100 and 1:1000 in sterile water, and plate onto 10 cm SC -Leu -Trp
11. Plate each transformation on one of 30 15 cm 3AT plates (must determine optimum 3AT concentration before hand).
12. Grow plates for 3 days at 30˚C. Count colonies on 10 cm plates to find efficiency.
13. Replica clean using a velvet replicator the 15 cm plates and grow for another 2-3 days.

Appendix R: Reporter assays

Testing Transformants: testing initial transformants for positive hits.

1. From a 3AT plate with fresh colonies, streak out each colony onto an SC -Leu -Trp plate and incubate at 30˚C for 2 days. Also prepare fresh colonies of the control cells (2 to 6) on SC -Leu -Trp plates.

2. Streak 4 isolated colonies of each hit onto another SC -Leu -Trp plate. Up to 4 separate hits can be streaked onto the same plate. Also streak 2 isolated colonies of each recommended control onto this plate.
3. Incubate plates for 18 hours at 30˚C.
4. Replica plate onto a YPD plate with a Whatman™ qualitative filter paper, an SC -Leu -Trp -Ura plate, and then onto a 3AT plate, making asymmetric marks onto the plates so they may be realigned with the master plate. A single velvet may be used to plate onto all plates. After plating onto the 3AT plate, use a fresh velvet to replica clean the plate.
5. Incubate all plates for 24 hours.
6. After incubation, replica clean the SC -Leu -Trp -Ura plates and return them to the incubator for another 2 days. For the YPD plate with the membrane, proceed to the X-gal assay.

X-gal assay: for testing beta-galactosidase activity.

1. For each filter, dissolve 10 mg of x-gal in 100 µL of DMF. Combine 100 µL of x-gal solution with 60 µL of BME in 10 mL of Z buffer.
2. Place 2 round Whatman™ 3 mm chromatography paper cut outs into a 10 cm plate. Saturate with ~8 mL of x-gal in z buffer while removing air bubbles.
3. Remove the membrane from the YPD plate with forceps and submerge in liquid nitrogen for 20 seconds. Place the frozen membrane directly onto the soaked filter papers and remove air bubbles between. Tip plate to remove excess buffer.
4. Cover the plate and incubate at 37˚C for 24 hours while monitoring the phenotype. Tip the plate at an angle so excess buffer accumulates under control 2. This will help reduce any bleeding of blue colour to improper cells. Score the final results at 24 hours.

Appendix S: Yeast plasmid isolation

Yeast Plasmid DNA Isolation: for extracting plasmids of positive hits to be sequenced and reconfirmed.

1. Grow at least 1.4 mL up to 5 mL of an overnight yeast culture in appropriate media at 30˚C.
2. Harvest cells in a 1.5 mL centrifuge tube at 1125 x g for 2 minutes discarding the supernatant.
3. Vortex tubes to resuspend cells in residual liquid and add 0.3 g of glass beads, 200 µL of Triton SDS Lysis buffer and 200 µL of phenol/chloroform/isoamylalcohol (25:24:1).
4. Vortex for 2 minutes and centrifuge at max speed for 5 minutes.
5. Transfer the aqueous top layer to a new microfuge tube.
6. Proceed to ethanol precipitation.

Ethanol Precipitation: for purifying plasmid DNA.

1. Adjust sample volume to 200 µL and add 550 µL of ice cold 95% ethanol.
2. Leave in -20˚C freezer for 15 minutes.

3. Centrifuge at max speed for 10 minutes at 4˚C.
4. Remove supernatant and wash with 4˚C 80% ethanol.
5. Carefully remove all liquid from tubes and allow to dry inverted on a Kimwipe for 20 minutes.
6. Resuspend pellet in 25 µL of sterile water and transfer to a clean tube.

Appendix T: Freezing yeast

1. Isolate a single colony and grow in 5 mL of appropriate liquid media overnight.
2. The next day, add 500 µL of sterile 30% glycerol and 500 µL of the overnight culture into a cryovial.
3. Cap it, invert to mix and freeze at -80˚C.

Appendix U: Nematode media

Nematode Growth Media (NGM)	Peptone	2.5 g
	NaCl	3.06 g
	Agar	17 g
	Water	to 1 L

After autoclaving, add 1 mL of sterile $MgSO_4$, 1 mL of sterile $CaCl_2$, 1 mL of 5 mg/mL Cholesterol and 25 mL of KPO_4

M9 Buffer	KH_2PO_4	3 g
	Na_2PO_4	6 g
	NaCl	5 g
	Water	to 1 L

After autoclaving, add 1 mL of 1 M $MgSO_4$

Appendix V: Single worm PCR

1. Prepare the lysis buffer as follows: 50 mM KCl, 10 mM Tris pH 8.2, 2.5 mM$MgCl_2$, 0.45% NP40, 0.45% Tween 20, 0.01% gelatin.
2. Add 2 µL of 20 mg/mL Proteinase K solution to 200 µL of lysis buffer and aliquot 5 µL of the resulting solution into as many tubes as worms you are genotyping.
3. Select worms of interest onto an unseeded NGM plate and allow them to crawl around and clean themselves off for 10 minutes.
4. Add a single worm to each tube with lysis buffer + Proteinase K and freeze them at -80˚C for 15 minutes.
5. Without thawing, lyse worms in a thermocycler as follows:

60˚C for 90 minutes, 95˚C for 15 minutes, 4˚C hold.

6. Add the components of the PCR reaction to the lysed worm tube and perform the PCR reaction with conditions necessary for the template and primers.

7 References

1. Watanabe Y. (2005) “Shugoshin: guardian spirit at the centromere.” *Current Opinion in Cell Biology* 17(6):590–595 DOI 10.1016/j.ceb.2005.10.003.
2. Kerrebrock, Anne W, *et al.* (1992) “The Drosophila Mei-S332 Gene Promotes Sister-Chromatid Cohesion in Meiosis Following Kinetochore Differentiation.” *Genetics*, vol. 130, no. 4, pp. 827–841.
3. Marston, Adele L. (2015) “Shugoshins: Tension-Sensitive Pericentromeric Adaptors Safeguarding Chromosome Segregation.” *Molecular and Cellular Biology*, vol. 35, no. 4, pp. 634–648., doi:10.1128/mcb.01176-14.
4. Grishaeva *et al.* (2016) Bioinformatical analysis of eukaryotic shugoshins reveals meiosis-specific features of vertebrate shugoshins. *PeerJ* 4:e2736; DOI 10.7717/peerj.2736
5. Nasmyth, K. and Hearing, C. (2009) “Cohesin: Its Roles and Mechanisms.” *Annual Review of Genetics*, vol. 43, no. 1, pp. 525–558., doi:10.1146/annurev-genet-102108-134233.
6. Ishiguro, K. and Watanabe, Y. (2007) “Chromosome Cohesion in Mitosis and Meiosis.” *Journal of Cell Science*, vol. 120, no. 3, pp. 367–369., doi:10.1242/jcs.03324.
7. Uhlmann, F. (2001) “Secured Cutting: Controlling Separase at the Metaphase to Anaphase Transition.” *EMBO Reports*, vol. 2, no. 6, pp. 487–492., doi:10.1093/embo-reports/kve113.
8. Yamada, H Y, *et al.* (2016) “Systemic Chromosome Instability in Shugoshin-1 Mice Resulted in Compromised Glutathione Pathway, Activation of Wnt Signaling and Defects in Immune System in the Lung.” *Oncogenesi*s, vol. 5, no. 8, doi:10.1038/oncsis.2016.56.
9. Yamada, H. *et al.* (2012) “Haploinsufficiency of SGO1 Results in Deregulated Centrosome Dynamics, Enhanced Chromosomal Instability and Colon Tumorigenesis.” *Cell Cycle*, vol. 11, no. 3, pp. 479–488., doi:10.4161/cc.11.3.18994.
10. Yamada, H. *et al.* (2015) “Tumor-Promoting/Progressing Role of Additional Chromosome Instability in Hepatic Carcinogenesis in Sgo1 (Shugoshin 1) Haploinsufficient Mice.” *Carcinogenesis*, vol. 36, no. 4, pp. 429–440., doi:10.1093/carcin/bgv011.
11. Watanabe Y, and Kitajima TS. (2005) “Shugoshin protects cohesin complexes at centromere.” *Philosophical Transactions of the Royal Society B: Biological Sciences* 360(1455):515–521 DOI 10.1098/rstb.2004.1607.
12. Mardin, B. and Schiebel, E. (2012) “Breaking the Ties That Bind: New Advances in Centrosome Biology.” *The Journal of Cell Biology*, vol. 197, no. 1, pp. 11–18., doi:10.1083/jcb.201108006.
13. Pouwels, Jeroen, *et al.* (2007) “Shugoshin 1 Plays a Central Role in Kinetochore Assembly and Is Required for Kinetochore Targeting of Plk1.” *Cell Cycle*, vol. 6, no. 13, pp. 1579–1585., doi:10.4161/cc.6.13.4442.
14. Katis, Vittorio L, *et al.* (2004) “Maintenance of Cohesin at Centromeres after Meiosis I in Budding Yeast Requires a Kinetochore-Associated Protein Related to MEI-S332.” *Current Biology*, vol. 14, no. 7, pp. 560–572., doi:10.1016/j.cub.2004.03.001.

15. Eshleman, H. and Morgan, D. (2014) “Sgo1 Recruits PP2A to Chromosomes to Ensure Sister Chromatid Bi-Orientation during Mitosis.” *Journal of Cell Science*, vol. 127, no. 22, pp. 4974–4983., doi:10.1242/jcs.161273.
16. Kitajima, TS *et al.* (2004) “The Conserved Kinetochore Protein Shugoshin Protects Centromeric Cohesion during Meiosis.” *Nature*, vol. 427, pp. 510–517.
17. Liu, Hong, *et al.* (2013) “Phospho-H2A and Cohesin Specify Distinct Tension-Regulated Sgo1 Pools at Kinetochores and Inner Centromeres.” *Current Biology*, vol. 23, no. 19, pp. 1927–1933., doi:10.1016/j.cub.2013.07.078.
18. Ricke, R. *et al.* (2012) “Bub1 Kinase Activity Drives Error Correction and Mitotic Checkpoint Control but Not Tumor Suppression.” *The Journal of Cell Biology*, vol. 199, no. 6, pp. 931–949., doi:10.1083/jcb.201205115.
19. Gregan, J. *et al.* (2008) “Solving the Shugoshin Puzzle.” *Trends in Genetics*, vol. 24, no. 5, pp. 205–207., doi:10.1016/j.tig.2008.02.001.
20. Tanaka,TU. (2010) “Kinetochore–Microtubule Interactions: Steps towards Bi-Orientation.” *The EMBO Journal*, vol. 29, no. 24, pp. 4070–4082., doi:10.1038/emboj.2010.294.
21. May, K. and Hardwick, K. (2006) “The Spindle Checkpoint.” *Journal of Cell Science*, vol. 119, no. 20, pp. 4139–4142., doi:10.1242/jcs.03165.
22. Sanhaji, M. *et al.* (2011) “Mitotic Centromere-Associated Kinesin (MCAK): a Potential Cancer Drug Target.” *Oncotarget*, vol. 2, no. 12, doi:10.18632/oncotarget.416.
23. Spieth *et al.* (2014) “Overview of gene structure in *C. elegans*”, *WormBook*, ed. The *C. elegans* Research Community, WormBook, doi/10.1895/wormbook.1.65.2, http://www.wormbook.org.
24. Subirana, Juan A., and Xavier Messeguer. “A Satellite Explosion in the Genome of Holocentric Nematodes.” *PLoS ONE*, vol. 8, no. 4, 2013, doi:10.1371/journal.pone.0062221.
25. Schvarzstein, M. *et al.* (2010) “Coordinating Cohesion, Co-Orientation, and Congression during Meiosis: Lessons from Holocentric Chromosomes.” *Genes & Development*, Cold Spring Harbor Lab, genesdev.cshlp.org/content/24/3/219.full.pdf html.
26. Carvalho, C. *et al.* (2008) “LAB-1 Antagonizes the Aurora B Kinase in *C. elegans*.” *Advances in Pediatrics*., U.S. National Library of Medicine, www.ncbi.nlm.nih.gov/pmc/articles/PMC2569883/.
27. Severson, A. (2016) “Analysis of Meiotic Sister Chromatid Cohesion in *Caenorhabditis Elegans*.” *Methods in Molecular Biology Cohesin and Condensin*, pp. 65–95., doi:10.1007/978-1-4939-6545-8_5.
28. Rogers, E. *et al.* (2002) “The Aurora Kinase AIR-2 Functions in the Release of Chromosome Cohesion in *Caenorhabditis Elegans* Meiosis.” *Advances in Pediatrics*., U.S. National Library of Medicine, www.ncbi.nlm.nih.gov/pmc/articles/PMC1855215/.
29. Tzur,YB., *et al.* (2012) “LAB-1 Targets PP1 and Restricts Aurora B Kinase upon Entrance into Meiosis to Promote Sister Chromatid Cohesion.” *PLOS Medicine*, Public Library of Science, journals.plos.org/plosbiology/article?id=10.1371/journal.pbio.1001378
30. Riddle, Donald L., Thomas Blumenthal, Barbara J. Meyer, and James R. Priess. (1997) eds. “*C. elegans II*.” Cold Spring Harbour Laboratory Press, Print.

31. Inglis P.N. *et al.* (2007) "The sensory cilia of *Caenorhabditis elegans*" *WormBook*, ed. The *C. elegans* Research Community, WormBook, doi/10.1895/wormbook.1.126.2, http://www.wormbook.org/chapters/www_ciliumbiogenesis.2/ciliumbiogenesis.pdf
32. Nance, J. and Zallen, J. (2011) "Elaborating Polarity: PAR Proteins and the Cytoskeleton." *Development for Advances in Developmental Biology and Stem Cells*, vol. 138, pp. 799–809., doi: 10.1242/dev.053538.
33. Nance, J. (2005) "PAR Proteins and the Establishment of Cell Polarity During *C. elegans* Development." *BioEssays*, vol. 27, no. 2, pp. 126–135., doi:10.1002/bies.20175.
34. Munro, E. *et al.* (2004) "Cortical Flows Powered by Asymmetrical Contraction Transport PAR Proteins to Establish and Maintain Anterior-Posterior Polarity in the Early *C. elegans* Embryo." *Developmental Cell*, vol. 7, no. 3, pp. 413–424., doi:10.1016/j.devcel.2004.08.001.
35. Achilleos, A., *et al.* (2010) "PAR-3 Mediates the Initial Clustering and Apical Localization of Junction and Polarity Proteins during *C. elegans* Intestinal Epithelial Cell Polarization." *Development*, vol. 137, no. 11, pp. 1833–1842., doi:10.1242/dev.047647.
36. David, D. J. V., *et al.* (2010) "The PAR Complex Regulates Pulsed Actomyosin Contractions during Amnioserosa Apical Constriction in *Drosophila*." *Development*, vol. 137, no. 10, pp. 1645–1655., doi:10.1242/dev.044107.
37. Georgiou, M., and Baum, B. (2010) "Polarity Proteins and Rho GTPases Cooperate to Spatially Organise Epithelial Actin-Based Protrusions." *Journal of Cell Science*, vol. 123, no. 7, pp. 1089–1098., doi:10.1242/jcs.060772.
38. Ward, S. *et al.* (1975) "Electron Microscopical Reconstruction of the Anterior Sensory Anatomy of the Nematode *Caenorhabditis elegans*." *Journal of Comparative Neurology* 1;160(3):313-37; PMID:1112927 http://www.wormatlas.org/ward_buildv0.1/Ward_buildv0.1.1.html#top
39. Oikonomou, G. and Shaham, S. (2011), "The Glia of *Caenorhabditis elegans*." *Glia*, 59: 1253–1263. doi: 10.1002/glia.21084 http://www.ncbi.nlm.nih.gov/pmc/articles/PMC3117073/
40. Altun, Z.F. and Hall, D.H. (2010) "Nervous system, neuronal support cells." In *WormAtlas*. doi:10.3908/wormatlas.1.19. http://www.wormatlas.org/hermaphrodite/neuronalsupport/mainframe.htm
41. Perens, E. and Shaham, S. (2005) "*C. elegans* Daf-6 Encodes a Patched-Related Protein Required for Lumen Formation." *Developmental Cell*, vol. 8, no. 6, pp. 893–906., doi:10.1016/j.devcel.2005.03.009.
42. Kolotuev, I. *et al.* (2009) "Secretion of Hedgehog-Related Peptides and WNT During *Caenorhabditis Elegans* Development." *Traffic*, vol. 10, no. 7, pp. 803–810., doi:10.1111/j.1600-0854.2008.00871.x.
43. Lints, R. and Hall, D.H. (2009) "Male neuronal support cells, rays." In *WormAtlas*. doi:10.3908/wormatlas.2.10
44. Barr, M.M. and Garcia, L.R. (2006) "Male mating behavior." *WormBook*, ed. The *C. elegans* Research Community, WormBook, doi/10.1895/wormbook.1.78.1, http://www.wormbook.org.
45. Heiman, M. G. and Shaham, S. (2009) "DEX-1 and DYF-7 Establish Sensory Dendrite Length by Anchoring Dendritic Tips during Cell Migration." *Cell*; 137:344–355.

46. Tardif, Steve, *et al.* (2010) "Zonadhesin Is Essential for Species Specificity of Sperm Adhesion to the Egg Zona Pellucida." *Journal of Biological Chemistry*, vol. 285, no. 32, pp. 24863–24870., doi:10.1074/jbc.m110.123125.
47. Legan, P. *et al*. (1997) "The mouse tectorins. Modular matrix proteins of the inner ear homologous to components of the sperm-egg adhesion system." *J Biol Chem*. 272:8791–8801.
48. Venkatesh, Deepak. (2017) "Primary Cilia." *Journal of Oral and Maxillofacial Pathology*, vol. 21, no. 1, p. 8., doi:10.4103/jomfp.jomfp_48_17.
49. Aldahmesh, M. A., *et al.* (2014) "IFT27, Encoding a Small GTPase Component of IFT Particles, Is Mutated in a Consanguineous Family with Bardet-Biedl Syndrome." *Human Molecular Genetics*, vol. 23, no. 12, pp. 3307–3315., doi:10.1093/hmg/ddu044.
50. Valverde, D. *et al.* (2015) "Alström Syndrome: Current Perspectives." The Application of Clinical Genetics, p. 171., doi:10.2147/tacg.s56612.
51. Mirvis, M. *et al.* (2018) "Cilium Structure, Assembly, and Disassembly Regulated by the Cytoskeleton." *Biochemical Journal*, vol. 475, no. 14, pp. 2329–2353., doi:10.1042/bcj20170453.
52. Serwas, D. *et al.* (2017) "Centrioles Initiate Cilia Assembly but Are Dispensable for Maturation and Maintenance in *C. elegans*." *The Journal of Cell Biology*, vol. 216, no. 6, pp. 1659–1671., doi:10.1083/jcb.201610070.
53. Cole, D. *et al.* (1998) "Chlamydomonas Kinesin-II–Dependent Intraflagellar Transport (IFT): IFT Particles Contain Proteins Required for Ciliary Assembly In *Caenorhabditis Elegans* Sensory Neurons." *The Journal of Cell Biology*, vol. 141, no. 4, pp. 993–1008., doi:10.1083/jcb.141.4.993.
54. Blacque, O. *et al.* (2004) "Loss of *C. elegans* BBS-7 and BBS-8 Protein Function Results in Cilia Defects and Compromised Intraflagellar Transport." *Genes & Development*, vol. 18, no. 13, pp. 1630–1642., doi:10.1101/gad.1194004.
55. Ou, G. *et al.* (2005) "Functional Coordination of Intraflagellar Transport Motors." *Nature*, vol. 436, no. 7050, pp. 583–587., doi:10.1038/nature03818.
56. Tobin, D. *et al.* (2002) "Combinatorial Expression of TRPV Channel Proteins Defines Their Sensory Functions and Subcellular Localization in *C. elegans* Neurons." *Neuron*, vol. 35, no. 2, pp. 307–318., doi:10.1016/s0896-6273(02)00757-2.
57. Qin, H. *et al.* (2005) "Intraflagellar Transport Is Required for the Vectorial Movement of TRPV Channels in the Ciliary Membrane." *Current Biology*, vol. 15, no. 18, pp. 1695–1699., doi:10.1016/j.cub.2005.08.047.
58. Badano, J. *et al.* (2006) "The Ciliopathies: An Emerging Class of Human Genetic Disorders." *Annual Review of Genomics and Human Genetics,* vol. 7, no. 1, pp. 125–148., doi:10.1146/annurev.genom.7.080505.115610.
59. Mukhopadhyay, A. *et al.* (2005) "*C. elegans Tubby* Regulates Life Span and Fat Storage by Two Independent Mechanisms." *Cell Metabolism*, vol. 2, no. 1, pp. 35–42., doi:10.1016/j.cmet.2005.06.004.
60. Bae, Y. and Barr, M. (2008) "Sensory Roles of Neuronal Cilia: Cilia development, morphogenesis, and function in *C. elegans*." *Frontiers in Bioscience,* 13, 5959-5974. http://www.ncbi.nlm.nih.gov/pmc/articles/PMC3124812/

61. Sundaram, M. and Buechner, M. (2016) "The *Caenorhabditis Elegans* Excretory System: A Model for Tubulogenesis, Cell Fate Specification, and Plasticity." *Genetics*, vol. 203, no. 1, pp. 35–63., doi:10.1534/genetics.116.189357.
62. Mancuso, V. P., *et al.* (2012) "Extracellular Leucine-Rich Repeat Proteins Are Required to Organize the Apical Extracellular Matrix and Maintain Epithelial Junction Integrity in *C. elegans*." *Development*, vol. 139, no. 5, pp. 979–990., doi:10.1242/dev.075135.
63. Polanska, U. *et al.* (2010) "The Cooperation of FGF Receptor and Klotho Is Involved in Excretory Canal Development and Regulation of Metabolic Homeostasis In *Caenorhabditis Elegans*." *Journal of Biological Chemistry*, vol. 286, no. 7, pp. 5657–5666., doi:10.1074/jbc.m110.173039.
64. Mello, C. *et al*. (1991) "Efficient Gene Transfer in *C.elegans*: Extrachromosomal Maintenance and Integration of Transforming Sequences." *EMBO Journal*, vol. 10, no. 12, pp. 3959–3970.
65. Herrmann, C. *et al*. (1996) "Differential Interaction of the Ras Family GTP-Binding Proteins H-Ras, Rap1A, and R-Ras with the Putative Effector Molecules Raf Kinase and Ral-Guanine Nucleotide Exchange Factor*." Journal of Biological Chemistry*, vol. 271, no. 12, pp. 6794–6800., doi:10.1074/jbc.271.12.6794.
66. Culotti, J. and Russel, R. (1978) "Osmotic Avoidance Defective Mutants of the Nematode *Caenorhabditis elegans*." *Genetics*, vol. 90, no. 2, pp. 243–256.
67. Lee, J. *et al.* (2011) "Methods for Evaluating the *Caenorhabditis Elegans* Dauer State: Standard Dauer-Formation Assay Using Synthetic Daumones and Proteomic Analysis of O-GlcNAc Modifications." *Methods in Cell Biology Caenorhabditis Elegans: Molecular Genetics and Development*, pp. 445–460., doi:10.1016/b978-0-12-544172-8.00016-5.
68. Duerr, J. S. (2006) Immunohistochemistry *WormBook*, ed. The *C. elegans* Research Community, WormBook, doi/10.1895/wormbook.1.105.1, http://www.wormbook.org.
69. Gilbert,S. (2000) "Early Development of the Nematode *Caenorhabditis Elegans*." *Developmental Biology*, vol. 6.
70. Totong, R., *et al*. (2007) "PAR-6 Is Required for Junction Formation but Not Apicobasal Polarization in *C. elegans* Embryonic Epithelial Cells." *Development*, vol. 134, no. 7, pp. 1259–1268., doi:10.1242/dev.02833.
71. Schouteden, C. *et al.* (2015) "The Ciliary Transition Zone Functions in Cell Adhesion but Is Dispensable for Axoneme Assembly In *C. elegans*." *The Journal of Cell Biology*, vol. 210, no. 1, pp. 35–44., doi:10.1083/jcb.201501013.
72. Swoboda, P. *et al.* (2000) "The RFX-Type Transcription Factor DAF-19 Regulates Sensory Neuron Cilium Formation in *C. elegans*." *Molecular Cell*, vol. 5, no. 3, pp. 411–421., doi:10.1016/s1097-2765(00)80436-0.
73. Serebriiskii, I. and Golemis, E. (2001) "Two-Hybrid System and False Positives: Approaches to Detection and Elimination." *Methods in Molecular Biology*, vol. 177, pp. 123–134., doi:10.1385/1-59259-210-4:123
74. Seeger-Nukpezah, T. and Golemis, E. (2012) "The Extracellular Matrix and Ciliary Signaling." *Current Opinion in Cell Biology*, vol. 24, no. 5, pp. 652–661., doi:10.1016/j.ceb.2012.06.002.

75. Hoh, R. *et al*. (2012) “Transcriptional Program of Ciliated Epithelial Cells Reveals New Cilium and Centrosome Components and Links to Human Disease.” *PLoS ONE*, vol. 7, no. 12, doi:10.1371/journal.pone.0052166.
76. Mollet, G. *et al*. (2005) “Characterization of the Nephrocystin/Nephrocystin-4 Complex and Subcellular Localization of Nephrocystin-4 to Primary Cilia and Centrosomes.” *Human Molecular Genetics*, vol. 14, no. 5, pp. 645–656., doi:10.1093/hmg/ddi061.
77. Miyamoto, T. *et al*. (2011) “Insufficiency of BUBR1, a Mitotic Spindle Checkpoint Regulator, Causes Impaired Ciliogenesis in Vertebrates.” *Human Molecular Genetics*, vol. 20, no. 10, pp. 2058–2070., doi:10.1093/hmg/ddr090.
78. Smith, K. *et al*. (2011) “A Role for Central Spindle Proteins in Cilia Structure and Function.” *Cytoskeleton*, vol. 68, no. 2, pp. 112–124., doi:10.1002/cm.20498.
79. Khanna, H. *et al*. (2005) “RPGR-ORF15, Which Is Mutated in Retinitis Pigmentosa, Associates with SMC1, SMC3, and Microtubule Transport Proteins.” *Journal of Biological Chemistry*, vol. 280, no. 39, pp. 33580–33587., doi:10.1074/jbc.m505827200.
80. Peset, I. and Vernos, I. (2008) “The TACC Proteins: TACC-Ling Microtubule Dynamics and Centrosome Function.” *Trends in Cell Biology*, vol. 18, no. 8, pp. 379–388., doi:10.1016/j.tcb.2008.06.005.
81. Bot, N. *et al*. (2003) “TAC-1, a Regulator of Microtubule Length in the *C. Elegans* Embryo.” *Current Biology*, vol. 13, no. 17, pp. 1499–1505., doi:10.1016/s0960-9822(03)00577-3.
82. Bhalla, N., and Dernberg, A. (2005) “A Conserved Checkpoint Monitors Meiotic Chromosome Synapsis in *Caenorhabditis Elegans*.” *Science*, vol. 310, no. 5754, pp. 1683–1686., doi:10.1126/science.1117468.
83. Bohr, T. *et al*. (2018) “Shugoshin Is Essential for Meiotic Prophase Checkpoints in *C. Elegans*.” *Current Biology*, vol. 28, no. 20, doi:10.1016/j.cub.2018.08.026.
84. Colaiácovo, M. *et al*. (2003) “Synaptonemal Complex Assembly in *C. Elegans* Is Dispensable for Loading Strand-Exchange Proteins but Critical for Proper Completion of Recombination.” *Developmental Cell*, vol. 5, no. 3, pp. 463–474., doi:10.1016/s1534-5807(03)00232-6.
85. Hall, D.H., Herndon, L.A. and Altun, Z. Introduction to *C. elegans* Embryo Anatomy. In *WormAtlas*.